Numerical Simulation of Streamflow Distribution, Sediment Transport, and Sediment Deposition along Long Branch Creek in Northeast Missouri

By David C. Heimann

Abstract

This report presents the results of a study conducted by the U.S. Geological Survey in cooperation with the Missouri Department of Conservation to describe the hydrology, sediment transport, and sediment deposition along a selected reach of Long Branch Creek in Macon County, Missouri. The study was designed to investigate spatial and temporal characteristics of sediment deposition in a remnant forested riparian area and compare these factors by magnitude of discharge events both within and outside the measured range of flood magnitudes.

The two-dimensional finite-element numerical models RMA2-WES and SED2D-WES were used in conjunction with measured data to simulate streamflow and sediment transport/deposition characteristics during 2-, 5-, 10-, and 25-year recurrence interval floods. Spatial analysis of simulated sediment deposition results indicated that mean deposition in oxbows and secondary channels exceeded that of the remaining floodplain areas during the 2-, 5-, 10-, and 25-year recurrence interval floods. The simulated mass deposition per area for oxbows and secondary channels was 1.1 to 1.4 centimeters per square meter compared with 0.1 to 0.60 centimeters per square meter for the remaining floodplain.

The temporal variability of total incremental floodplain deposition during a flood was found to be strongly tied to sediment inflow concentrations. Most floodplain deposition, therefore, occurred at the beginning of the streamflow events and corresponded to peaks in sediment discharge. Simulated total sediment deposition in oxbows and secondary channels increased in the 2-year through 10-year floods and decreased in the 25-year flood while remaining floodplain deposition was highest for the 25-year flood.

Despite increases in sediment inflows from the 2-year through 25-year floods, the retention ratio of sediments (the ratio of floodplain deposition to inflow load) was greatest for the 5-year flood and least for the 25-year flood. The decrease in retention ratio at greater flows is likely the result of higher velocities on the floodplain, resulting in higher bed shear stress, greater suspension time of deposited material, and greater sediment transport through the system.

Simulated sediment deposition was most sensitive to sediment inflow concentrations and modification of floodplain roughness—factors that can be controlled through management practices. The increase in floodplain sediment deposition resulting from a simulated increase in vegetation density (increase in floodplain roughness from a Manning's n of 0.11 to 0.12) was 142,000 kilograms, or 6.5 percent for a 10-year recurrence interval flood. This increase was comparable to total oxbow and secondary channel deposition mass in the simulations, but would result in a mean increase in floodplain deposition thickness of only 0.025 centimeter.

The hydrodynamic model results show the importance of the secondary channels and meander cutoff channels in this system because these areas quickly bring floodwaters and sediment to areas not close to the main channel. The meander cutoff channels in the simulation also effectively decrease flow and velocities in some main channel sections thereby affecting sediment deposition in the vicinity of these features.

INTRODUCTION

Historically, mesic and wet-mesic bottomland forests associated with riparian zones were found throughout Missouri (Nelson, 1987). In the glaciated plains of northern Missouri, the conversion of upland prairies and floodplains to agriculture production began in the late 1800's (Schroeder, 1982). Presently (2001), natural examples of these bottomland forest types are rare and fragmented because most of this area has been cleared for agricultural uses. Also, many streams in this region have been channelized, resulting in higher velocities and potentially increased sediment loads. Consequently, many of the remaining riparian forests are thought to receive large quantities of sediment during overbank flow.

The Riparian Ecosystem Assessment and Management (REAM) project is an ongoing multi-disciplinary and multi-agency research effort with a focus on characterizing remaining examples of forested riparian areas in northern Missouri. Initiated in 1993, the objective of the REAM project is to determine Best Management Practices for maintaining or enhancing wildlife habitat, biodiversity, forest resources, and aquatic resources. Overall goals are to characterize the functional system and biota of riparian forest ecosystems of northern Missouri; develop management strategies to protect and enhance riparian resources; and determine the effects of management applications on riparian forests of northern Missouri. The REAM project includes investigations of both the physical and biological components of riparian systems including the interactions of the hydrology, sediment deposition, and the vegetation characteristics of the floodplain. Both the suspended sediment load and streamflow characteristics were significant factors describing the variability in the magnitude of median event deposition during overbank events on the Long Branch Creek floodplain (Heimann and Roell, 2000). The riparian system hydrology and sediment deposition characteristics are contributing factors in vegetation composition and succession in bottomland forests. Vegetation composition and succession has been attributed to the hydrologic conditions (inundation frequency and duration) of the flooded system (Hardin and Wistendahl, 1983; Metzler and Damman, 1985; Patterson and others, 1985; Hupp and Osterkamp, 1985, 1996; Brinson, 1990; Gregory and others, 1991). Microtopographical features of the floodplain also may have a determining effect on the distribution of vegetation (Hardin and Wistendahl, 1983; Hodges, 1997), as well as the particle size of sediment deposits (Sigafoos, 1976; Wolfe and Pittillo, 1977), and aggradation/degradation effects as the result of channelization (Hupp and Osterkamp, 1996). The vegetation characteristics will, in turn, be a determining factor in the wildlife community (Geier and Best, 1980; Abernethy and Turner, 1987; Murray and Stauffer, 1995) supported by the area.

A study from October 1998 to December 2000 by the U.S. Geological Survey (USGS), in cooperation with the Missouri Department of Conservation (MDC), simulated streamflow, sediment transport, net sediment deposition rates, and controlling factors in sediment deposition along a selected reach of Long Branch Creek, a REAM study site in Macon County, Missouri. This is the second of two reports describing streamflow and sediment transport and deposition characteristics of this stream system. The first is a summary of streamflow, suspended sediment, and sediment deposition data collected between 1995 and 1998 in the Long Branch Creek Basin (Heimann and Roell, 2000) and these data are used in the verification of the numerical models used in this study.

Purpose and Scope

This report summarizes the results of a study conducted from October 1998 to December 2000 to determine streamflow and sediment transport, and sediment deposition characteristics of a small northeast Missouri stream system from onsite observations and numerical simulations. Two-dimensional hydrodynamic simulations of the streamflow provide insight into the velocity distribution, water depths, and inundation area resulting from flood discharges for recurrence intervals of 2, 5, 10, and 25 yrs (years). A two-dimensional sediment transport and deposition model pro-

vides insight into the spatial distribution of streambed change, sediment concentration, and bed shear stress for multiple time steps during these same four floods.

Description of Study Area

The study reach consists of a 2.7-km (kilometer) section of Long Branch Creek located in the 1,800-hectare Atlanta Conservation Area in Macon County, Missouri (fig. 1). The Atlanta Conservation Area is managed by the MDC for recreation and wildlife. The Long Branch Creek Basin drains 60 km^2 (square kilometers) upstream from a continuously recording streamflow gaging station (06910500) and drains 65 km^2 above the upstream end of the study reach. Land use in the basin upstream from the Conservation Area primarily is agriculture with a thin forest buffer along much of the stream channel. The average bankfull stream width along the study reach is 11.7 m (meter), the sinuosity is 2.3, and the slope is 0.61 m/km (meter per kilometer). The stream bed in the study reach predominantly is sand and silt. No constructed levees exist along the stream, but evidence of channelization exists upstream of the study area. Comparisons of 1908 and 1979 topographic maps of the area, along with onsite observations, indicate approximately 0.80 km of Long Branch Creek has been channelized between the streamflow gaging station and the upstream end of the study reach.

Acknowledgments

The author acknowledges Darren Gonzalez, Environmental Modeling Research Laboratory, Brigham Young University, Provo, Utah, and Gary Freeman, WEST Consultants, Tempe, Arizona, for their assistance in the development of the numerical model simulations. The author also acknowledges Mike Roell, Missouri Department of Conservation, for acquiring elevation data points and woody debris survey information for Long Branch Creek.

STUDY APPROACH

Hydrology and Sediment Transport

A continuous streamflow gaging station was established by the USGS, in July 1995, approximately 2.4 km upstream from the study area, to monitor streamflow and suspended-sediment concentrations. Two crest-stage indicators (CSI; fig. 1) were established along the stream in the study area to monitor peak stages during floods.

Suspended-sediment samples were collected at the streamflow gaging station at discharges larger than 0.3 m^3/s (cubic meter per second) using an automatic sampler. Periodic manual samples were collected using the equal-width increment method (Guy and Norman, 1970) and analyzed using methods described in Guy (1969). Automatic sample concentrations were adjusted, if necessary, to account for differences between the point-sampled automatic samples and multiple manual samples. These adjustments were determined from differences between suspended-sediment concentrations in concurrent automatic and manual samples. Suspended-sediment concentrations and loads were determined from discrete suspended-sediment concentration samples and interpolated estimates along with corresponding stream discharge using the USGS computer program SEDCALC (Koltun and others, 1994).

Sediment Deposition

Sediment deposition was measured on the floodplain along the study reach using a network of feldspar clay pads and sediment disks (fig. 1). There were 82, 0.25-m^2 (square meter) clay pads and 14 sediment disks (0.09-m^2 Plexiglas disks) located in the study area. Flood sediment deposition and corresponding flood characteristics are summarized in Heimann and Roell (2000) from an extended 132 clay pad and 31 sediment disk network sampled from July 1995 through September 1998. Particle-size information was gathered from the sediment disk samples following individual overbank floods and from floodplain sediment samples collected during an elevation survey of the model reach. A 5-cm (centimeter)-diameter core was used to collect soil samples from the top 10 cm of the floodplain. Forty-seven sediment disk samples (collected following individual floods) and 80 floodplain samples (collected during a June 1997 elevation survey) were analyzed for particle size at the University of Missouri Soil Characterization Laboratory in Columbia, Missouri, using methods described in U.S. Department of Agriculture (1996).

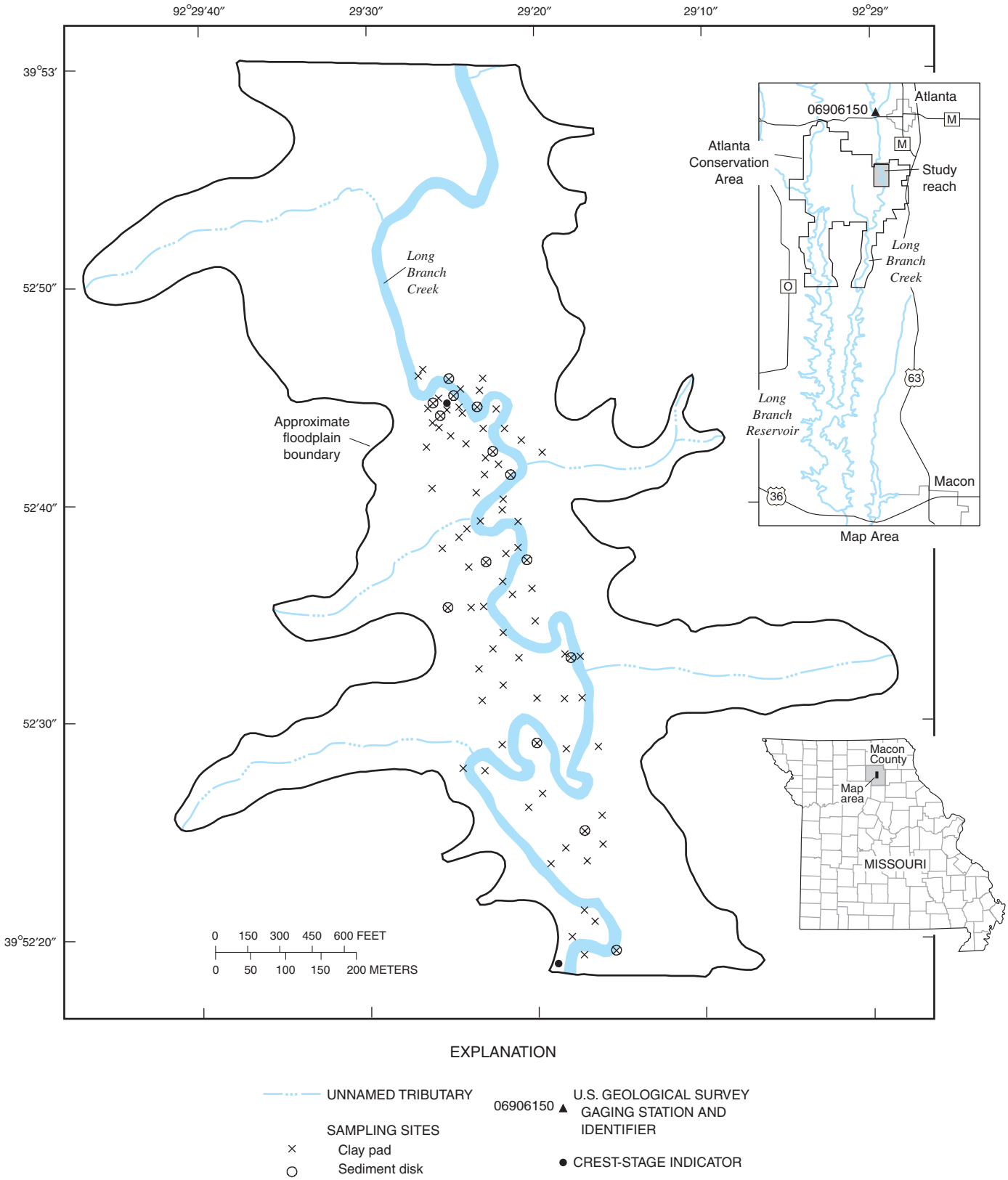

Figure 1. Location of study reach.

Numerical Simulations

Streamflow Distribution

Velocities and inundation areas under different streamflow conditions were determined using RMA2-WES—a two-dimensional finite element hydrodynamic numerical model. The RMA2-WES version 4.35 was used in conjunction with the Surface-Water Modeling System (SMS) version 6.0, which serves as a pre- and post-processor for both RMA2-WES and SED2D-WES simulation data (Environmental Modeling Research Laboratory, 1999). The RMA2-WES solves for depth-averaged velocity and hydraulic head using the Reynolds form of the Navier-Stokes equation for both steady-state and dynamic simulations (King, 1990; U.S. Army Corps of Engineers, 1996). Friction was calculated using the Manning's or Chezy equations. Limitations of the RMA2-WES include the assumption that vertical accelerations are negligible and that the simulation is under subcritical flow conditions. Four floods were simulated including two measured floods for verification (2- and 5-yr recurrence intervals and two simulated larger-recurrence interval floods (10- and 25-yr recurrence intervals). Other studies that have used the RMA2 model include Bates and others (1992), Apicella and others (1994), Hall and Engel (1995), Sanchez and Roig (1997), and Crowder and Diplas (2000).

Model Setup and Requirements

The setup procedure included developing a finite element mesh, interpolating surface elevations onto the mesh, determining material properties, and developing input streamflow and stage hydrographs. Output consists of nodal water-surface elevations, water depths, and velocity magnitudes and directions for each time step.

The mesh developed for the RMA2-WES and SED2D-WES simulations represents approximately 2,700 m of the study reach, and includes a 600-m focus area and approximately 1,000-m extensions upstream and downstream (fig. 2). The focus area corresponds to approximately two mean floodplain widths (mean floodplain width of 317 m) and represents the area with the most intensive elevation and sediment deposition data. The upstream and downstream extensions are used to minimize the effects of boundary conditions and allow for equilibration of the water-surface elevation and velocities entering and leaving the focus area. CSIs were located upstream from the focus area and near the downstream boundary of the model reach (fig. 2). The lateral extent of the mesh was designed to contain the estimated water-surface elevation of the largest simulation flood (25-yr recurrence interval). The mesh contains 7,065 elements and 16,750 nodes. The overall mean area per element was 81.8 m^2 although near-channel elements are refined to an average area of about 22 m^2. The near-channel elements are in the active wetting and drying mesh area, and these elements were refined to decrease the possible numerical destabilizing effects that can occur during wetting and drying and also to prevent conservation of mass problems that may occur with inadequate mesh refinement (Berger, 1990). The maximum front width (maximum number of nodes for which equations are solved simultaneously) was 567.

The simulation geometry was developed using data from onsite surveys and digitized contour data from a 7.5-minute USGS topographic map. Survey data for the 600-m focus area was collected using a total station and consisted of about 2,600 horizontal and vertical coordinates. Included in this survey were 37 stream cross sections and numerous floodplain elevations and sediment-characterization sampling points. These data were augmented with elevations from 37 feldspar clay pad sites (sediment deposition monitoring sites) within the focus area. The elevations of the feldspar clay pads were determined by a survey conducted by MDC. The geometry of the area of the mesh upstream and downstream of the focus area was developed primarily using 5-m mesh elevation points developed by the MDC from digitized data for 7.5-minute USGS topographic maps. These mesh points were adjusted, if necessary, using data from the detailed survey in the focus area and an additional 44 clay pad elevation points outside of the focus area. The streambed elevation within the focus area was surveyed along the 37 channel cross sections spaced at approximately 17-m intervals. The stream channel elevations outside of the focus area were determined by interpolating from the ending study-reach cross sections to the upstream and downstream ends of the reach using the mean channel gradient. The mean channel gradient was determined from MDC survey points, which included 14 mid-channel elevation points collected throughout the model reach. The 14 survey points also were used as check points to verify interpolated elevations. The horizontal and vertical-coordinate data points were interpolated onto the developed mesh using the linear interpolation method within SMS. The

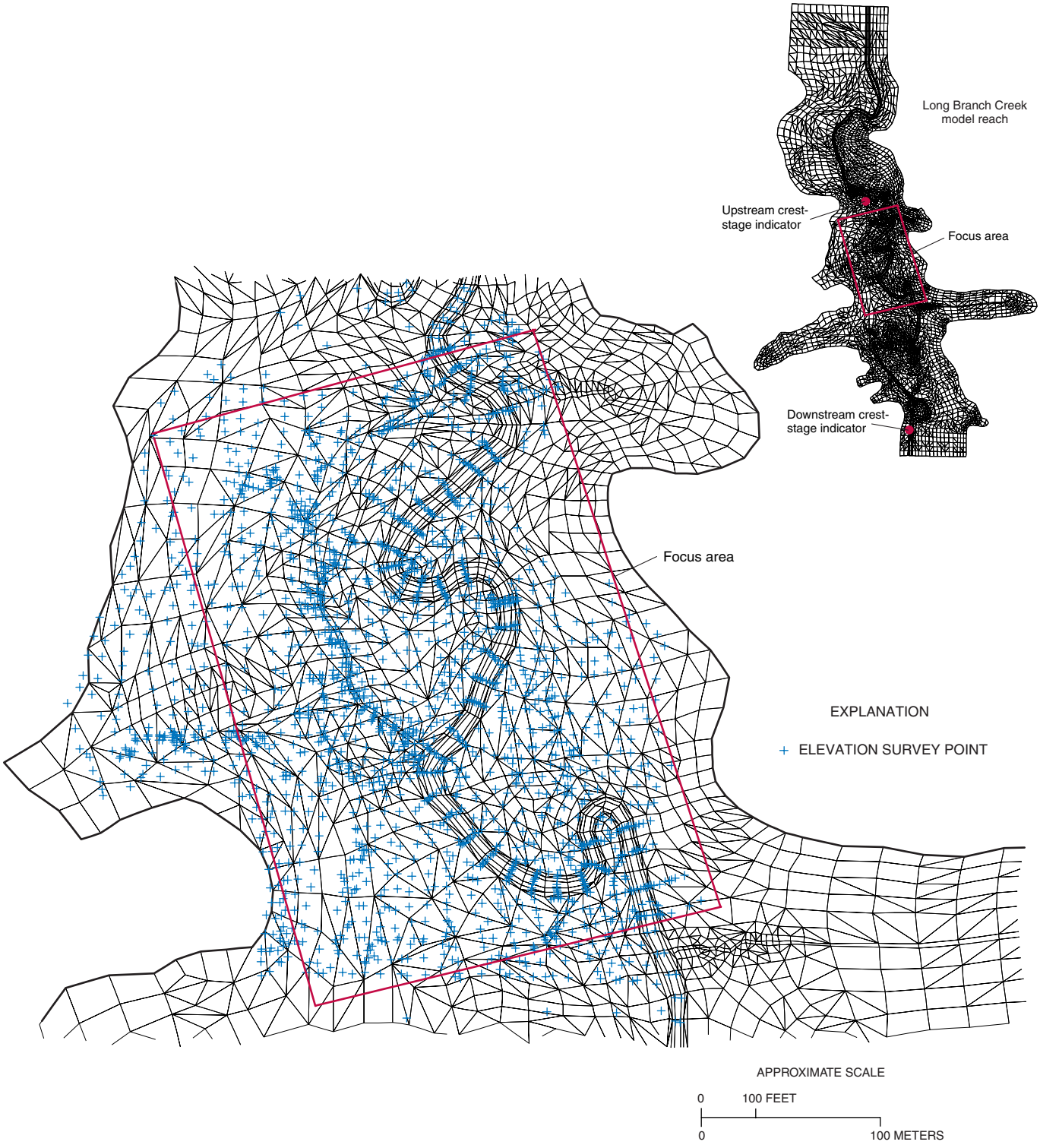

Figure 2. Finite-element mesh of Long Branch Creek model reach and focus area (showing elevation survey points).

minimum elevation value in the mesh (fig. 3) was 245.50 m above sea level and the maximum elevation was 254.78 m above sea level for a range of 9.28 m. Artificial sumps were placed into the upstream and downstream end of the model reach to ensure that the boundary strings (nodes defining the upper and lower boundary conditions) would not become dry during dynamic simulations, which would result in an unstable numerical condition.

The model mesh elements were developed to follow elevation contours and facilitate a smooth elemental boundary during wetting and drying periods in the dynamic simulations. Wetting and drying in a simulation was accomplished by the elemental elimination method in which a mesh element is turned off when the water depth at one or more nodes is less than a user specified minimum (U.S. Army Corps of Engineers, 1996). Elements are re-wet when all nodes in an element exceed a user specified maximum value of water depth. A minimum water depth of 0.08 m (drying depth) and maximum water depth (rewetting depth) of 0.20 m were used in all simulations and these criteria were checked following every fifth model iteration. Wetting and drying criteria that are too low result in frequent drying and rewetting of elements and leads to numerical instability and divergence from a numerical solution. Wetting and drying threshold elevations that are too high result in unrealistic wetting/drying scenarios. A solution for each time step in the dynamic simulation was complete when the change in water-surface elevation for an iteration was less than the specified 0.005-m convergence criteria at all nodes. The convergence criteria of 0.005 m was used for all four simulations.

User specified material properties, including roughness coefficients (Manning's n) and eddy viscosity values (turbulence exchange factor), were assigned to each element in the mesh. A Manning's n value of

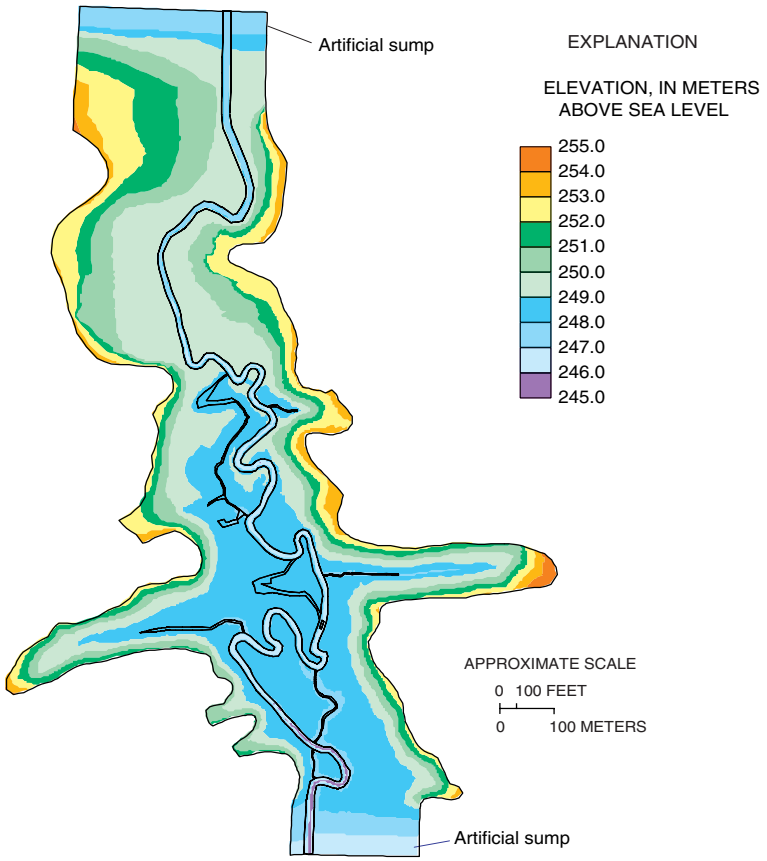

Figure 3. Model mesh elevations.

0.05 was used for the stream channel elements in all simulations and was determined using empirical data and developed guidelines provided in Arcement and Schneider (1989) and Barnes (1967). A value of 0.11 was determined to be suitable for the floodplain areas in a simulation of the April 4, 1997, conditions (approximately 2-yr recurrence interval flood). This was determined by selecting a starting value of Manning's n from Arcement and Schneider (1989) and adjusting this value to obtain a desired maximum water-surface elevation corresponding to that obtained from the upstream CSI for the flood. A Manning's n of 0.13 was used for simulating the July 4, 1998, flood (approximately 5-yr recurrence interval), for the simulated water-surface elevation to match the measured maximum CSI water-surface elevation for this flood. The higher Manning's n required for simulating the July flood could be explained by vegetation cover during the active growing season. A Manning's n of 0.11 was selected for the entire floodplain area in the 10- and 25-yr flood to represent a more typical flooding scenario that would occur in the spring prior to substantial vegetation cover.

All elements in the final mesh design were assigned an eddy viscosity of 900 Pa-s (pascal seconds) as determined during model "spin-down" (see following section). The eddy viscosity values control the transfer of momentum between waters of differing velocities and can therefore have a direct effect on simulated stream velocities. In dynamic simulations the recommended starting values of eddy viscosity were 1,000-5,000 Pa-s and these values were then decreased to find a stability threshold point and then slightly increased to a working level (Darren Gonzalez, Environmental Modeling Research Laboratory, Brigham Young University, written commun., 1999).

Model "Spin Down"

The first step in running the dynamic simulations was to obtain a stable starting point for the simulated hydrographs, and the process of developing the stable starting point is referred to as "spinning-down" the model. In this step the mesh is "filled with water" (in this simulation a water-surface elevation of 255 m above sea level was used) and the downstream boundary hydraulic head is lowered incrementally to the desired dynamic simulation starting point. The "spin-down" procedure also allows for testing of the mesh geometry to better ensure smooth boundaries during wetting and drying and to eliminate ponding (isolated wet elements), which can result in numerically unstable solutions. Some node elevations were modified (by 0.1 m or less) to eliminate ponding and the eddy viscosity values were also modified during the spin down to obtain a stable numerical solution. Inflow during the spin-down procedure corresponds to that of the target downstream hydraulic head. Inflow used throughout the spin down was 9.0 m^3/s and the corresponding ending downstream hydraulic head was 247.5 m; these corresponded to bankfull conditions in the model reach. A 10-hr (hour) increment time was used in the spin down to ensure a stable solution. The output solution from the spin down (hotstart output) was then used as the starting point for all four dynamic simulations.

A lag time of 1 hr was included between the upstream boundary inflow and the corresponding downstream boundary hydraulic head to compensate for the 2.7 km travel distance between the upstream and downstream mesh boundaries. The lag time of 1 hr was estimated based on a stream length of 2.7 km and a mean velocity of 0.75 m/s (meter per second)—determined from velocity measurements collected during floods at the gaging station and from initial simulations.

Streamflow and stage data from two measured floods—April 4, 1997 (approximately a 2-yr recurrence interval) and July 4, 1998 (approximately a 5-yr recurrence interval)—were used to verify the RMA2-WES solutions. The April 4, 1997, flood had an instantaneous peak flow of 35.0 m^3/s, approximately corresponding to a 2-yr recurrence interval flood (table 1; fig. 4). The approximate recurrence interval was determined from equations developed by Alexander and Wilson (1995) for instantaneous peak streamflows in ungaged basins in Missouri. The July 4, 1998, flood had an instantaneous peak flow of 73.2 m^3/s, approximately corresponding to a 5-yr recurrence interval flood (table 1; fig. 4). The 15-min (minute) incremental measured stage data from the gaging station was related to the downstream CSI elevations by linear regression analyses of peak stages ($y = 0.67x + 79.71$, adjusted $r^2 = 0.91$, fig. 5) so these data could be used as model input. An input streamflow and stage hydrograph with a time step of 0.5 hr was used in the 2-yr flood simulation, and a time step of 0.25 hr was used in the larger 5-yr recurrence interval flood simulation to limit stage and streamflow incremental changes.

Table 1. Streamflow and peak water-surface elevation characteristics of 2-, 5-, 10-, and 25-year recurrence interval floods

[--, no data]

Measured or simulated flood	Measured instantaneous peak flow, in cubic meter per second and (cubic foot per second)[1]	Measured instantaneous peak water-surface elevation at gaging station, in meters above sea level	Calculated upstream reach peak water-surface elevation, in meters above sea level	Calculated downstream study reach peak water-surface elevation, in meters above sea level
April 4, 1997	35.0 (1,235)	252.37	249.66	248.48
Simulated 2-year recurrence interval	38.8 (1,370)[1]	--	249.76	248.62
July 4, 1998	73.3 (2,590)	253.06	250.19	249.13
Simulated 5-year recurrence interval	67.4 (2,380)[1]	--	250.07	248.96
Simulated 10-year recurrence interval	89.2 (3,150)[1]	--	250.16	249.09
Simulated 25-year recurrence interval	120 (4,230)[1]	253.41	250.27	249.23

[1]Values calculated from equations in Alexander and Wilson (1995).

Hydrographs were developed for 10- and 25-yr recurrence interval floods using a dimensionless hydrograph developed by Becker (1990) for small basins in Missouri. Hydrograph development using this technique required the determination of a mean basin lag time and an instantaneous peak streamflow for the desired event. The mean basin lag time (time between the centroid of rainfall and measured streamflow hydrograph peak), determined from five selected events, was 13.25 hrs. The calculated instantaneous peak streamflow for the 10-yr recurrence interval flood was 89.2 m^3/s and 120 m^3/s for the 25-yr flood (fig. 4) based on regional equations developed by Alexander and Wilson (1995) for ungaged basins. A time step of 0.33 hr was used in the 10- and 25-yr recurrence interval simulations. A lag time of 0.66 hr (two-time steps) was used between the inflow streamflow and the corresponding outflow hydraulic head in the 10- and 25-yr simulations (rather than the 1-hr lag used in the 2- and 5-yr simulations) to account for greater channel velocities and greater part of flow in cutoff channels that effectively decrease the travel distance and time.

Sediment Transport and Deposition

Sediment transport and deposition were simulated using the numerical model SED2D-WES version 3.2. The SED2D-WES is currently (2001) supported by the U.S. Corps of Engineers Waterways Experiment Station (Roig and others, 1996). The SED2D-WES can be applied to cohesive (clay) or noncohesive (sand) bed sediments where flow velocities are considered two-dimensional in the horizontal plane. The sediment transport model uses the Galerkin finite-element formulation to solve the advection-dispersion equation for suspended-sediment transport in the water column. The governing equations for the sediment transport model are provided in Roig and others (1996) and Letter and others (1998). The channel bed is considered to be a source or a sink depending on the bed shear stress that results from the velocity field calculated by RMA2-WES. The SED2D-WES can be applied to both erosion and deposition applications. Version 3.2 used in this study was limited to simulating transport and deposition of material in a single size class of substrate material although the size class can vary among nodes. It also was not found to be constrained to conserve mass, and the model verification process used in this study included adjustment of parameters to ensure reasonable mass conservation. Other studies that have used the SED2D-WES include Hall and Engel (1995) and Sanchez and Roig (1997).

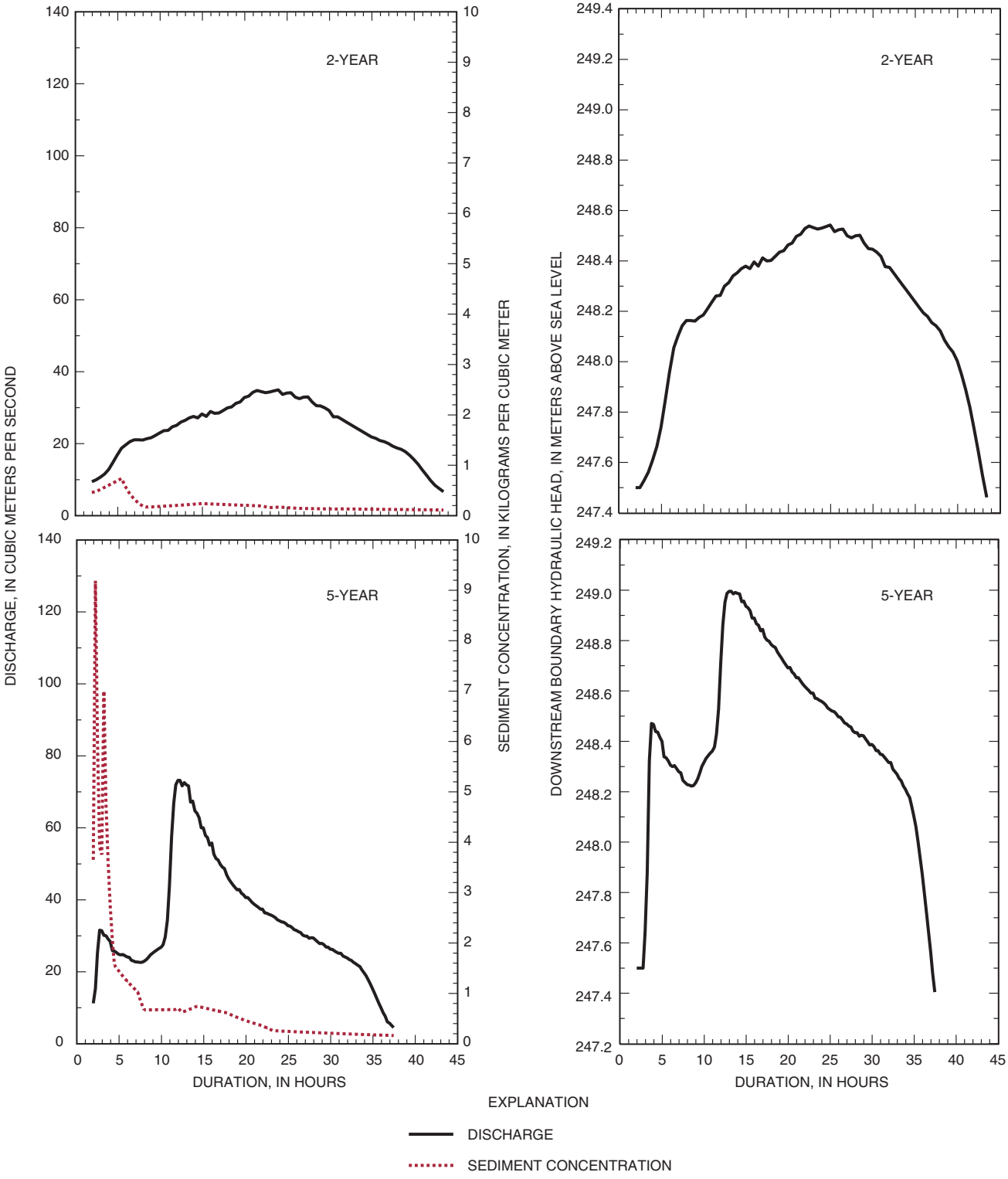

Figure 4. Input hydrographs and sedigraphs for approximate 2-year recurrence interval (April 4, 1997); approximate 5-year recurrence interval (July 4, 1998); and estimated 10- and 25-year recurrence interval floods.

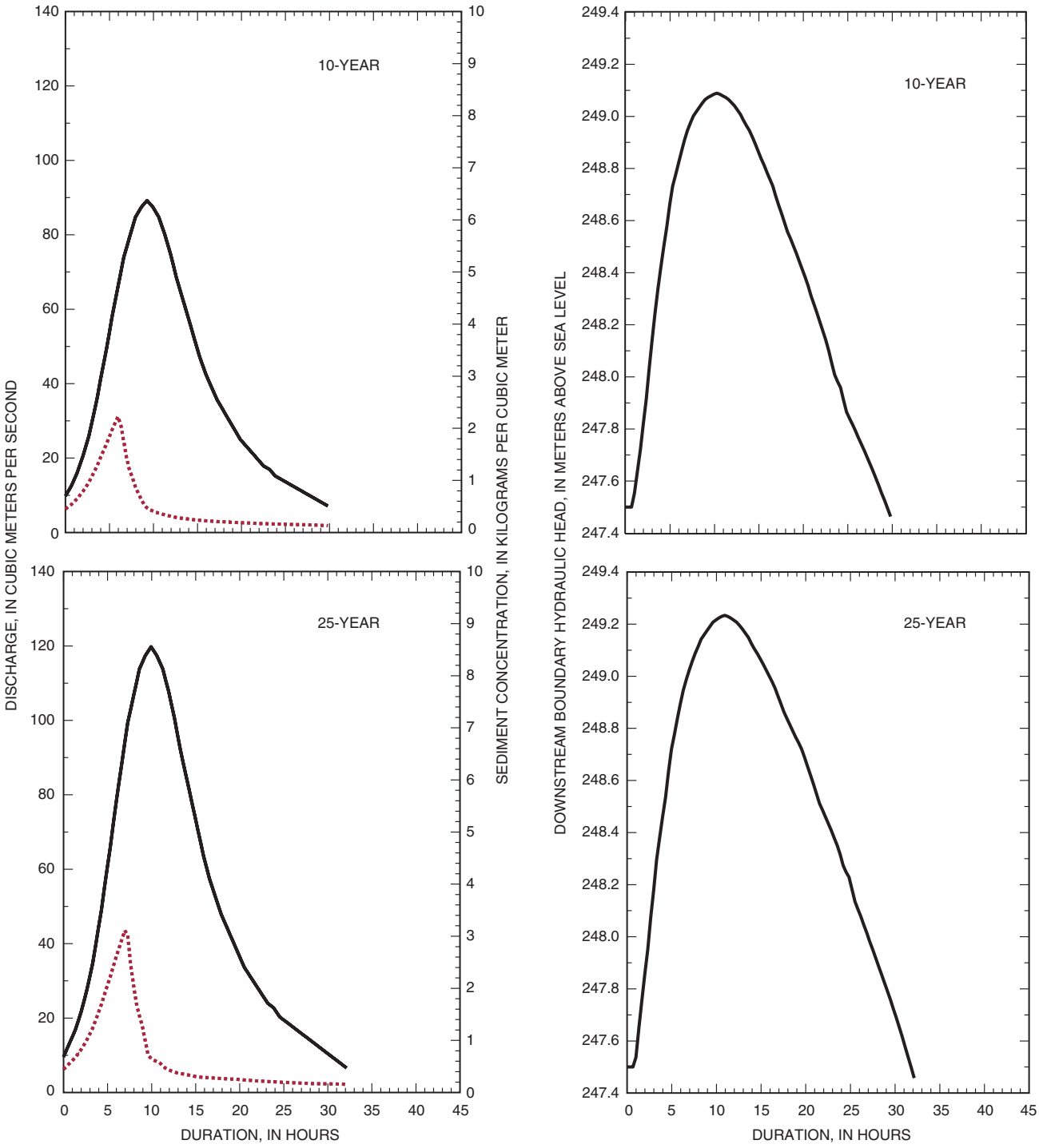

Figure 4. Input hydrographs and sedigraphs for approximate 2-year recurrence interval (April 4, 1997); approximate 5-year recurrence interval (July 4, 1998); and estimated 10- and 25-year recurrence interval floods—Continued.

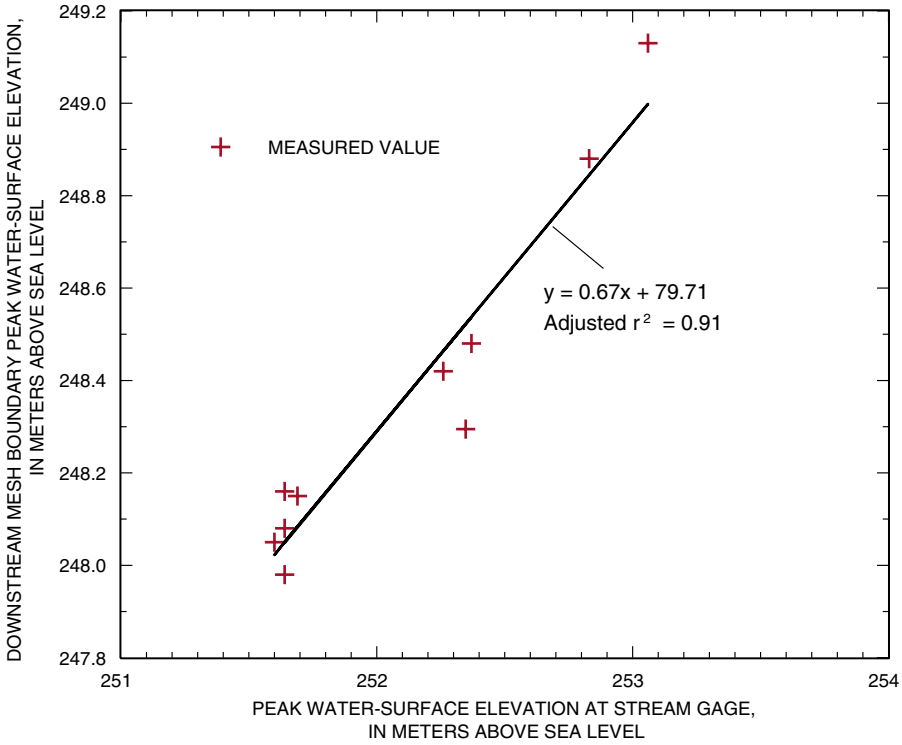

Figure 5. Relation between peak water-surface elevations at the upstream continuous gaging station and the downstream crest-stage gage in the study reach.

Data Setup and Requirements

The SED2D-WES uses the existing mesh geometry, nodal velocity, and water depth output from the RMA2-WES simulation to calculate bed shear stress and transport/deposition characteristics of the specified streambed and floodplain substrate. Input data consist of suspended-sediment concentrations at the upstream nodal boundary and global and local bed characteristics. Output data consist of nodal values of bed shear stress, sediment concentration, and bed elevation change for each time step. Sediment concentrations corresponding to the streamflow values and time increments used in the RMA2-WES simulation are specified for the inflow boundary. Particle-size analyses of floodplain samples indicated that most of the bed material was fine sand, therefore, the global characteristics were selected for a sand substrate. The global sand bed characteristics included sediment particle size, specific gravity of bed material, bed thickness, sand grain roughness, diffusion coefficients, settling velocity, gravity, shear stress equation (Manning's shear stress equation was used), bed change threshold, and fluid density. Global parameter values were selected based on default/suggested values, empirical relation, and model verification adjustments. Bed factors that could be modified for localized areas included particle size, bed thickness, diffusion coefficients, settling velocity, sand grain roughness, and initial sediment concentration. Minor localized bed changes (thickness, grain size, and eddy diffusion) were used in selected floodplain areas and at the streambed nodes to improve verification and mass balance results. A summary of the primary bed characteristics and values used in the simulations is provided in table 2. A description of all parameters used in the SED2D-WES are in Roig and other (1996) or Letter and others (1998). These values represent those for which the SED2D-WES was most sensitive to modifications within the variable working limits used for this study. For those values not listed in table 2, the default value from SMS (Environmental Modeling Research Laboratory, 1999) or Roig and others (1996) was used in each simulation. Settling velocity was estimated from developed relations between sphere diameter and settling velocity (Interagency Committee, 1957). Effective diffusion values were

Table 2. Selected input parameters used in SED2D-WES simulations

[mm, millimeter; m/s, meter per second; m^2/s, square meter per second; m, meter]

Model variable	Description	Recurrence interval			
		2-year	5-year	10-year	25-year
Particle size	Effective particle size of bed and transported material	0.085 mm floodplain, 0.1 mm streambed	0.085 mm floodplain and streambed	0.085 mm floodplain and streambed	0.085 mm floodplain and streambed
Deplimit	Deposition limit at which time SED2D stops and RMA2 flow field needs to be rerun	25 percent of water depth	25 percent of water depth	25 percent of water depth	25 percent of water depth
Settling velocity	Settling velocity of specified particle size	0.009 m/s	0.009 m/s	0.009 m/s	0.009 m/s
Effective diffusion	Variable incorporating effects of dispersion and turbulent diffusion	100 m^2/s	4 m^2/s	100 m^2/s	100 m^2/s
Bed thickness	Thickness of bed material available for erosion per time step	0.01 m floodplain, 0.07 m streambed	0.01 m floodplain, 0.10 m streambed	0.01 m floodplain, 0.08 m streambed	0.01 m floodplain, 0.10 m streambed

selected from a recommended range provided in Roig and others (1996); the default values for bed threshold, erosion length, deposition length, and water density were used. The bed thickness was determined through the verification process.

Particle-size characteristics were determined from 127 floodplain sediment samples collected and analyzed for particle-size distribution. These samples included 47 flood deposition samples collected from sediment disks and 80 transect samples collected during a June 1997 ground elevation survey. Overall average values for texture classes were 13 percent clay, 42 percent silt, and 45 percent sand. The proportion of deposited material in the sand fraction increased with flood stage at most sediment disk monitoring sites with multiple event samples (fig. 6; see fig. 7 for sediment disk locations). The mean particle size (d_{50}) of deposited material also increased with larger floods based on data from those sites with multiple samples (table 3). Whereas 20 percent of sediment disk samples from the flood with a 3.20 m peak stage (April 8, 1998) had a sample with a d_{50} in the 0.05 mm (millimeter) or greater size class, 78 percent of samples for the flood with a 4.66 m stage (July 9, 1998) had a d_{50} in a size class greater than 0.05 mm.

The limitations of the SED2D-WES necessitate that all suspended sediment in transport or that is deposited be of a single effective particle size, although the specified effective particle size may vary for localized bed areas. Initially, a global particle size was selected in the 0.1 to 0.24 mm size class because material in this particle size class was the largest proportion of the total mass of material deposited in samples from the floodplain. Even though material in this size class made up only 30 to 40 percent of deposited material (by mass), as a result of model limitations it represented 100 percent of transported and deposited material. Therefore, for verification purposes, material of the effective particle size was assumed to be 100 percent of the target measured deposition. The effective particle size value was adjusted during the verification process so that deposition quantities better correlated with those measured on the floodplain, and a global effective particle size of 0.085 mm was later selected for all simulations because this value produced the best verification results. Maintaining the same effective particle size and global SED2D-WES simulation parameters between simulations allowed for the opportunity to focus on the relative differences in deposition and erosion with flood magnitude.

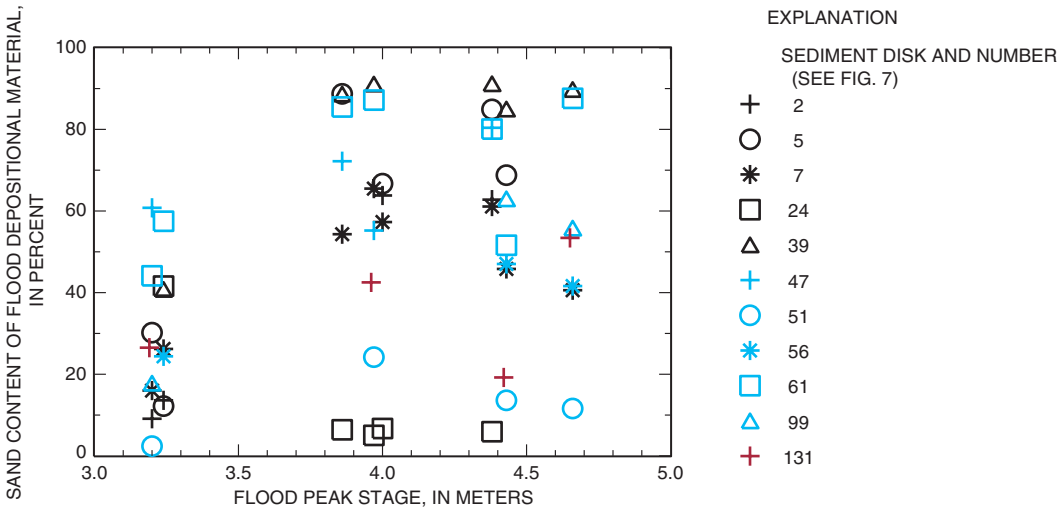

Figure 6. Variability in sand content of depositional material with flood magnitude at selected sediment disk monitoring sites.

Equilibration was made with RMA2-WES and SED2D-WES, and this was used as a starting point for each of the SED2D-WES dynamic hydrograph simulations. Equilibration consisted of obtaining a RMA2-WES steady-state simulation at the starting simulation streamflows and using the initial sediment concentrations of each of the simulated floods. The equilibration run lasted for 4 to 5 time steps to allow for sediment concentrations to travel through the entire reach. In this way sediment concentrations and bed shear stress conditions would be more stable during the initial phases of the SED2D-WES simulation than starting with sediment-free waters.

Development of Simulation Sedigraphs

Input sedigraphs for the 2- and 5-yr recurrence interval floods were developed from measured data collected at the gaging station (fig. 4), whereas sedigraphs for the 10- and 25-yr recurrence interval floods were developed using simple regression and sedigraph characteristics of measured floods. Suspended sediment concentrations were specified for the upstream boundary of the mesh for each time step. The SED2D-WES time steps for each simulation matched those used in the RMA2-WES runs with 0.5, 0.25, 0.33 hr, and 0.33 hr for the 2-, 5-, 10-, and 25-yr floods.

Sediment concentrations were quite variable depending on streamflow hydrograph shape, time since last flood, and seasonal effects, and a combination of methods was used to develop an estimate of sediment transport for the 10- and 25-yr recurrence interval floods. The sedigraphs developed using these methods are intended to represent but one possible estimate of sedigraphs for these flood magnitudes. Streamflow and corresponding sediment concentrations from the rising limb of selected “simple” floods (single peak floods, at least 30 days from the previous flood, and “typical” sedigraph shape) were plotted to develop a simple regression. The streamflow and sediment concentration data from the April 4, 1997, flood were used to extrapolate sediment concentration data for the 10- and 25-yr floods using a simple linear regression (fig. 8)($y = 0.04x + 0.177$, adjusted $r^2 = 0.99$). Peaks for the 10- and 25-yr sedigraphs, developed using this method, were 2,800 and 3,900 mg/L (milligrams per liter). Based on analyses of other Long Branch Creek floods, the “typical” sedigraph peak occurred, on average, 3.5 hrs before the hydrograph peak, and the sediment concentration at the time of the hydrograph peak was, on average, 21 percent that of the sedigraph peak value. The regression was used to calculate sediment concentrations through the sedigraph peak (about 3.5 hrs before the streamflow peak), and a value corresponding to about 21 percent of the sediment peak was plotted at the hydrograph peak and the sedigraph recession was estimated manually. The inflow mass of suspended sediment for the 2- and 5-yr floods were 697,000 and

Figure 7. Location of selected simulation observation sites used in study.

Table 3. Proportion of samples with mean particle size (d_{50}) in selected particle size classes by flood

		Percent of samples with d_{50} in given size class					
		Silt		Sand			
Flood date	Peak stage, in meters	0.002-0.019 millimeter	0.020-0.049 millimeter	0.050-0.09 millimeter	0.10-0.24 millimeter	0.25-0.49 millimeter	Number of samples
July 9, 1998	4.66	0.0	22.2	33.3	44.4	0	18
October 28, 1998	4.43	5.9	47.1	11.8	35.3	0	17
May 30, 1996	4.34	18.2	0	63.6	18.2	0	11
May 22, 1996	3.96	16.7	0	50.0	33.3	0	6
April 22, 1997	3.93	11.1	33.3	5.6	44.4	5.6	18
March 6, 1997	3.87	14.3	0	14.3	71.4	0	7
March 24, 1998	3.26	16.7	58.3	8.3	16.7	0	12
April 8, 1998	3.20	13.3	66.7	20.0	0	0	15

3,260,000 kg (kilograms). The estimated inflow mass from the 10- and 25-yr simulation sedigraphs was 3,590,000 and 6,370,000 kg.

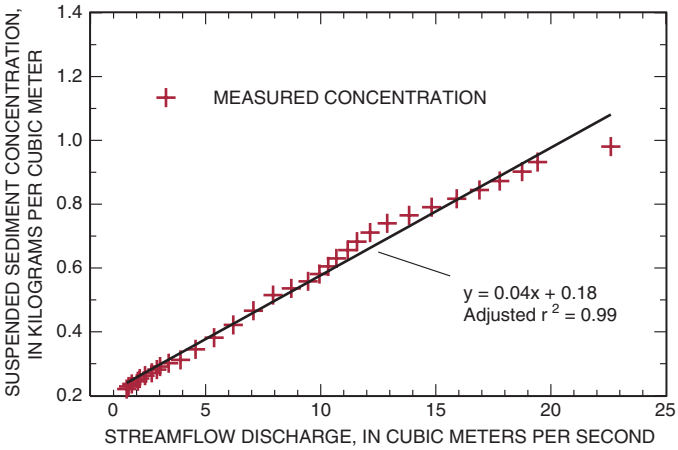

Figure 8. Linear regression used in estimating sediment concentrations for 10- and 25-year interval floods.

SIMULATION OF STREAMFLOW DISTRIBUTION

RMA2-WES Sensitivity Analyses

Sensitivity analyses of the RMA2-WES simulations included modification of input parameters to quantify the relative effects of a specific parameter on the hydrodynamic solution. The results of the sensitivity analyses were used in the verification process to determine which values could be changed to gain the desired effect and what degree of modification was necessary. The user's manual for RMA2-WES lists the relative importance of parameters on the verification of the results. The geometry constitutes 60 percent of the relative importance, boundary conditions—20 percent, roughness—10 percent, viscosity—6 percent, and other factors—4 percent (U.S. Corps of Engineers, 1996). Modifications used in the sensitivity analyses for this study included (1) increasing the floodplain roughness to simulate an increase in understory vegetation or possible effects of woody debris obstructions (Manning's n increased from 0.11 to 0.12); (2) decreasing the stream channel roughness to simulate an increase in stream channel efficiency (Manning's n decreased from 0.05 to 0.04); (3) increasing eddy viscosity from 900 to 1,800 Pa-s to indicate the effects of a decrease in momentum exchange and turbulence; (4) modifying floodplain geometry (decrease elevation 0.2 m at 10 nodes representing 161 m^2 in selected mesh regions; and (5) modifying the channel bed geometry and channel roughness to simulate a debris jam or other in-channel obstructions. Modifications of eddy viscosity and floodplain Manning's n values both represent about a 10 percent difference in the working range of the variables.

Velocities

All modifications resulted in noticeable changes at the stream and floodplain locations, indicating the model is sensitive to all of the factors. The effects of the modifications varied with time and location. The modifications were conducted on the first 10.26 hrs (including the flood peak at hour 9.93) of the 10-yr recurrence interval flood. Results from selected stream and floodplain locations (fig. 9; see fig. 7 for observation point locations) show the temporal effects of these modifications on mean velocities. At stream site 1 the increase in eddy viscosity from 900 to 1,800 Pa-s resulted in the most noticeable change from the original simulation by decreasing stream velocities by 0.1 to 0.2 m/s (15-30 percent) throughout the simulation. Both the decrease in channel roughness and modification of the floodplain geometry also resulted in noticeable differences from the original simulation at floodplain site 1 by increasing velocities by about 0.1 m/s through the first several hours of the simulation. At stream site 2 the increase in eddy viscosity also decreased in-stream velocities. The decreased channel roughness and the upstream floodplain modification resulted in increased in-stream velocities. The simulated debris jam resulted in a decrease in stream velocities at stream site 2, immediately upstream from of the obstruction. The effects of a channel obstruction would be quite variable depending on the location and size of the obstruction.

Geometry modifications and modification of floodplain roughness had the largest effects on floodplain velocities and also on the timing of floodplain inundation. Overall, the velocities at the selected floodplain sites were about one-half that of stream velocities, and the effects of the modifications were proportional, resulting in variations from the original simulation of generally less than 0.05 m/s. The geometry modification and increase in floodplain roughness had the most apparent effect on velocities at floodplain site 1. The lowered nodal elevations at floodplain site 1 resulted in increased velocities (0.02 to 0.03 m/s) relative to the original simulation and also resulted in an earlier inundation time of about 3 hrs. The increased floodplain roughness from 0.11 to 0.12 resulted in smaller floodplain velocities (0.03 to 0.05 m/s) and a delayed inundation time of about 1 hr at floodplain site 1. The decrease in eddy viscosity also resulted in a delayed inundation time of about 1 hr at that site.

Floodplain site 2 was at an elevation control point for flows over this area of the floodplain as determined from the original RMA2-WES simulation. Slight modifications of elevations of nodes in this area or modification of input parameters can result in substantial changes in overbank flows evidenced by the spikes in velocities in several of the simulation results. Velocities at floodplain site 2 were affected most by the increase in floodplain roughness and increased eddy viscosity. Both modifications resulted in decreased velocities of about 0.04 m/s at this site relative to the original simulation. The increase in floodplain roughness and decrease in channel roughness also resulted in a delay of 1 to 2 hrs in the timing of inundation at floodplain site 2.

Water-Surface Elevation/Water Depths

Of the five modifications, the increase in eddy viscosity, followed by the increase in floodplain roughness, caused the most substantial change in peak water-surface elevation and depths, as measured at the upstream CSI (table 4). The decrease in channel roughness, modification of floodplain geometry, and the simulated channel obstruction had no effect on water-surface elevation at the location of the upper CSI.

Model Verification

Verification of the 2- and 5-yr simulations was conducted by comparing the simulated velocities to those measured at the gaging station and on the floodplain, comparing water-surface elevations to measured elevations, comparing simulated area of inundation to that determined from high water marks (HWM), and checking for conservation of mass between upstream and downstream streamflows. The input parameters (floodplain roughness and eddy viscosity) were adjusted, if necessary, to minimize the differences between measured and simulated values.

Velocities

Measured mean and maximum channel velocities were similar to those of the simulation at the same stage conditions for increasing streamflow but differed at the same stage conditions on simulated recessions (table 5). In-stream velocities measured near bankfull stage on May 10, 1996, at the gaging station (on the hydrograph recession) and those from the 2- and 5-yr recurrence interval simulation were examined. Main channel velocity comparisons were restricted to stages in which flows remained within the bank at both the gaging station and focus area because overbank flow

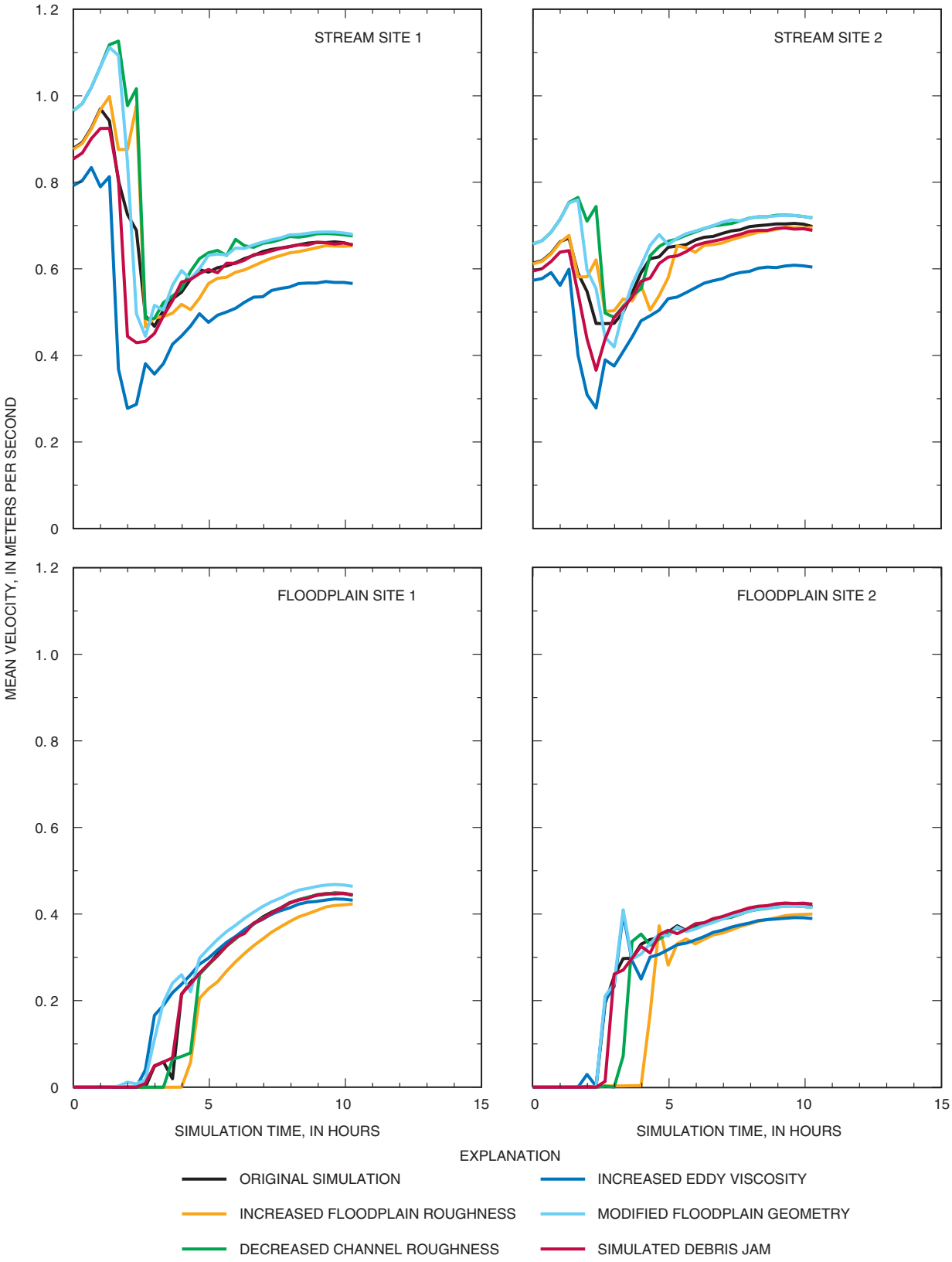

Figure 9. Summary of RMA2-WES sensitivity analyses at selected stream and floodplain locations.

Table 4. Change in peak water-surface elevation at the upstream crest-stage indicator location as a result of parameter modifications during RMA2-WES sensitivity analyses

Modification	Simulated peak water-surface elevation at upstream crest-stage indicator, in meters	Resulting change in peak water-surface elevation at upstream crest-stage indicator, in meters
Increase in eddy viscosity (from 900 to 1,800 Pascal-seconds)	250.34	+ 0.13
Increase in floodplain roughness Manning's n (from 0.11 to 0.12)	250.27	+ 0.06
Decrease in channel roughness Manning's n (from 0.05 to 0.04)	250.21	0
Modification of floodplain geometry (decrease nodal elevation by 0.2 meter) in selected regions	250.21	0
Simulated channel obstruction	250.21	0

Table 5. Comparison of measured and simulated stream channel and floodplain velocities and water depths

	Channel velocity, in meters per second		Floodplain			
			Velocity, in meters per second		Water depth, in meters	
	Measured	Simulated rise/recession	Measured	Simulated	Measured	Simulated
May 10, 1996						
Mean	0.66	0.68/0.34	0.34	0.68	--	--
Maximum	.84	.86/.62	.62	.86	--	--
April 16, 1999						
Maximum	--	--	.33	.33	0.36	0.57
Minimum	--	--	.06	.07	--	--

conditions varied greatly between the constricted flows at the bridge at the gaging station and those in the unrestricted focus area. The mean cross-sectional velocity measured on May 10 at the gaging station was 0.66 m/s with a maximum cross-sectional velocity of 0.84 m/s (table 5). The downstream elevation corresponding to the stage on this date was 247.67 m. Simulated velocity data were determined for 10 main channel regularly spaced "observation" points from simulations at the corresponding stage conditions. The simulated velocity under rising conditions (0.68 m/s) was similar to the measured velocity at the same stage condition (0.66 m/s), but the simulated velocity for the recession was less than measured value at the same stage level (0.34 m/s). Floodwaters were not yet fully confined to the stream channel at a downstream elevation of 247.67

during the recession, whereas flow at the upstream gaging station was restricted to the main channel. This fact could account for lower velocities under the conditions.

Water-Surface Elevations

Measured and simulated water-surface elevations were similar for both the 2- and 5-yr floods at the upstream CSI site. The measured (249.66 m) and simulated (249.70 m) elevation for the 2-yr flood were within 0.04 m and the measured (250.19) and simulated (250.17 m) elevation for the 5-yr flood were within 0.02 m.

Inundated Area

Measured and simulated inundated areas also were similar under comparable flood conditions. A series of HWM were collected by the MDC for a May 9, 1996, flood, and these were used to verify the inundated area depicted in the simulations. The HWM data were located using the Global Positioning System with a 5-m horizontal accuracy. The peak stage for this flood was 4.00 m (elevation 252.40 m) at the gaging station, which corresponded to an elevation of 248.55 m at the downstream CSI site. The inundated area, resulting from measured HWM, and the simulated inundated area from the 5-yr simulation at a time step of 9.75 hrs (corresponding to an elevation 248.53 m at the downstream CSI site) were determined. The inundated area in the focus area was about 60,400 m^2 using the HWM delineation and 57,600 m^2 using the inundated area from the simulation—a difference of about 5 percent.

Overbank flow velocities and depths were measured during an April 16, 1999, flood along a short transect in the focus area and determined from a flood simulation under similar conditions. Velocity and depth measurements were made on the floodplain at a water-surface elevation corresponding to a downstream hydraulic head of 248.02 m. The range of measured velocities (0.06 to 0.33 m/s) and water depths (0.36 m) were similar to those conditions (0.07 to 0.33 m/s, 0.57 m) for the simulated 2-yr recurrence interval flood (elevation 248.05 m) listed in table 5.

Conservation of Mass

The difference between the input streamflow and the simulated outflow streamflow was zero in three of the four simulations and 2 percent in the remaining simulation (fig. 10). Flood-peak attenuation between the upstream maximum peak inflow streamflow and the downstream simulated peak streamflow was less than 3 percent.

Sources of Error

Sources of error in the RMA2-WES simulations include a simplified floodplain and channel model geometry, a simplified assignment of floodplain and channel material properties, the use of input streamflow data from the gaging station upstream from the model reach, the estimation of the downstream stage hydrograph, and the estimation of the 10- and 25-yr flood hydrographs. The sensitivity analyses indicated that all the factors could result in errors that could affect velocity, water depth, and water-surface elevation. Anytime an actual condition is depicted in a mathematical simulation, some simplifications are necessary; however attempts were made to balance the practical period of onsite data collection of floodplain and channel topography with the necessary simulation scale that would allow the study objectives to be fulfilled. Features with relief less than about 0.3 m were likely unaccounted in the original USGS elevation survey and some features were omitted. For example, 12 elevation points could be represented by 4 element nodes. The gaging station is about 2.4 km upstream from the area of the model reach and the computed streamflows from the gaging station data were used at the upstream model boundary without an adjustment for this difference. Assuming the increase in streamflow was proportional to basin size, the change in basin size (10 percent) is within the range of error in streamflow measurements made during flood conditions. The input stage and streamflow hydrographs for the 10- and 25-yr floods were estimated using calculated instantaneous peak streamflows and a dimensionless hydrograph developed for small Missouri streams. Errors associated with using a generalized hydrograph for a specific basin exist, but the use of this hydrograph provides a reproducible method and is intended to represent but one of many possible hydrographs for these floods. The conservation of streamflow mass, the measured and simulated inundation area, and water surface elevations and stream velocities were used to verify the simulation results, and they were used to adjust these results if necessary to minimize the sources of error.

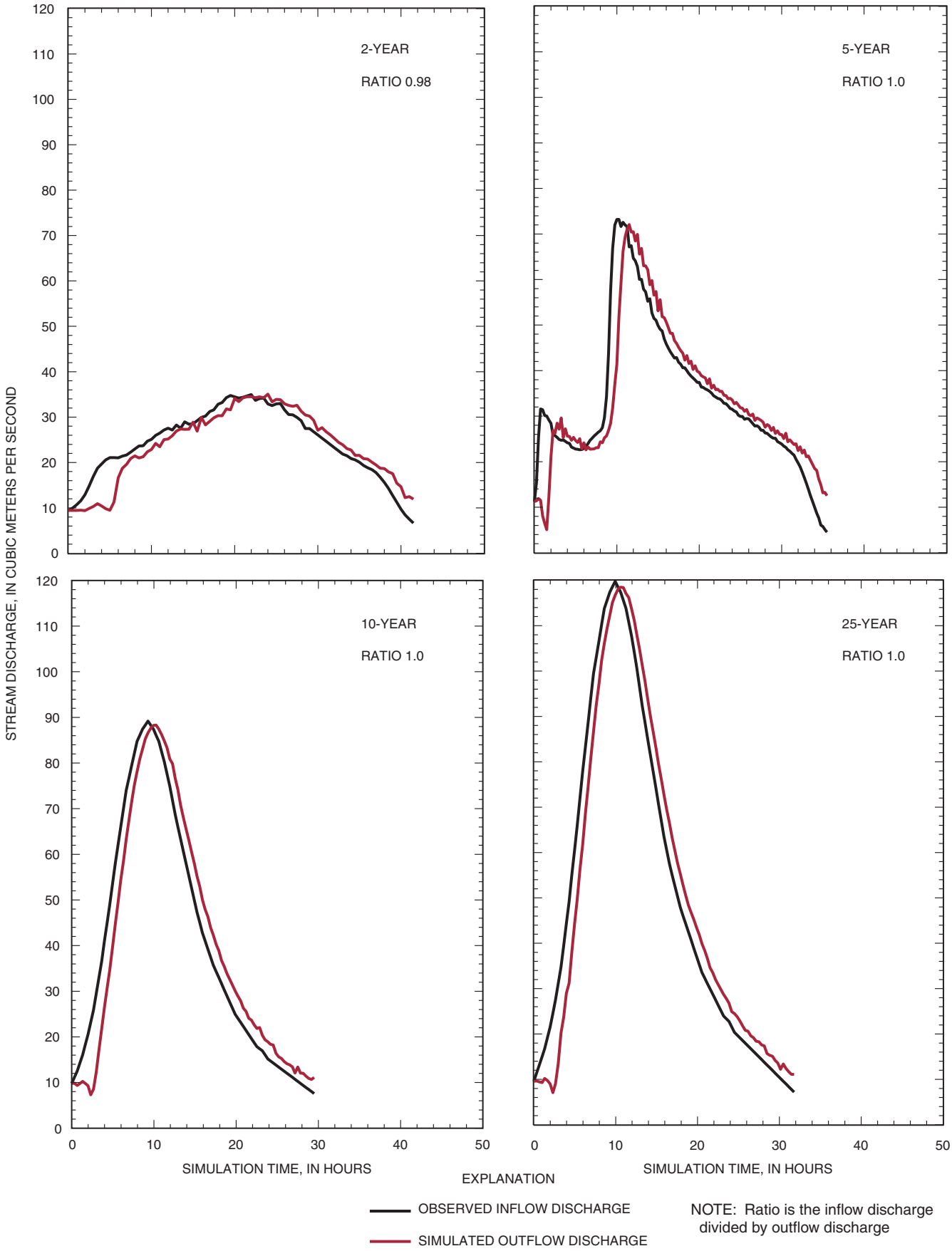

Figure 10. Inflow and simulated outflow streamflow hydrographs for 2-, 5-, 10-, and 25-year recurrence interval floods.

Comparison of 2-, 5-, 10-, and 25-yr Floods

Graphical Comparisons

Velocities

Graphs of the dynamic simulations indicate the temporal variability in main channel velocities when water streamflow inundates the floodplain and also illustrate the importance of secondary/cutoff channels and selected elevation control points in this system. A generalized view of both spatial and temporal velocities for each flood is available from films generated from simulation results for the model reach (films 1–4, on compact disk at the back of this report) or for the focus area (films 5–8). Films 1 through 8 show a decrease in main-channel velocities, particularly in meander bends, when substantial overbank flow occurs from an apparent transfer of momentum of the main channel flows to the floodplain flows as referred to by Sellin (1964) and Knight and Shiono (1996). As flows increase, velocities increase in the straight reaches, but lag in the meander bends. This process is reversed on the recession when flows are again restricted to the main channel, and main channel velocities increase as a result. The films also show the importance of the secondary cutoff channels in this system. The secondary channels are a source of streamflow and sediment to floodplain areas not close to the main channel even before bankfull conditions. The secondary cutoff channels also can account for some of the decrease in main channel velocities as noted previously, because these features carry a substantial part of the streamflow during the floods (films 1–8). This condition is particularly evident for the sinuous main channel area downstream from the focus area in which simulated main channel velocities do not exceed 0.4 m/s at peak conditions even during the 25-yr flood (fig. 11).

Maximum simulated velocities occurred in straight reaches of the main channel and in secondary/cutoff channels, whereas minimum simulated channel velocities occurred downstream from secondary channel/cutoff locations and on floodplain/hillslope boundaries. Velocity conditions during peak stage/streamflow for each of the 2-, 5-, 10-, and 25-yr floods for the entire model reach and the focus area are shown in figures 11 and 12. Velocities larger than 0.4 m/s primarily were restricted to the main channel and the downstream cutoff channel (immediately upstream from the downstream artificial sump) in the 2-yr recurrence interval flood simulation (fig. 11). The highest velocities in all simulations occurred in the straight main-channel reach and bend upstream from the beginning of the focus area. Within the focus area, the highest velocities were in the straight reaches of the main channel (fig. 12). Because of large velocities of the straight reaches, channelization can substantially alter velocity (and sediment transport characteristics) in sinuous reaches such as the one represented in the model reach.

Differences between the velocity distribution during the 2-yr flood and that of the 5-yr flood included an increase in both the floodplain and main-channel velocities during the 5-yr flood as most of the floodplain had velocities greater than 0.2 m/s. At peak conditions during the 10-yr flood, part of the floodplain had velocities exceeding 0.4 m/s with areas less than 0.2 m/s restricted to the tributary arms and floodplain/hillslope boundaries. Velocities in the secondary/cutoff channels also were increased. During the peak-flow conditions of the 25-yr flood, most of the floodplain area had simulated velocities exceeding 0.4 m/s.

Water Depths

The most dramatic change in water depths with flood magnitude occurred between the 2- and 5-yr floods. An overview of the spatial and temporal changes in water depths over the model reach can be viewed in films 9 through 12 and for the focus area in films 13 through 16. Water depths at peak flows in the focus area are shown in figure 13. During the 2-yr flood peak water depths exceeding 2.0 m were restricted to the main channel and tributary channels. The main secondary channel in the focus area had peak water depths of 1 to 1.5 m, but a large part of the floodplain had water depths of less than 0.5 m under peak conditions. Nearly all the inundated area in the 5-yr flood simulation had peak water depths exceeding 0.5 m. Water depths in the secondary channel in the focus area exceeded 1.5 m, and the location of the minor secondary/cutoff channels become more evident. Water depths increased in the 10- and 25-yr simulations. During the 25-yr peak, water depths were greater than 1.0 m over much of the floodplain, and water depths in the deepest areas of the main channel exceeded 4.0 m in depth.

The floodplain secondary/cutoff flow channels are most evident in illustrations showing the 2-, 5-, and 10-yr flood water depths (fig. 13). During the construction of the mesh and subsequent early simulation runs, the importance of selected floodplain control points

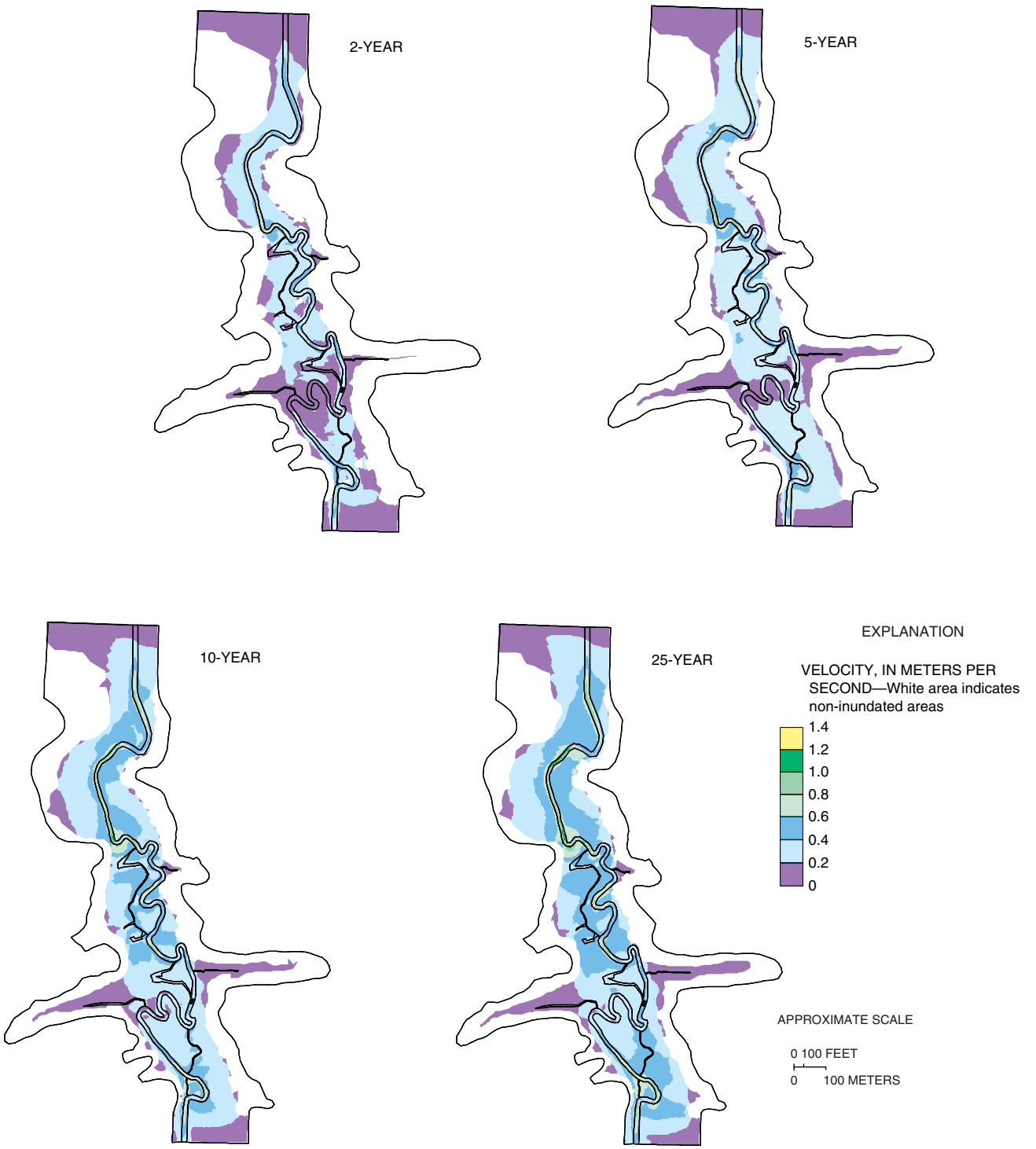

Figure 11. Spatial distribution of velocities in the model reach at peak-flow conditions for 2-, 5-, 10-, and 25-year recurrence interval floods.

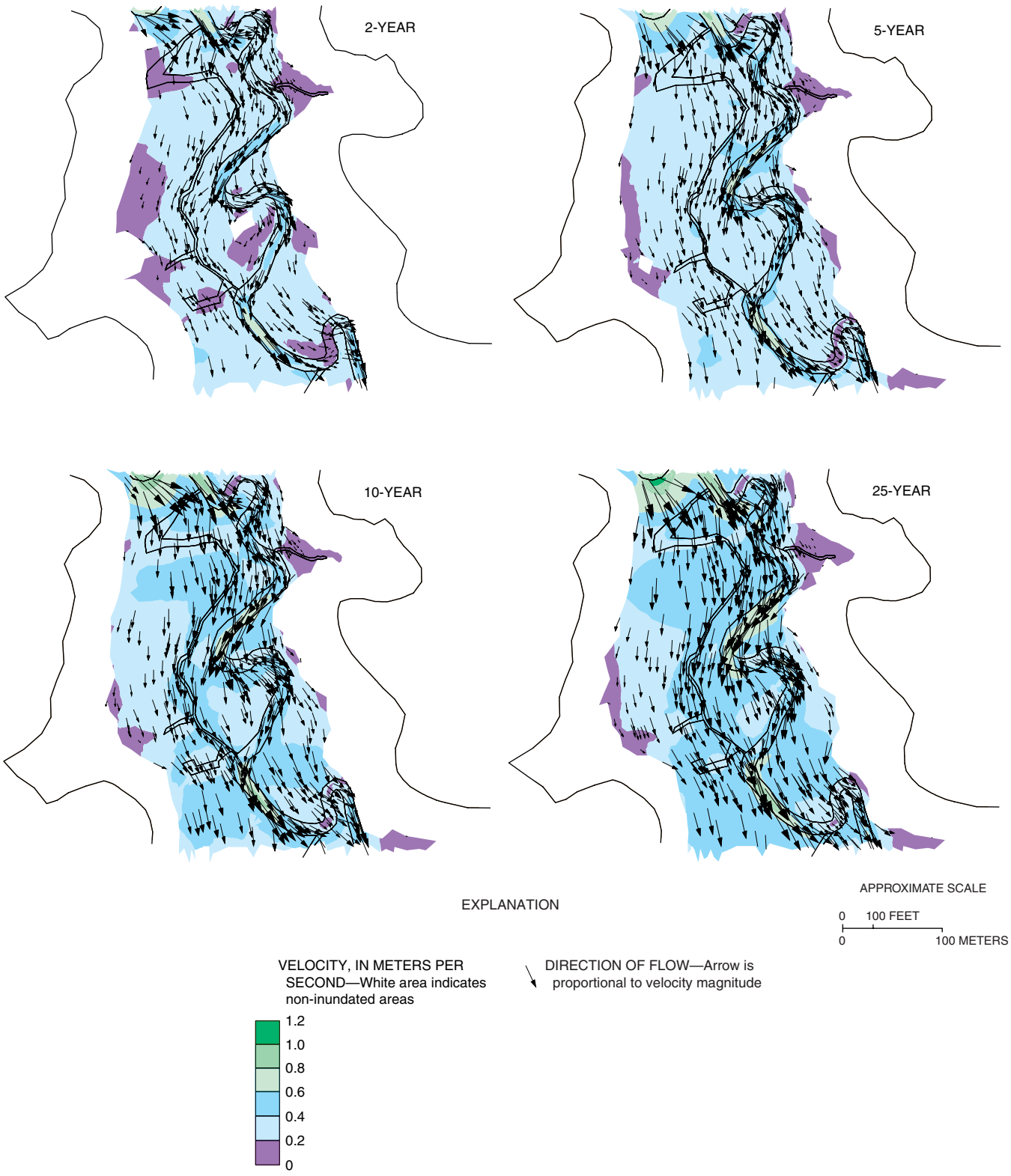

Figure 12. Spatial distribution of velocities in the focus area at peak-flow conditions for 2-, 5-, 10-, and 25-year recurrence interval floods.

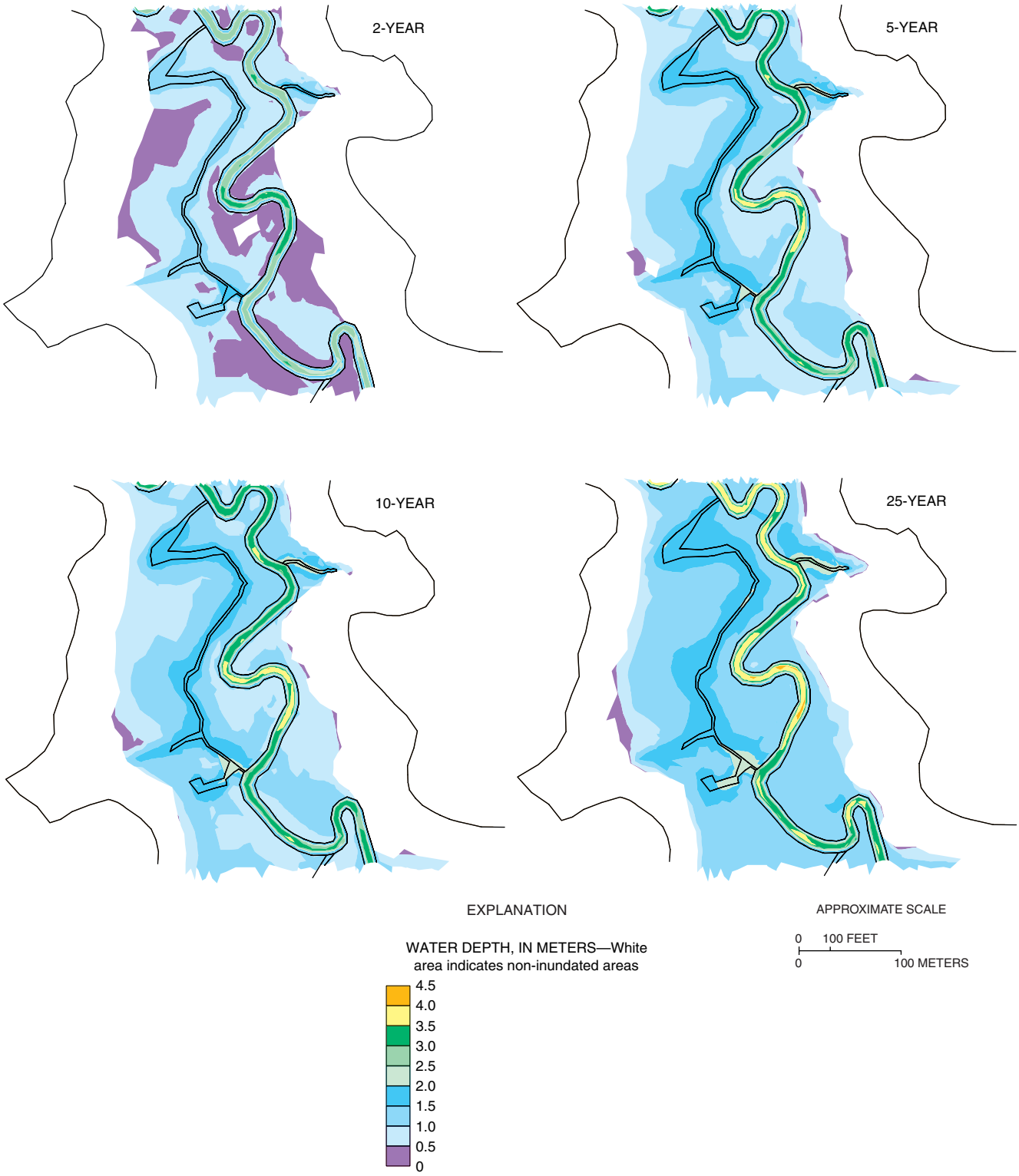

Figure 13. Spatial distribution of water depths in the focus reach at peak-flow conditions for 2-, 5-, 10-, and 25-year recurrence interval floods.

became apparent. The elevations at these selected control points determine, to a great extent, the timing, duration, extent, and direction of overbank flows. These points include the inflow and outflow points of secondary channel and meander cutoffs, natural levee low points/breaks, and low points on microtopographical "ridges" on floodplain areas without secondary cutoff channels (fig. 14).

Water-Surface Elevations

The largest change in water-surface elevations over the model reach occurred between the 2- and 5-yr floods (films 17–20; fig. 15), with an increase of about 0.5 m in water-surface elevation between the two simulations. The increase between the maximum water-surface elevations for the 5- and 25-yr flood simulations, at the upstream CSI location, was only about 0.25 m. The range in water-surface peak elevations was 2.3 m for all four simulations.

Quantitative Comparisons

Data from "observation" points, corresponding to clay pad locations, were used to quantify temporal and spatial differences in simulated velocities and water depths. As would be expected, floodplain velocities and water depths increased with flood magnitude at selected observation points, and large spatial and temporal differences were evident. The observation points corresponded to clay pad locations that were classified into landform types (John Kabrick, Missouri Department of Conservation, oral commun. 1999; Heimann and Roell, 2000), thus providing the opportunity to determine the relation between floodplain flow characteristics and geomorphic features (fig. 16).

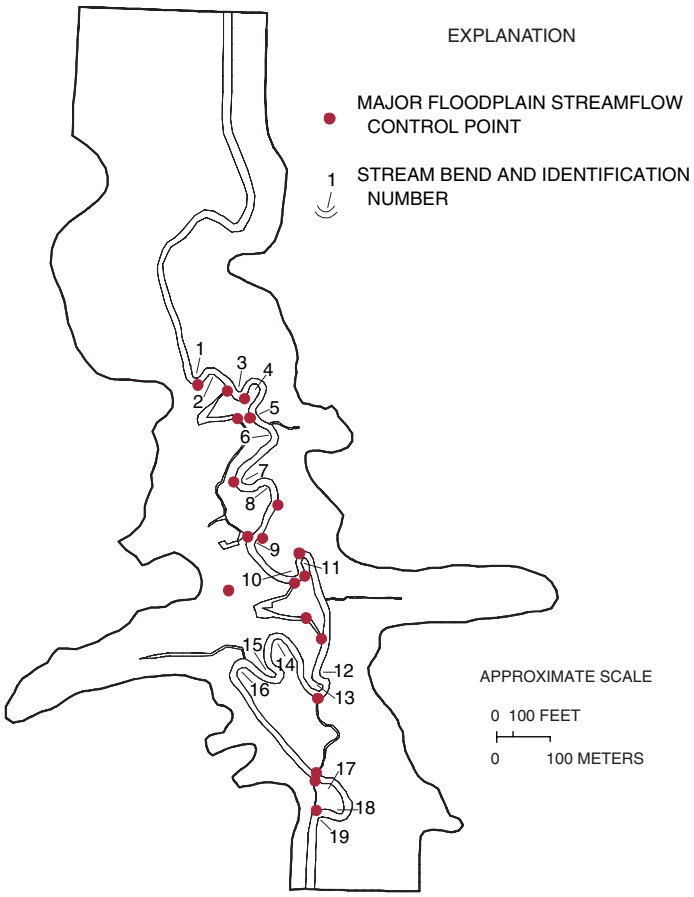

Figure 14. Location of major floodplain streamflow control points and identified stream bend.

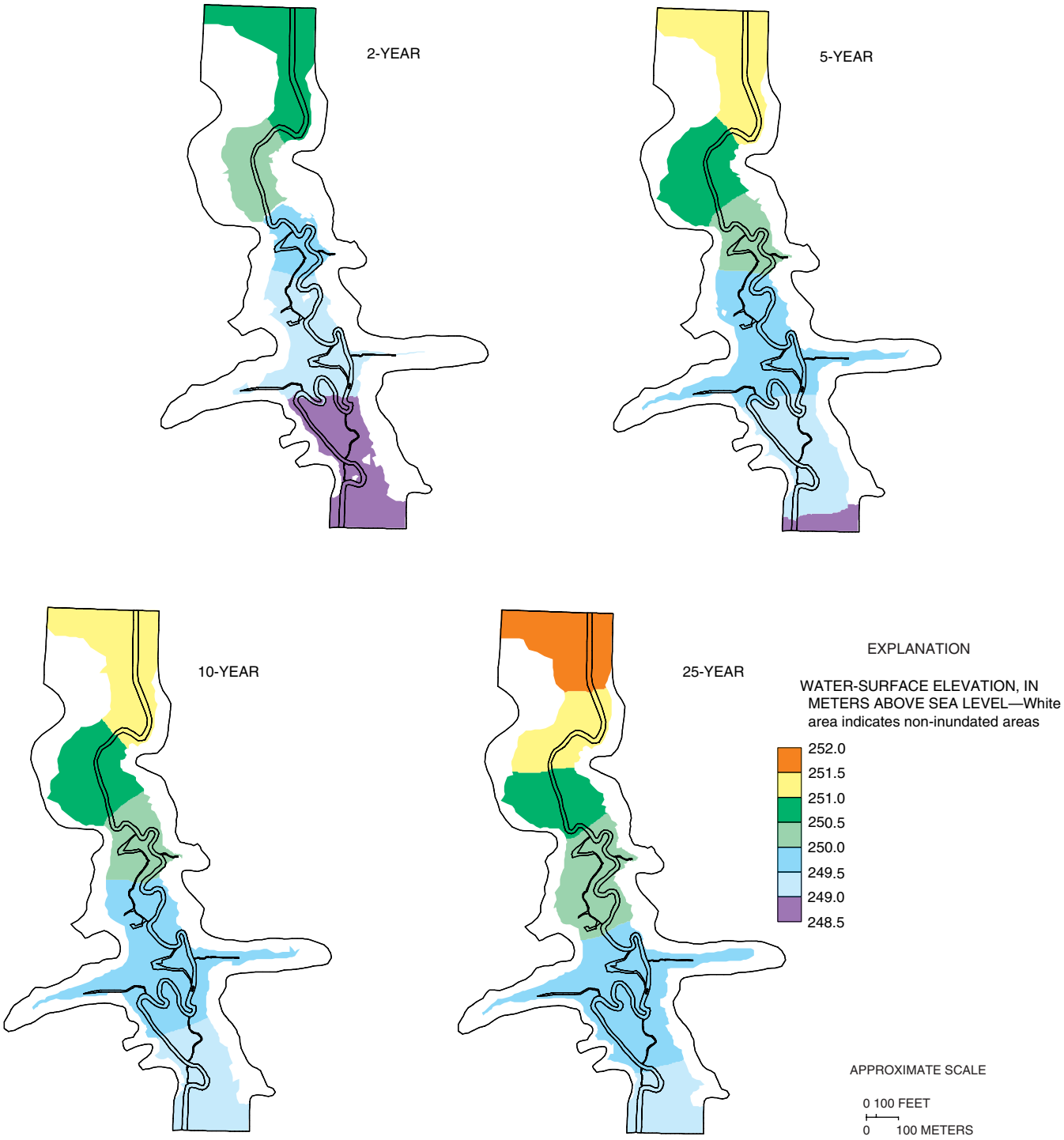

Figure 15. Spatial distribution of water-surface elevations in the model reach at peak-flow conditions for 2-, 5-, 10-, and 25-year recurrence interval floods.

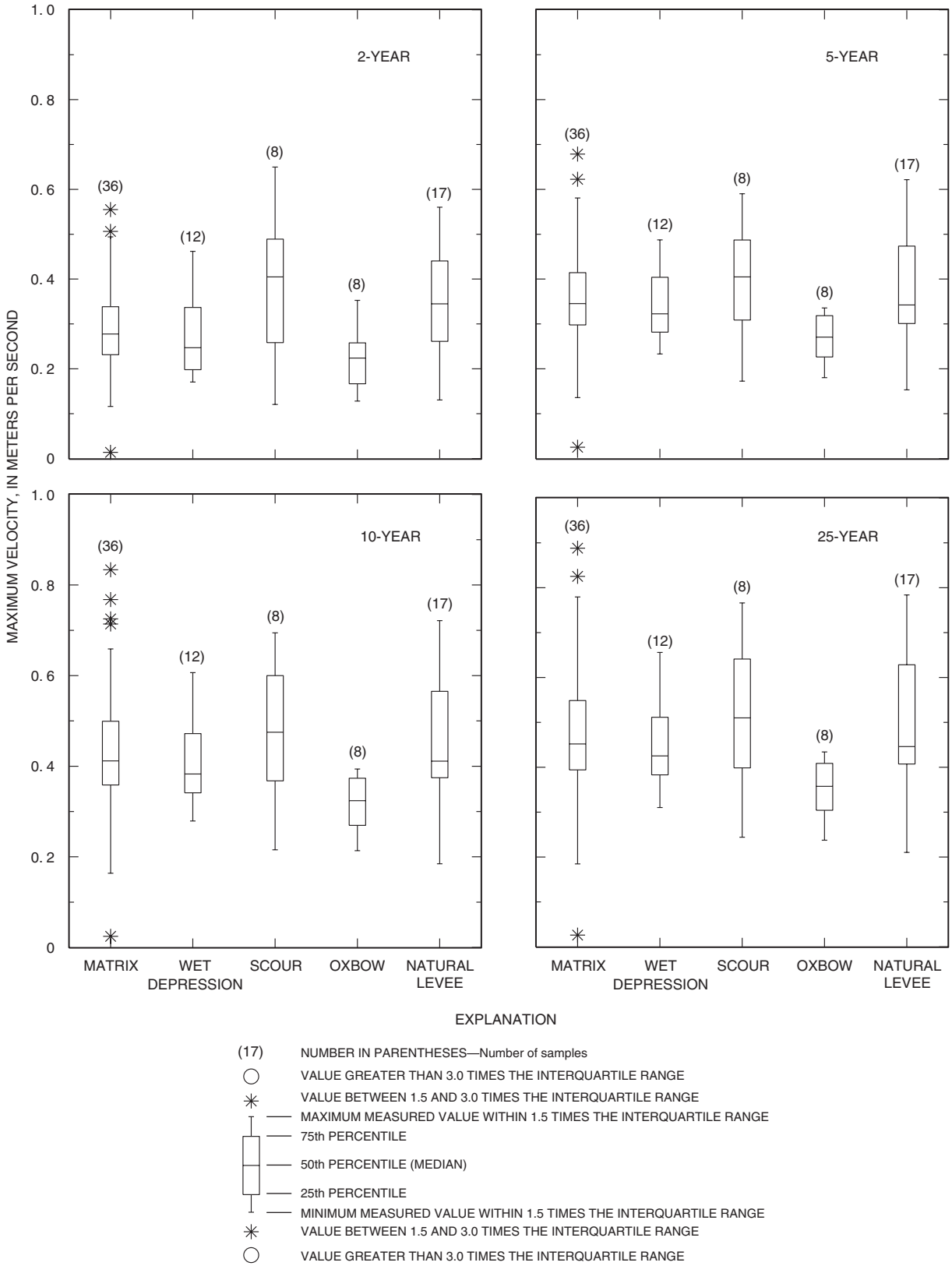

Figure 16. Maximum velocity and water depth distribution, by landform type, for 2-, 5-, 10-, and 25-year recurrence interval floods.

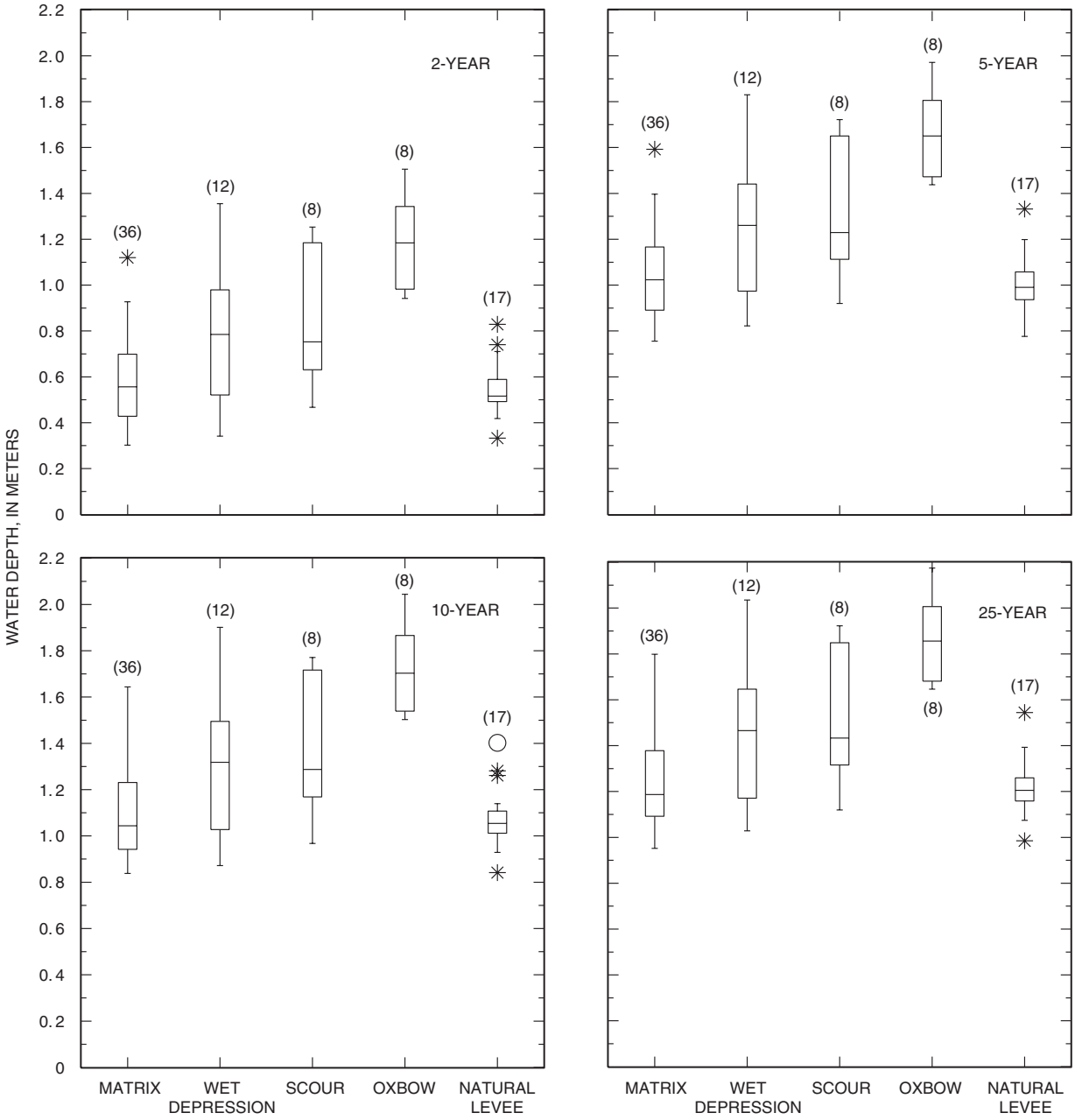

Figure 16. Maximum velocity and water depth distribution, by landform type, for 2-, 5-, 10-, and 25-year recurrence interval floods—Continued.

Median maximum velocities were consistently highest at observation points classified as scours (discontinuous overbank flow channel similar to an ephemeral channel) and lowest at points classified as oxbows (abandoned main channel). The greatest median velocity change over the range of floods occurred in wet depression (isolated, usually oval, depressions) sites (+86 percent) and the lowest change occurred in scours (+24 percent). The greatest variability in the distributions of maximum velocities within landform types occurred in floodplain matrix sites (featureless floodplain area) and the least variability in oxbows.

The temporal variability in velocities were also compared at selected clay pad sites (fig. 7) representing major landform types (fig. 17). The shape of the plots of temporal changes in velocities mirrored that of the respective stage/streamflow hydrographs at the clay pad sites and was similar between sites and landform types. Differences in the temporal changes in velocities between floodplain sites included the magnitude of maximum velocities and the initial and ending simulation velocities at the selected sites.

The distribution of simulated maximum water depths by landform type indicates that median depths were consistently highest in the oxbow sites and lowest at the natural levee (narrow raised feature adjacent to the main channel) and floodplain matrix sites (fig. 16). The change in water depths between the 2- and 5-yr floods was higher than that between the 5- and 10-yr or 10- and 25-yr recurrence floods. The greatest range in median maximum water depths over the range of floods occurred at natural levee sites with a 130 percent increase in depth between the 2- and 25-yr floods. The greatest variability in maximum water depths within a landform type was at wet depression sites and the least variability was at natural levee sites. The temporal changes in water depth at selected clay pad sites representing various landforms reflected that of the stage/streamflow hydrograph (fig. 17). The starting and ending depths, as well as maximum depths, differed between sites—the oxbows and wet depressions had higher depths at the near-bankfull conditions represented at the start and end of the simulation and these sites had greater maximum depths than other landform types.

As would be expected, the inundation area associated with the flood peaks also increased with magnitude (table 6). As with water depths, the greatest change in inundation area occurred between the 2- and 5-yr floods (the 5-yr and larger floods were “valley wall to valley wall”) and the inundated area for the 25-yr flood peak was about 32 percent greater than the 2-yr maximum inundation area.

Velocity and stream bend characteristics, as well as water depth and stream bend characteristics, were determined from observation points located on the inside and outside of 19 meander bends depicted in the model reach (fig. 14) to determine if generalized relations could be discerned. The stream bend characteristics were calculated using a dimensionless ratio of bend radius to channel width to use units that were transferable and comparable with other northern Missouri stream systems. In general, the range in maximum velocities were similar at inside and outside meander bends during the four floods, with overall range of 0.25 and 0.9 m/s (fig. 18). No clear discernible relations could be determined between the inside and outside bend characteristics and the measured velocities and water depths at the 19 meander bends. Further examination indicates that possible relations may exist on a larger scale, as evidenced in the outside bend characteristics and velocities for the 2-yr flood (points 1–9, 10–11, 13–16, and 18–19, fig.19), indicating the controlling factor for velocities in these bends may be at the channel reach scale. The location and carrying capacity of secondary cutoff channels will greatly affect velocities in meander bends with similar radius/channel width characteristics.

In general, the maximum water depths were greater at the outside of meander bends than at the inside of bends for all four floods (fig. 18). The variability in water depths was less than that for velocities for both inside and outside bend points, but the bend radius/channel width ratio explained little of the variability present. In all situations velocities and water depths increased with flood magnitude, although the magnitude of change was not constant between simulation observation points.

The range of velocities for the inside bend points seemed to increase with increasing bend radius/channel width ratio, but this increase was not measured in the outside meander bends. One explanation for this is that the larger the inside meander bend radius the more variable the cutoff flow conditions will be, resulting in a wider range of velocities in smaller radius meanders. The increase in water depths was greatest between the 2- and 5-yr floods than for other larger floods for both inside and outside bend points.

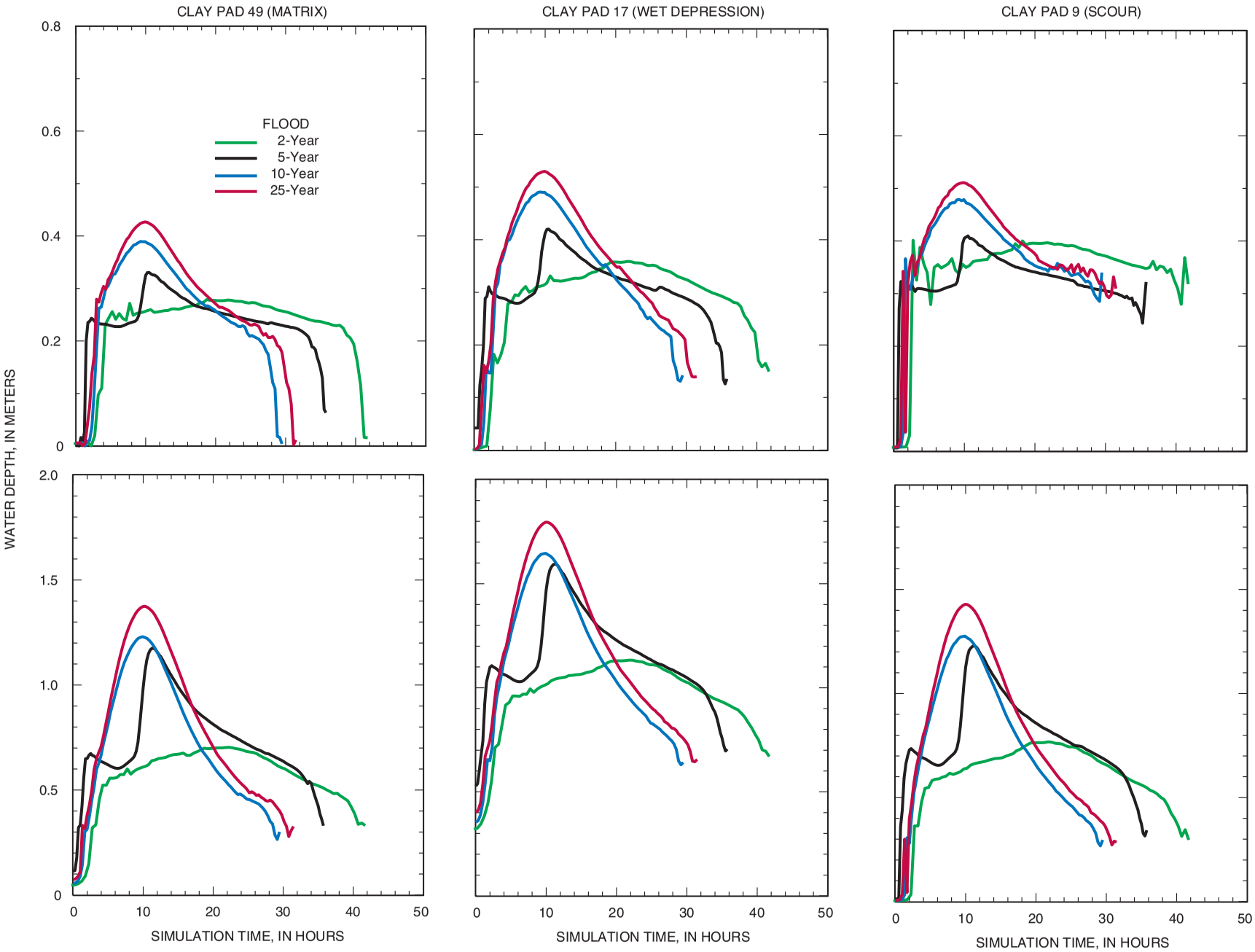

Figure 17. Temporal variablity in velocity and water depth values at selected clay pad observation points for 2-, 5-, 10-, and 25-year recurrence interval floods.

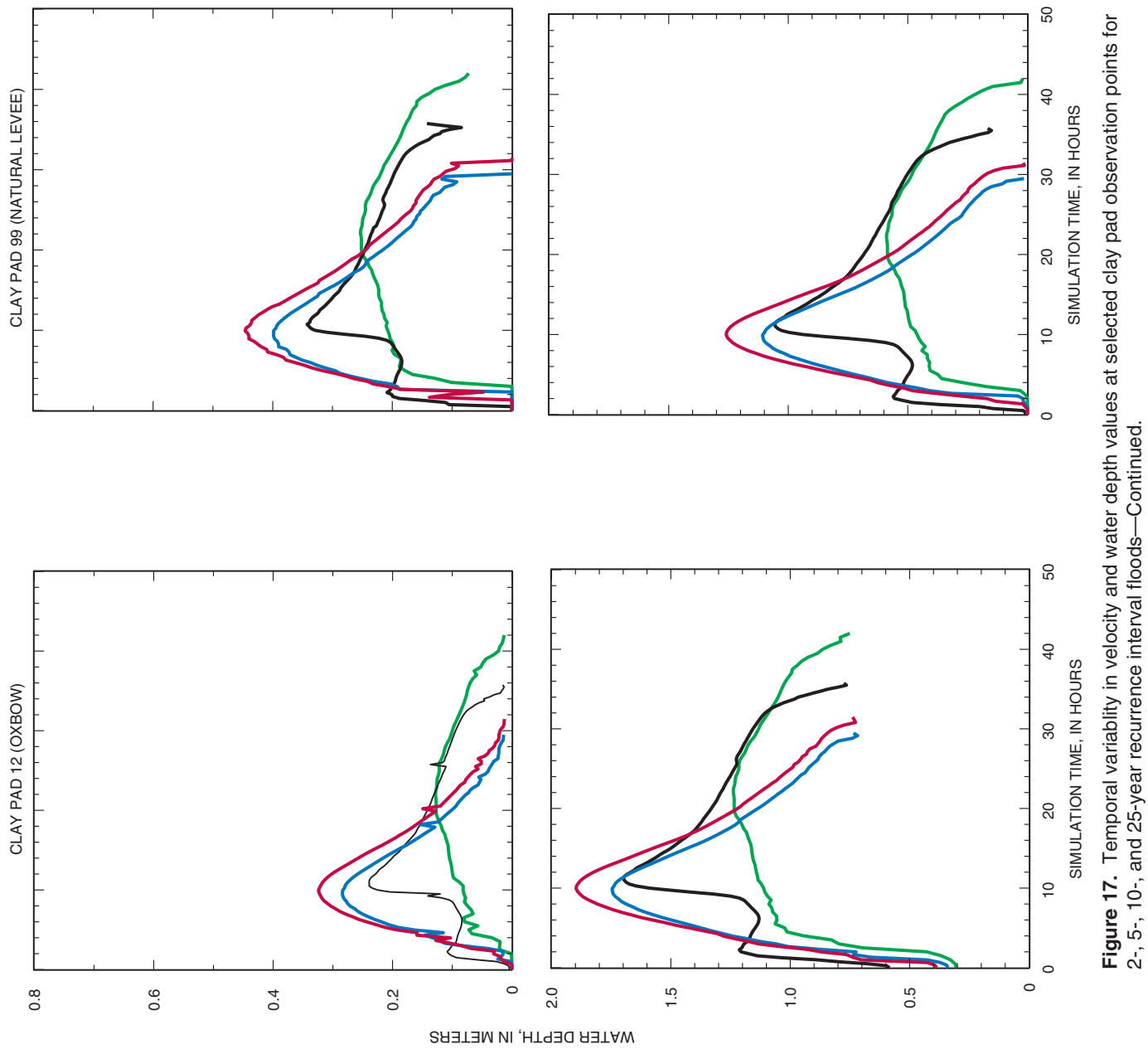

Figure 17. Temporal variablity in velocity and water depth values at selected clay pad observation points for 2-, 5-, 10-, and 25-year recurrence interval floods—Continued.

Table 6. Maximum inundation area for 2-, 5-, 10-, and 25-year recurrence interval flood simulations

Magnitude of flood	Inundation area at flood peak, in square meters	Percent difference from 2-year recurrence flood area
2-year	281,000	0
5-year	348,000	23.8
10-year	350,000	24.6
25-year	370,000	32.0

Simulated Velocities and Coarse Woody Debris

An important natural component of many northern Missouri streams, including Long Branch Creek, is coarse woody debris (CWD—logs, branches, and root wads greater than 10 cm in diameter). The CWD accumulations can affect the velocity distribution and direction of flow in both the main channel and floodplain. The distribution of CWD in a stream system depends on the size (length and diameter) and orientation of source CWD and the size and transport capability of the stream system. The distribution of CWD is more random in headwater streams incapable of transporting delivered material and more clustered in larger systems capable of redistributing CWD. The objective of examining the distribution of CWD in Long Branch Creek is to determine the nature of the distribution (random, regular, or clustered) and how this distribution relates to velocities and occurrence of meander bends in a stream of this size. The CWD data for the model reach were obtained by MDC (Mike Roell, Missouri Department of Conservation, written commun., 2000) during a March 1995 survey. Morisita's Index of Dispersion (Elliot, 1977) was used to determine the nature of the CWD distribution using numbers of pieces of CWD in 25 m length segments (quadrats). The formula of the index is

$$I_\delta = n \frac{\Sigma(x^2) - \Sigma x}{(\Sigma x)^2 - \Sigma x}$$

where n is number of sample quadrats and x is the number of samples in each quadrat.

The index equals 1 for a random distribution, is greater than 1 for a clustered distribution, and is less than 1 for a regular distribution. The calculated Index of Dispersion for the model reach was 1.66, indicating a clustered distribution. The CWD is proportionately greater in meander bends in the model reach than straight reaches as 74 percent of the debris pieces were in meander bends that represent only 62 percent of the stream reach.

A histogram showing simulated velocities from the 5-yr flood (the largest measured flood during the monitoring period) associated with individual CWD pieces is presented in fig. 20 and may explain, in part, the spatial distribution of CWD. The distribution of CWD at any point in time is the cumulative result of floods—particularly the largest recent flood. Velocities were simulated without the inclusion of CWD and provide a generalized view of velocity distributions associated with floods in Long Branch Creek. The peak in the number of CWD pieces corresponded with the 0.3 to 0.39-m/s peak velocity category and more than one-half of the debris pieces were in these channel areas or a lower velocity category area. The peak CWD velocity category may provide an indication of the threshold transport velocity because the number of pieces decreased with an increase in velocity category. The flood conditions of measured debris distribution were unknown and, therefore, the 0.3 to 0.39-m/s velocity values provide only a possible indication of this threshold value. Debris pieces associated with the lower (less than 0.4 m/s) velocities are likely random inputs that are not capable of being moved by smaller floods, and debris pieces associated with larger velocities were observed to be those associated with large debris accumulations spanning the stream channel. No CWD pieces were associated with the 0.9 to 1-m/s peak velocity category areas (fig. 20). The CWD distribution in Long Branch Creek is likely to be determined both by the random nature of the delivery of source material (timber stand characteristics, size, and orientation of delivered material) and also, to some extent, by the redistribution of CWD during floods.

SIMULATION OF SEDIMENT TRANSPORT AND DEPOSITION

SED2D-WES Sensitivity Analyses

Several SED2D-WES input parameters were modified to determine the relative effects of these parameters on net floodplain deposition from a selected simulation covering the model reach. The first 3 hrs (6 time steps) of the 2-yr flood were selected to determine the effects of the modifications. In each case only a single variable was modified at one time, and the net

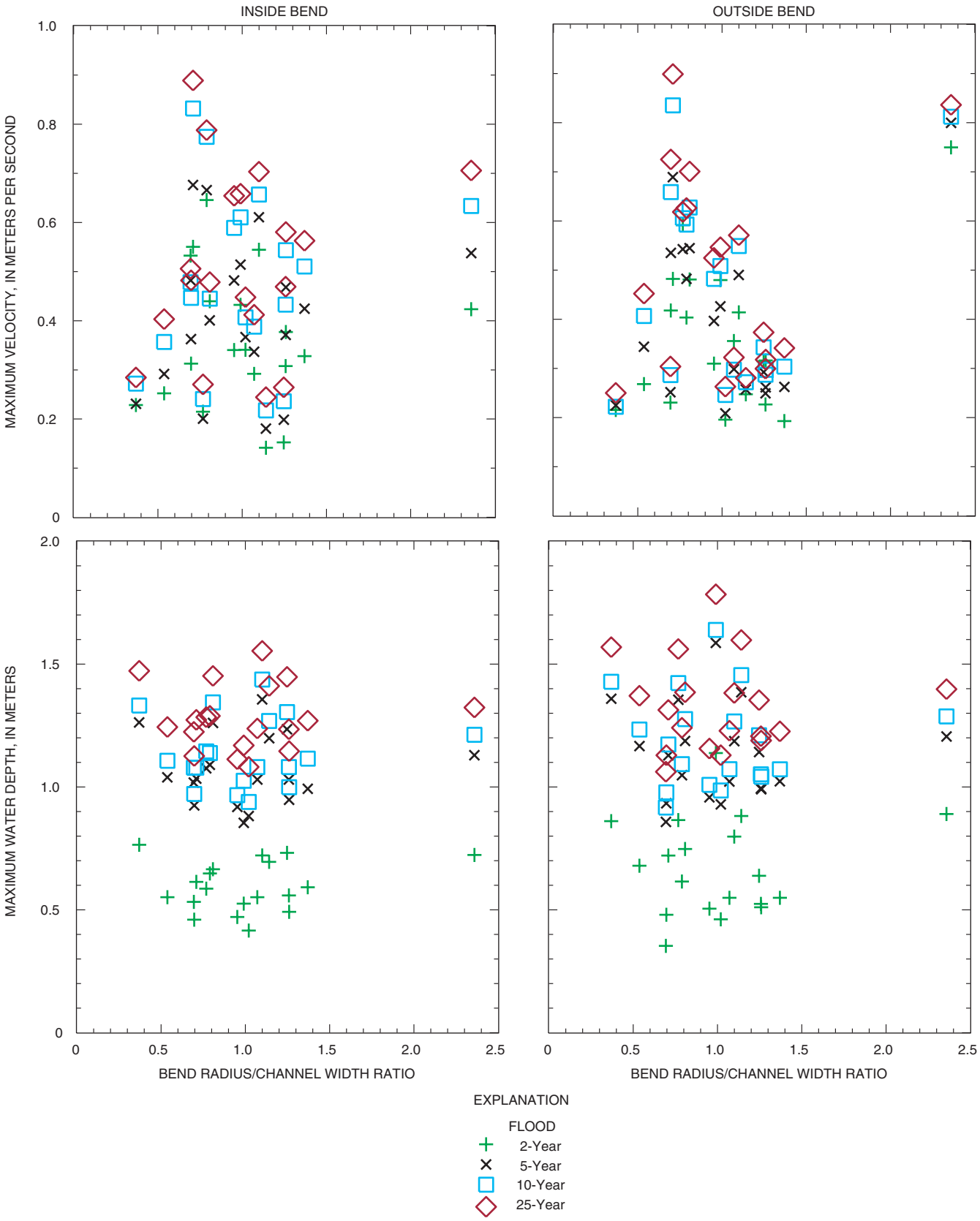

Figure 18. Comparison of simulated maximum velocities and water depths with meander bend characteristics at inside and outside meander bend observation points for 2-, 5-, 10-, and 25-year recurrence interval floods.

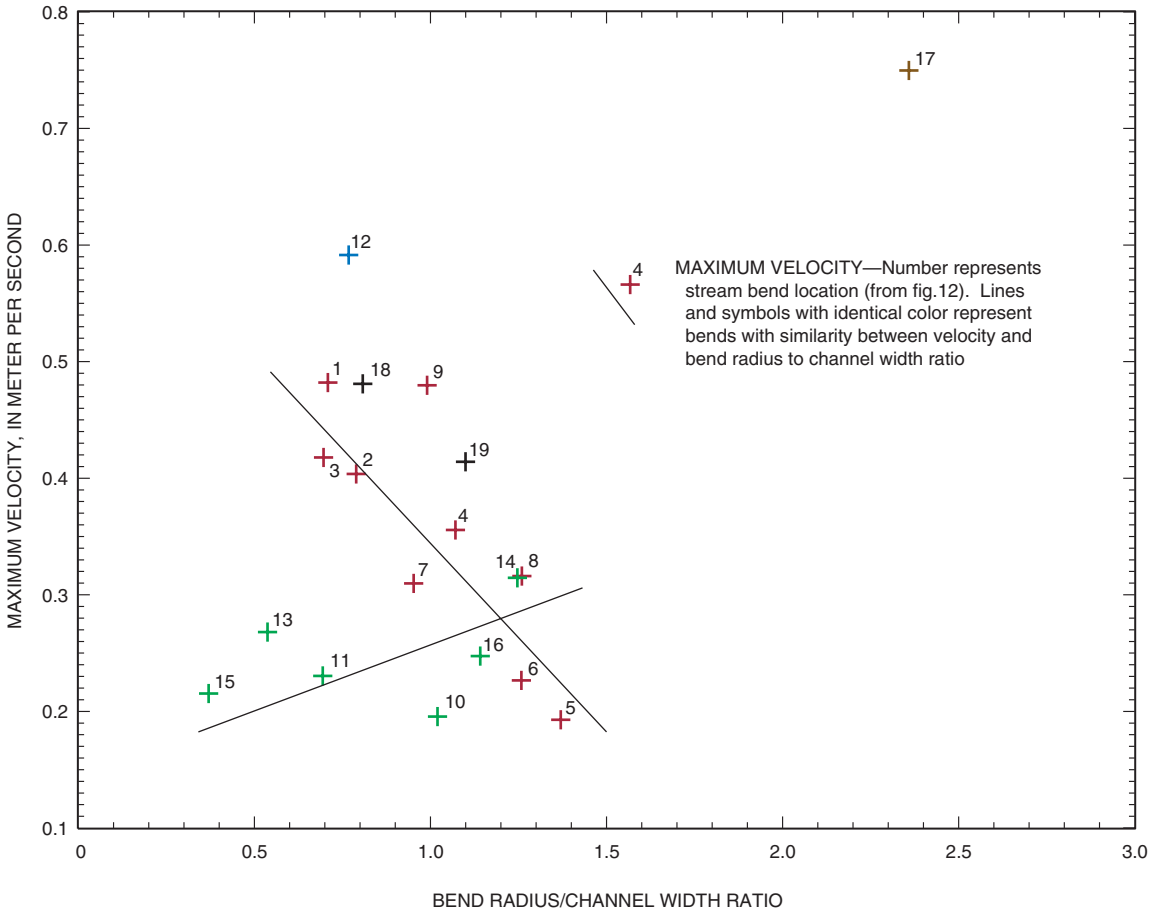

Figure 19. Detailed view of outside meander bend simulated maximum velocities for 2-year recurrence interval flood and bend characteristics (fig. 18) showing possible sub-reach correlations.

effects are summarized in table 7. The model was most sensitive to changes in sediment particle size, but changes in inflow concentrations, bed thickness, and effective diffusion also produced substantial changes in net deposition over the model reach within the applied ranges of these parameters. Modification of fall velocity, grain size for roughness calculations, and erosion length had minimal effects, although lowering of fall velocity to values outside the applied range of sand particles did have substantial effects on deposition.

Of the input parameters, the only one that could be modified as a result of management efforts in the basin is sediment input. Based on this partial simulation, efforts to decrease sediment inflows could substantially decrease sediment deposition in the model reach. A full-length simulation would be required to estimate the net effects of modifications of inflows and other parameters on sediment deposition for the entire flood. The objective of the partial sensitivity analyses was to determine what parameters were most effective in producing changes in sediment deposition before attempting the full-length simulations.

Those factors to which the model was sensitive were more effective in producing a decrease in sedimentation than an increase in sedimentation. The RMA2-WES input flow conditions and mesh geometry were more important in determining sediment deposition than the modification of any input parameters (within applied ranges) in SED2D-WES. Within SED2D-WES the parameter that was most effective in increasing global deposition was an increase in the sediment concentration input. The SED2D-WES input parameters most effective in increasing deposition in localized areas were an increase in particle size and effective diffusion along with a decrease in bed thickness.

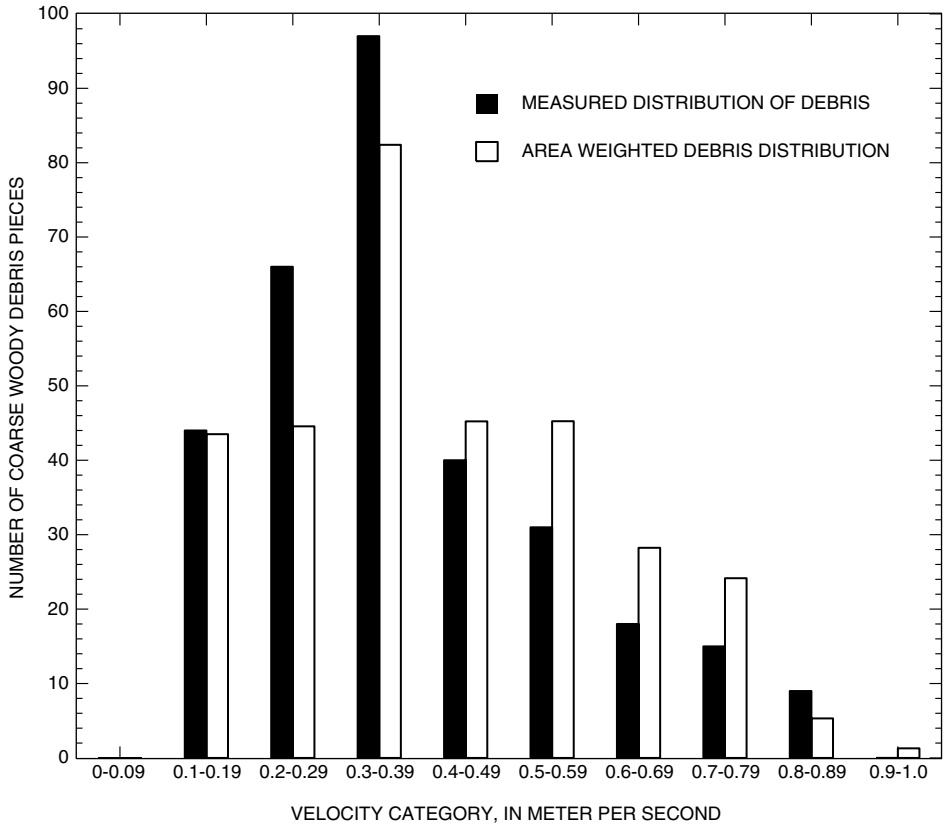

Figure 20. Distribution of measured in-channel coarse woody debris pieces by velocity category for simulated 5-year flood peak flow.

To relate how measured deposition for a particular landform type is related to hydrologic conditions, the measured deposition distribution from selected clay pad sites (and landforms) for the 2- and 5-yr floods were graphed with RMA2-WES simulation results (including velocities, water depths, and inundation period) at the same locations (fig. 21). The ranking of landform sediment deposition distributions for the 2-yr flood and the relative ranking of those landforms for simulated velocities, water depths, and inundation period indicates that deposition distributions were, in general, inversely related to the velocity distribution for that landform and directly related to water depth and inundation period distributions. For example, oxbow sites had the largest mean deposition, the smallest mean velocity, and the largest mean water depths and inundation period whereas scours had the smallest mean deposition, largest velocities, and small mean water depths and inundation period. The relative differences in the distribution of measured sediment deposition with those of simulated hydrologic characteristics for the 5-yr flood provide fewer generalized correlations and, unlike the 2-yr flood, the overall relation seemed to differ by landform type. Natural levees had the largest deposition but relatively small velocities, water depths, and inundation period. The floodplain matrix sites (featureless floodplain landform), as a group, had a small mean deposition, water depths, and inundation period, but large velocities.

The differences between the 2- and 5-yr flood deposition and hydrologic characteristics illustrate the difficulties in attempting to use generalities for describing sediment deposition in Long Branch Creek. These differences in deposition not only indicate the effects of hydrologic differences, but also are likely an indicator of the variability in particle size of material being transported with flood magnitude. For the 2-yr flood, landforms with large deposition had low velocities and large water depths and inundation periods. These hydrologic conditions would likely be associated with the transport and deposition of fine particle size materials. For the 5-yr flood, inconsistencies between the

Table 7. Summary of SED2D-WES sensitivity analyses results

Bed thickness		Particle size		Effective diffusion		Erosion length	
Thickness, in meters	Algebraic sum of floodplain bed change, in cubic meters	Size, in millimeters	Algebraic sum of floodplain bed change, in cubic meters	Value, in square meters	Algebraic sum of floodplain bed change, in cubic meters	Length, in multiples of water depth	Algebraic sum of floodplain bed change, in cubic meters
0.001	18.5	0.0625	40.9	1	12.9	0.1	17.5
.01	18.5	.08	21.2	10	15.8	1	17.5
.03	14.3	.1	17.5	50	17.5	10	17.5
.1	17.0	.2	16.8	100	18.3	50	17.5
1	17.0	.5	16.8	200	18.9	100	17.5

Deposition length		Fall velocity		Roughness		Sediment concentration	
Length, in multiples of water depth	Algebraic sum of floodplain bed change, in cubic meters	Velocity, in meters per second	Algebraic sum of floodplain bed change, in cubic meters	Grain size, in millimeters	Algebraic sum of floodplain bed change, in cubic meters	Percent of measured concentration	Algebraic sum of floodplain bed change, in cubic meters
0.1	17.5	0.0001	6.93	0.01	17.5	50	12.1
.5	17.5	.001	17.5	.1	17.5	100	17.5
1	17.5	.01	17.5	1	17.5	200	28.4
5	17.5	.1	17.5				
10	14.6	1	17.5				
25	10.1						

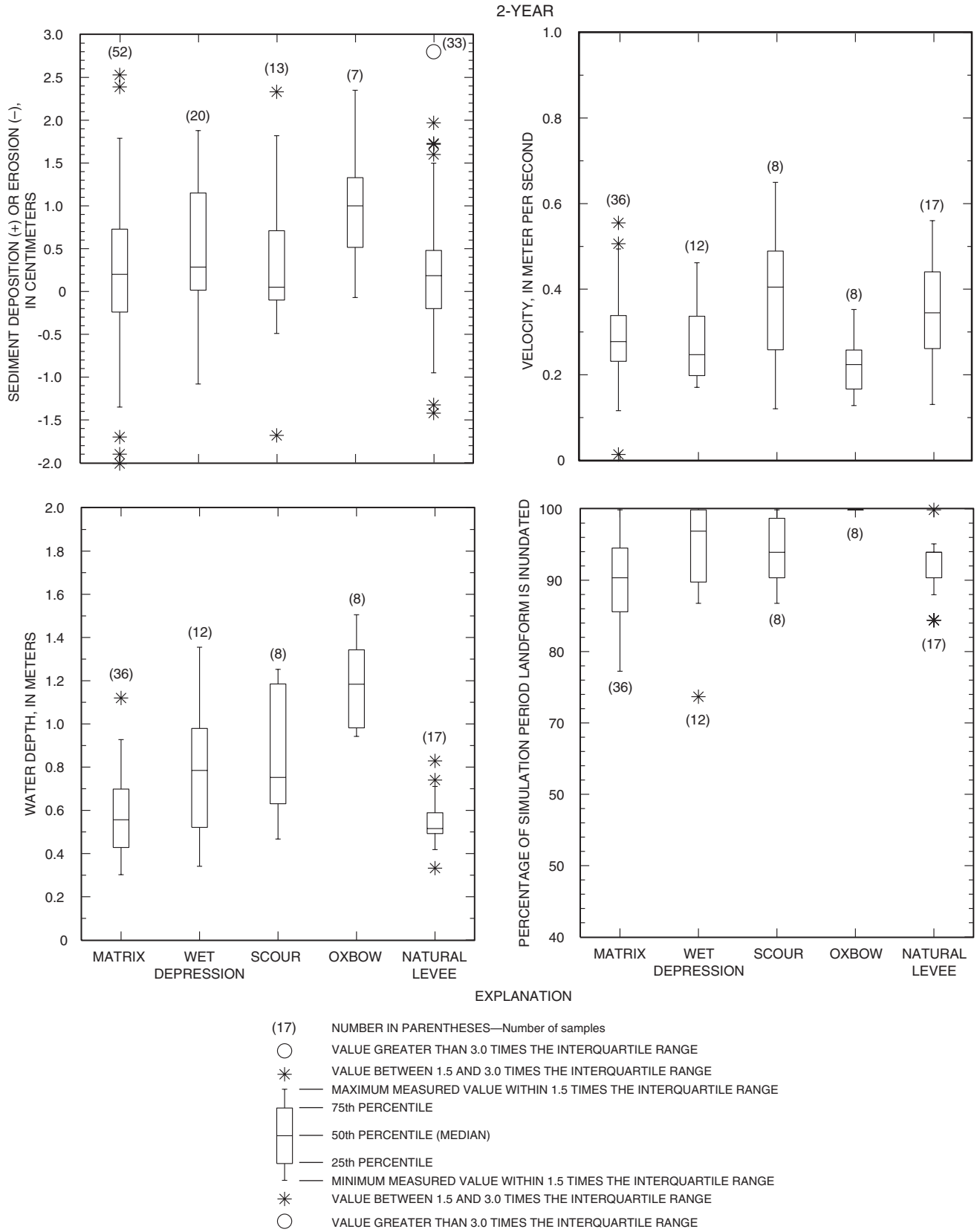

Figure 21. Measured sediment deposition distributions and simulated velocity, water depth, and inundation period distributions for 2- and 5-year recurrence interval floods.

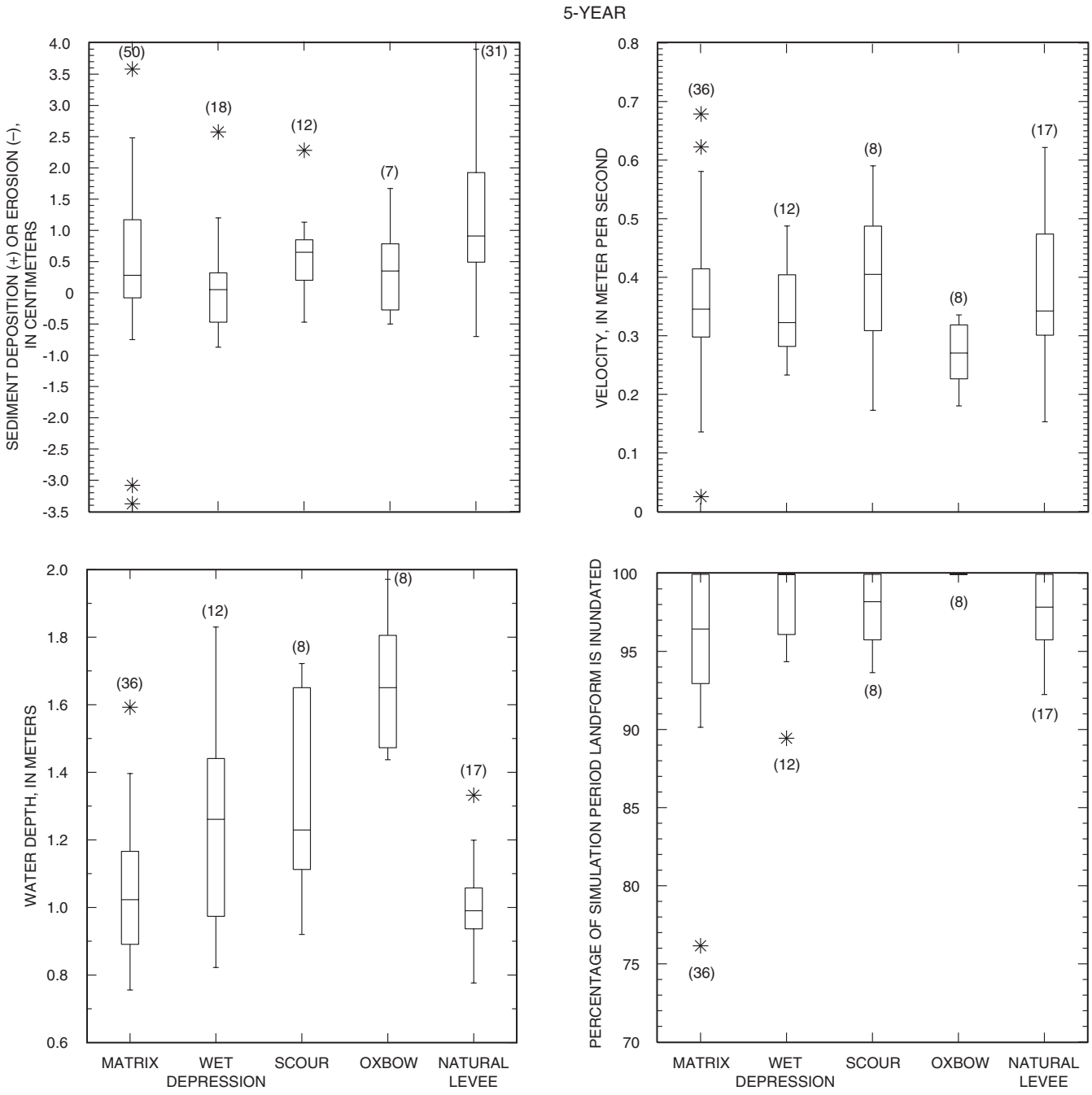

Figure 21. Measured sediment deposition distributions and simulated velocity, water depth, and inundation period distributions for 2- and 5-year recurrence interval floods—Continued.

relation among landform deposition and associated hydrologic conditions were noted. The largest deposition amounts were associated with the largest floodplain velocities, shallowest depths, and shortest inundation period—hydrologic factors likely associated with the transport and deposition of a coarse particle size material from the channel. Despite the evidence of depositional differences between landform types, measured deposition amounts were not statistically significantly different by landform type following the 5-yr flood (Heimann and Roell, 2000).

Model Verification

The SED2D-WES simulation results were similar to measured sediment deposition values for both the 2- and 5-yr floods, but the simulation did tend to overestimate deposition in oxbows and tributaries and underestimate near-channel natural levee and matrix deposition for the 5-yr flood (fig. 22). Initial verification attempts were conducted using global SED2D-WES parameters to determine if simulated deposition values were similar to measured deposition on clay pads and also to determine if sediment mass was con-

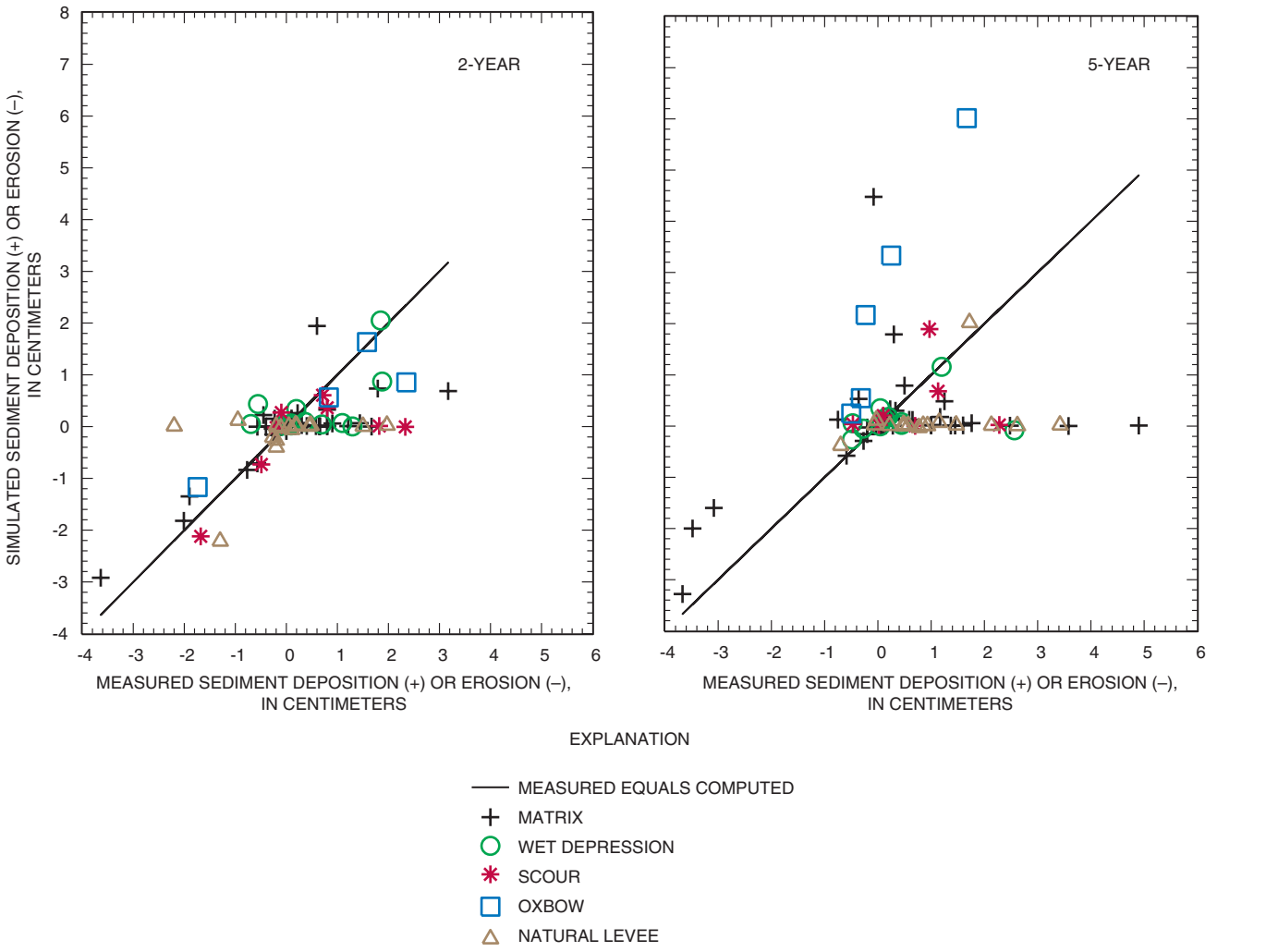

Figure 22. Measured and simulated sediment deposition at selected observation points (classified by landform type) for the 2- and 5-year recurrence interval floods.

served. After these conditions (similar simulated and measured results; mass conserved) were met, local settings were used or adjusted at selected node and element locations to "fine tune" simulated deposition. The addition of localized adjustments in three of the four flood simulations resulted in a less than 1 percent change in overall floodplain deposition in each case. Therefore, this process could be considered to represent a redistribution of existing floodplain sediment.

Measured deposition data collected from 82 clay pads within the model reach were used to verify deposition in floodplain mesh elements that averaged 22 m^2; therefore, some differences could be expected. An objective of the design of the mesh was to be able to predict deposition characteristics at a landform scale or floodplain scale. The ability to predict sediment deposition on the scale of the 0.25-m^2 clay pads was calculated using the root mean square (RMS) error between the measured flood and simulated sediment deposition at the clay pad sites. The equation used to calculate the RMS error was:

$$RMS = \sqrt{\frac{e_1^2 + e_2^2 + e_3^2 + \ldots\ldots e_n^2}{n}}$$

where e is the difference between measured event sediment deposition and the simulated sediment deposition, and n is the number of observation points.

The RMS error for the 2-yr flood simulation was 0.87 cm and the RMS error for the 5-yr flood simulation was 1.54 cm. These RMS errors were greater than the 0.30-cm mean standard deviation associated with the variability in the measurement of flood sediment deposition on all clay pads, but were less than the 3.5-cm maximum standard deviation associated with the variability in sediment deposition at an individual clay pad. Those sites for which the 5-yr simulation overestimated the measured values were in oxbows and tributary areas, but these areas represent less than 2 percent of the peak inundated floodplain in the mesh. Simulated (RMA2-WES) velocities in these areas apparently were not large enough to erode materials despite modifications of local particle size and bed thickness values.

The simulations lacked "robustness" in predicting deposition at several points, particularly for the 5-yr flood, as evidenced by the line of simulated deposition points near zero (fig. 22). As discussed in the "sensitivity analysis" section, the simulations were insensitive to attempts to increase deposition by modification of localized parameters. The lack of robustness can be explained, in part, by the underestimation of deposition in the natural levee and near-channel floodplain matrix areas. These areas represent only about 3 percent of the peak 5-yr inundated area in the mesh. Many of the greatest discrepancies between measured and simulated deposition occurred in near-channel locations in which sand splays were responsible for the localized deposition. About 65 percent of the clay pad verification points, in which simulated deposition underestimated measured deposition by more than 0.5 cm, were located within 5 m of the main channel and 92 percent of the underestimated sites were within 10 m of the channel. Measured floodplain deposition from the clay pad monitoring network indicated that the natural levee areas had the largest median deposition in the 5-yr flood (fig. 21).

The inability of SED2D-WES to replicate these near-channel deposition conditions is likely an effect of the simplified single-particle size transport feature of SED2D-WES, because deposition in these natural levee areas would be of a characteristically coarser particle size than the effective particle size used in the simulations. Another limitation of SED2D-WES that could affect near-channel deposition is the lack of a lateral gradient in suspended sediment concentrations across the floodplain (fig. 23). Longitudinal suspended sediment gradients were more apparent than lateral gradients under the governing equations used in the SED2D-WES model. Discrepancies between the measured and simulated values in the oxbow and near-channel areas were within the maximum variability associated with the measurement of sediment deposition at an individual clay pad, and discrepancies occurred in areas that represent only about 5 percent of the total inundated area during the 5-yr flood.

For one-half of the 82 clay pad verification points in the model reach, either no localized modifications were necessary or similar local modifications were needed to optimize both the 2- and 5-yr floods. For the other points, the local modifications necessary to match the measured and simulated depositions for the 5-yr flood were the opposite of those needed to match the 2-yr flood, or modifications were needed for one flood and not the other. Those modifications that were consistent for both the 2- and 5-yr floods were used in creating a parameter set that was applied to the 10- and 25-yr floods.

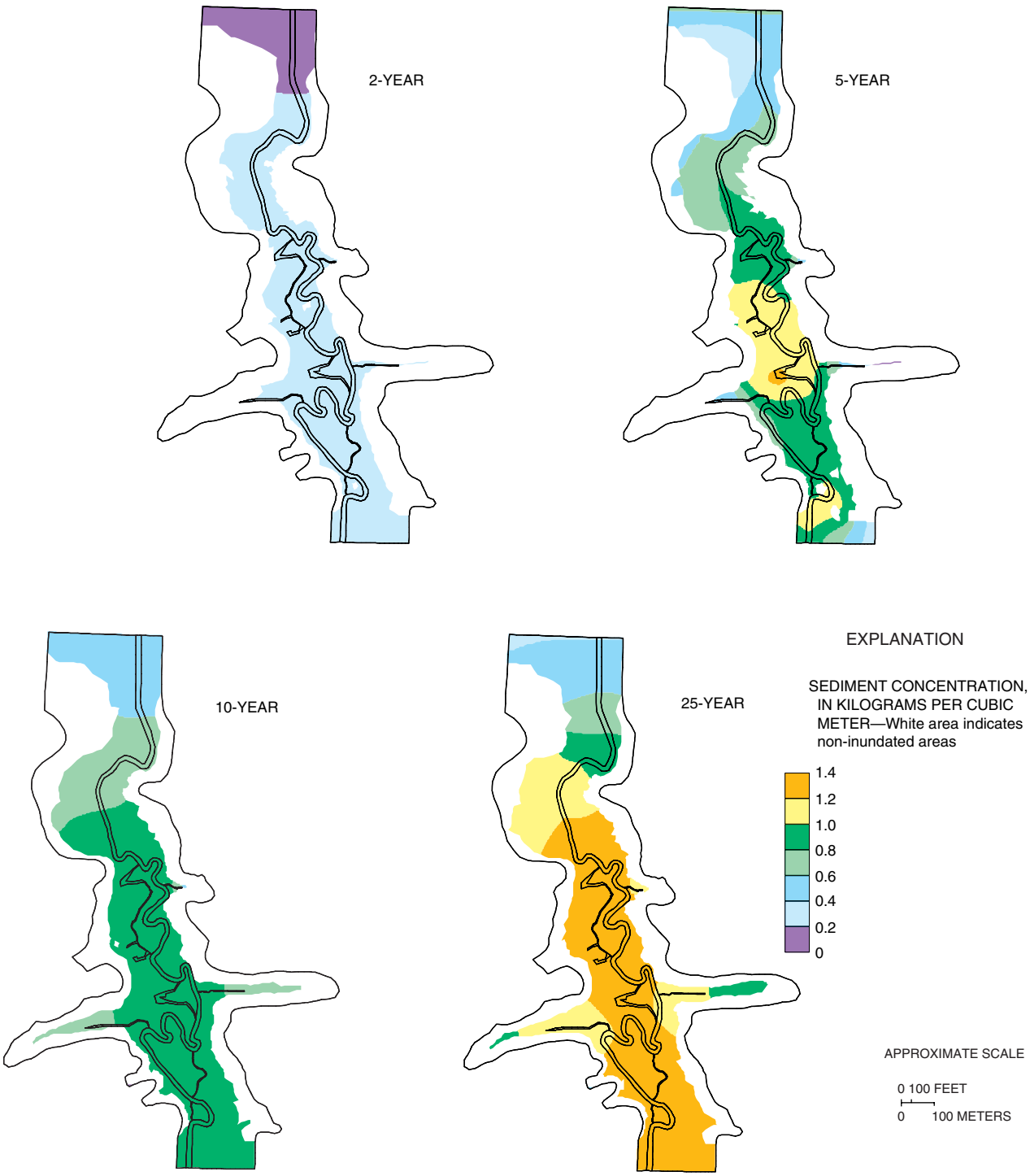

Figure 23. Spatial distribution of suspended sediment concentrations in the model reach at peak-flow conditions during 2-, 5-, 10-, and 25-year recurrence interval floods.

Sources of Error

Simulations have inherent errors associated with the simplification of actual conditions. This situation is compounded because SED2D-WES relies on results of the RMA2-WES as input. Sources of error, therefore, include those associated and discussed with the RMA2-WES model (for example, simplified geometry, use of upstream gaging station data, and simplified material properties) and those associated with the simplification of the sediment transport and deposition process. Errors that could arise as a result of the simplification of the sediment transport and deposition process in SED2D-WES include the constraint of using a single particle size for transport and deposition, sediment mass balance errors, an error in SED2D-WES to update the wetted boundary, necessity of adding an artificial sump in the mesh, use of upstream suspended sediment data for 2- and 5-yr flood model input, and the estimation of the 10- and 25-yr sedigraphs. All of the discussed sources of error could contribute to differences between measured and simulated sediment deposition values.

Use of a single size category of material for transport and deposition is a gross simplification of the sediment transport and deposition process. The effects of using a single effective particle size on the suspended sediment transport and deposition processes are unclear. The verification process becomes complicated as a result of this simplification because the actual deposition amounts can be attributed to multiple size categories of material rather than a single size category. The total measured input concentrations and the total measured deposition amounts were used as targets for verification purposes because little basis existed for the magnitude of any modifications necessary to account for the simplification.

A comparison of sources of sediment mass (suspended sediment inflow and streambed net erosion) to mass losses/sinks (floodplain deposition and suspended-sediment outflow) for initial simulations had differences of as much as 60 percent. In only one of four simulations (25-yr flood) was the ratio of sediment inputs and losses, in the initial simulation attempt, within 5 percent. Changes, primarily in streambed thickness and particle size characteristics, possibly could increase or decrease sources and sinks of material and better balance mass conservation in the simulations. An iterative process by which parameters were selected to best attain measured sediment thicknesses was used and the sediment thickness was then adjusted to try to attain conservation of mass. In some cases (particularly the 5-yr flood) the results of this iterative process came at the expense of the optimum floodplain sediment depths for the verification process. Adjustments were made to the input parameters so that inputs and losses in all simulations were within 5 percent while attempting to maintain desired deposition amounts.

An error was detected in the SED2D-WES version 3.2 code after the completion of the simulations and during the generation of the SED2D-WES simulation result films. The error indicated the wetted boundary of the transient RMA2-WES solution was not updated properly in SED2D-WES. The RMA2-WES wetted boundary was updated only for the initial time step of a transient SED2D-WES simulation, whereas the velocity and depth flow fields were updated for each time step. The error was reported, but no correction was available before completion of this analysis. The effects of this error would be greatest if the simulation was completed in a single run from start to finish because the wetted boundary would only be updated once. The bed threshold limit (maximum change in bed thickness before the RMA-2 solution is deemed unusable) required that the SED2D-WES and, therefore, RMA2-WES simulations in this study be completed in multiple separate runs (between 29 and 44 separate runs were made for each of the four SED2D-WES simulations and then combined for a final solution using a utility program SEDUTIL.EXE, on compact disk at the back of this report). In this way, the wetted boundary layer was updated 29 times in the 2-yr simulation and as many as 44 times during the 25-yr simulation, or about every 2 to 4 time steps, thereby limiting, to some degree the effects of this error. To completely eliminate the error, a separate RMA2-WES and SED2D-WES solution would have to be created for each of the 82 to 144 time steps in the SED2D-WES runs. The quantitative error in the final SED2D-WES simulation associated with this error is unknown, but was thought to be no greater than any other source of error associated with the simulation.

The artificial sumps added to the upstream and downstream ends of the mesh (fig. 3) to keep the boundary conditions from drying also served to trap sediment during the simulations. The effect was to trap inflow sediments thereby greatly overestimating floodplain deposition in these areas, which resulted in greater erosion from the streambed to compensate for the inflow transport losses. The artificial sumps

accounted for 61 to 71 percent of total deposits on the floodplain in the four simulations. By using the utility program SEDUTIL.EXE those elements not affected by the artificial sumps were selected and those values were used for the flood summary information. The SED2D-WES summary output file lists the net algebraic and absolute bed change volumes for each time step, and the SEDUTIL.EXE utility program was developed to determine the net bed change volume for each time step by material type (specified in the construction of the model mesh and corresponding to the floodplain, oxbow plus secondary channel, and the main channel) or list of selected elements (those floodplain elements not affected by artificial sumps). The net bed change volume was converted to a mass using the bulk density of 1,590 kg/m^3 (kilograms per cubic meter) that was used in SED2D-WES.

Similar to RMA2-WES simulation, the assumption was made for SED2D-WES that the suspended sediment concentrations at the upstream gaging station were similar to those at the upstream boundary of the model reach for the 2- and 5-yr floods. Suspended sediment concentrations can vary both longitudinally and laterally in a stream channel, so this assumption could account for some error in input concentrations. Errors in the measurement of suspended sediment also are compounded by errors associated with the determination of streamflow discharge.

The 10- and 25-yr flood sedigraphs were determined from an extrapolation of a suspended sediment concentration and streamflow relation for a measured flood. Measured flood sedigraphs were quite variable, and the characteristics of these sedigraphs—time of peak relative to streamflow peak and the relative concentration at streamflow peak—were incorporated in the estimation process to better represent the simulated sedigraphs. Flood sedigraphs were more variable than streamflow and stage hydrographs and those sedigraphs used in the simulations in this study represent but one of many possible sediment discharge scenarios.

Comparison of 2-, 5-, 10-, and 25-yr Floods

Graphical Comparisons

Maximum simulated floodplain deposition occurred in the oxbows and tributary channels whereas maximum erosion on the floodplain typically was on the outside of meander bends and in cutoff channels (full model reach shown in fig. 24 and films 21–24; focus area shown in fig. 25 and films 25–28). Localized maximum cumulative deposition on the floodplain (tributary channels) in the focus area was about 4 cm at the end of the 2-yr flood, 12 cm for the 5-yr flood, and 10 cm for the 10- and 25-yr floods. Localized maximum cumulative erosion on the focus area was about -4 cm for the 2-yr flood, -5 cm for the 5-yr flood, and -2 cm for the 10- and 25-yr floods. The 10- and 25-yr floods had smaller maximum localized erosion but larger areas of erosion in the 0 to -1 cm range than the 2- and 5-yr flood simulations.

Substantial simulated deposition in the focus area (fig. 25) has occurred in tributary channels, secondary channels, and oxbows—all areas of microtopographical depressions with low bed shear stress—by the time of the streamflow peak discharge (fig. 26; films 29–32). Deposition continues to occur in these features between the peak streamflow and final simulation time step. Floodplain erosion takes place primarily between the peak and final time step in all flood simulations. Erosion is likely the result of decreased suspended sediment inflows on the hydrograph recession. Again, localized maximum erosion primarily was observed onsite on outside meanders and cutoff channels; these areas displayed the highest floodplain bed shear stress values at peak flood conditions (fig. 26; films 29–32). No substantial lateral gradient in simulated sediment deposition on the floodplain is evident from the main channel outward as suspended sediment concentrations also lack lateral differences (fig. 23; films 33–36).

Quantitative Comparisons

The overall sediments budgets (table 8) of the four flood simulations were dominated by total floodplain deposition and streambed erosion, but these components were affected by the artificial sumps in the mesh (fig. 3). The artificial sumps were sediment traps, and the stream system compensated for the trapped inflows by scouring the streambed. Both total floodplain deposition and streambed deposition were overestimated in the simulations. The following discussion will, therefore, focus on the suspended sediment inflows and sediment deposition on the oxbows and secondary channels, and deposition on the floodplain—excluding the artificial sumps.

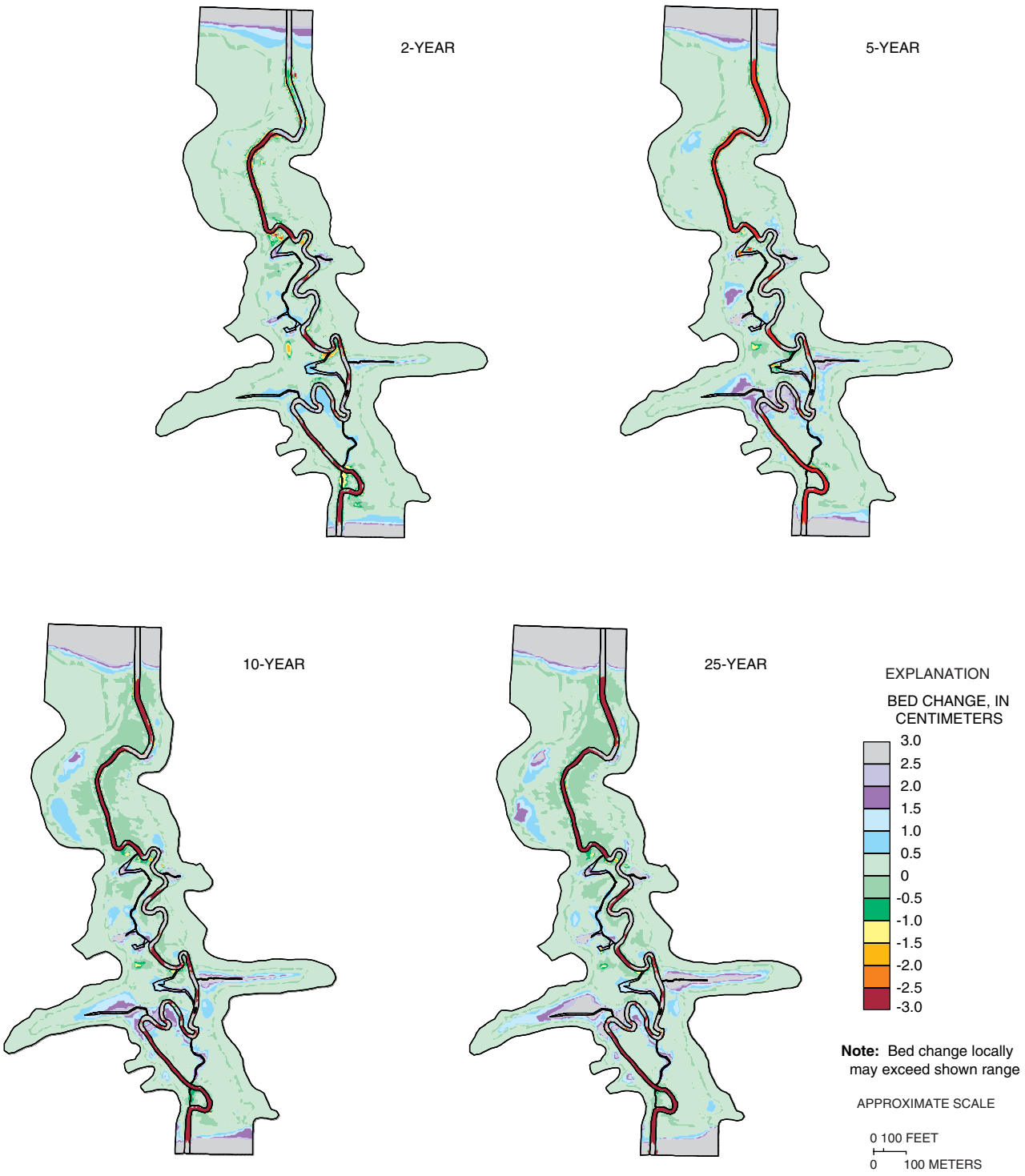

Figure 24. Spatial distribution of cumulative bed change in the model reach at peak-flow conditions during 2-, 5-, 10-, and 25-year recurrence interval floods.

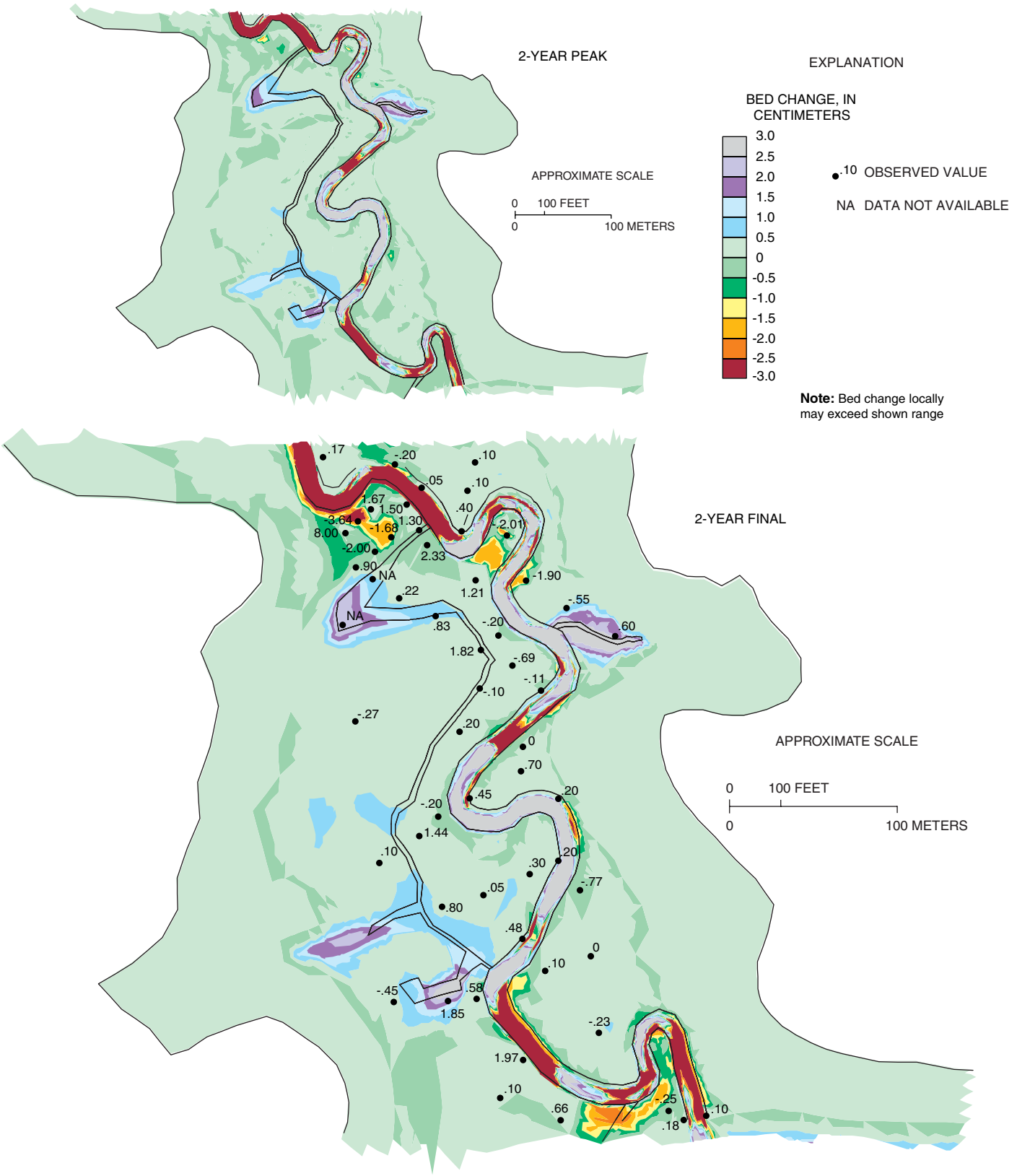

Figure 25. Spatial distributions of cumulative bed change in the focus area at peak flow and final simulation steps for 2-, 5-, 10-, and 25-year recurrence interval floods.

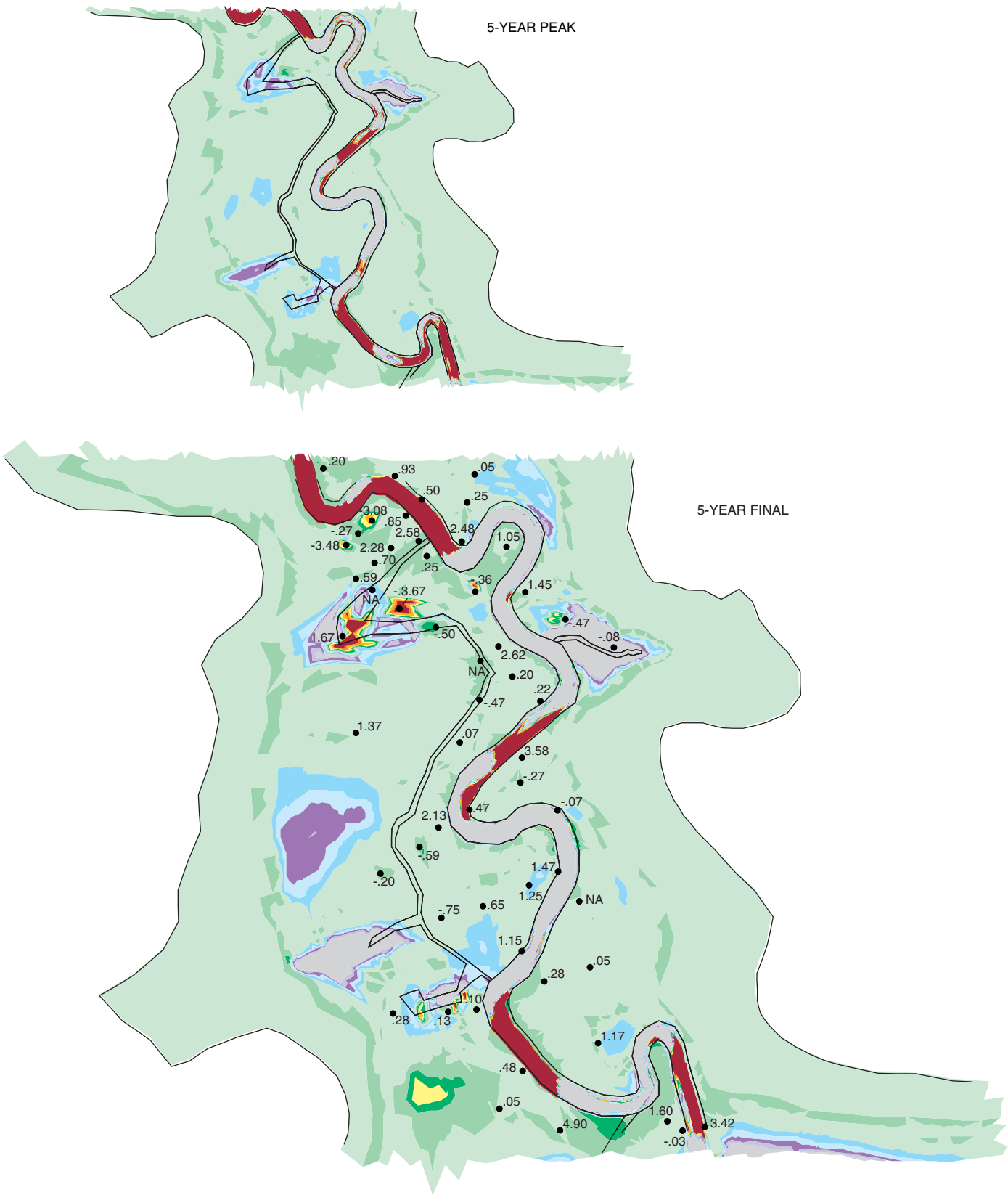

Figure 25. Spatial distributions of cumulative bed change in the focus area at peak flow and final simulation steps for 2-, 5-, 10-, and 25-year recurrence interval floods—Continued.

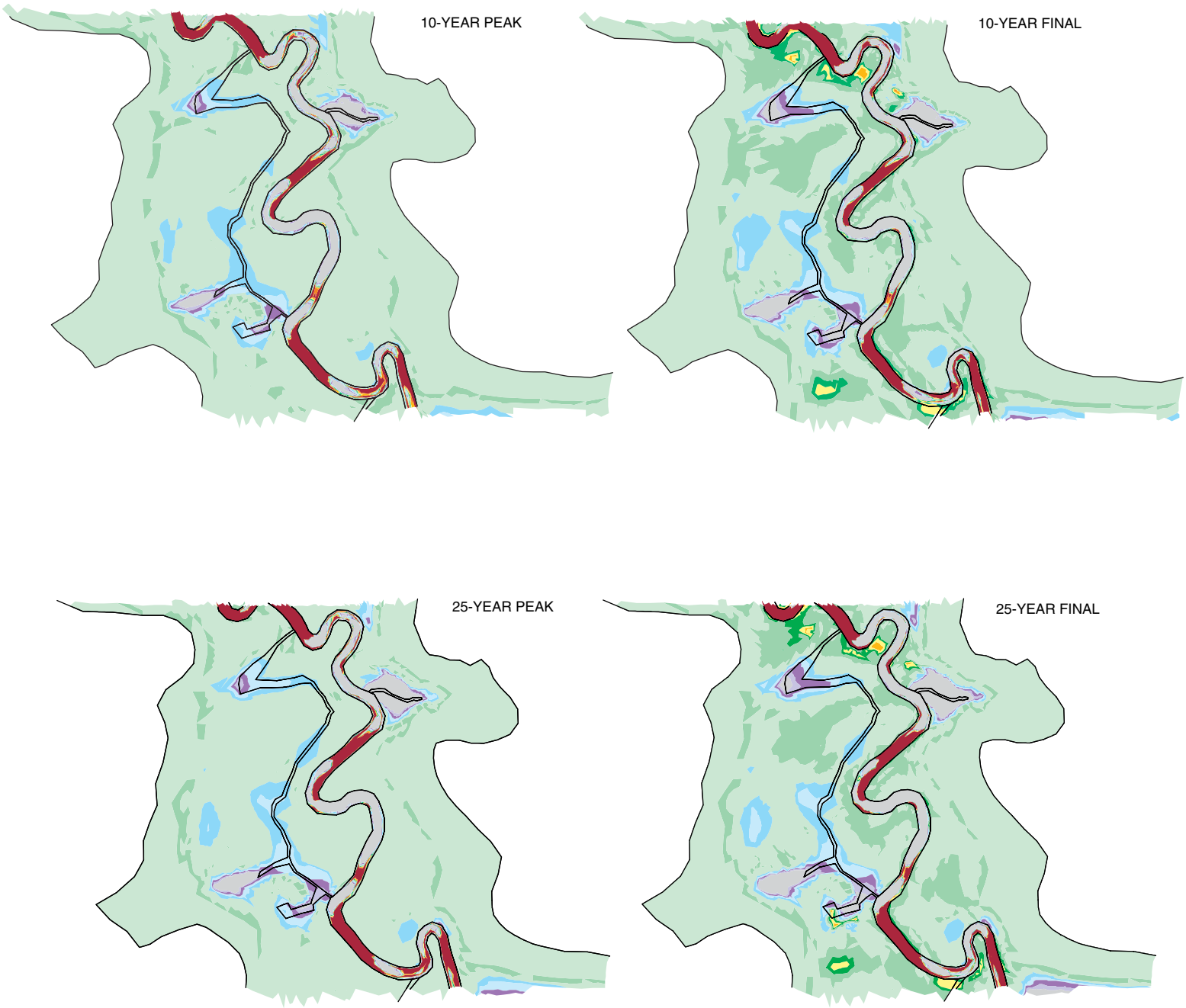

Figure 25. Spatial distributions of cumulative bed change in the focus area at peak flow and final simulation steps for 2-, 5-, 10-, and 25-year recurrence interval floods—Continued.

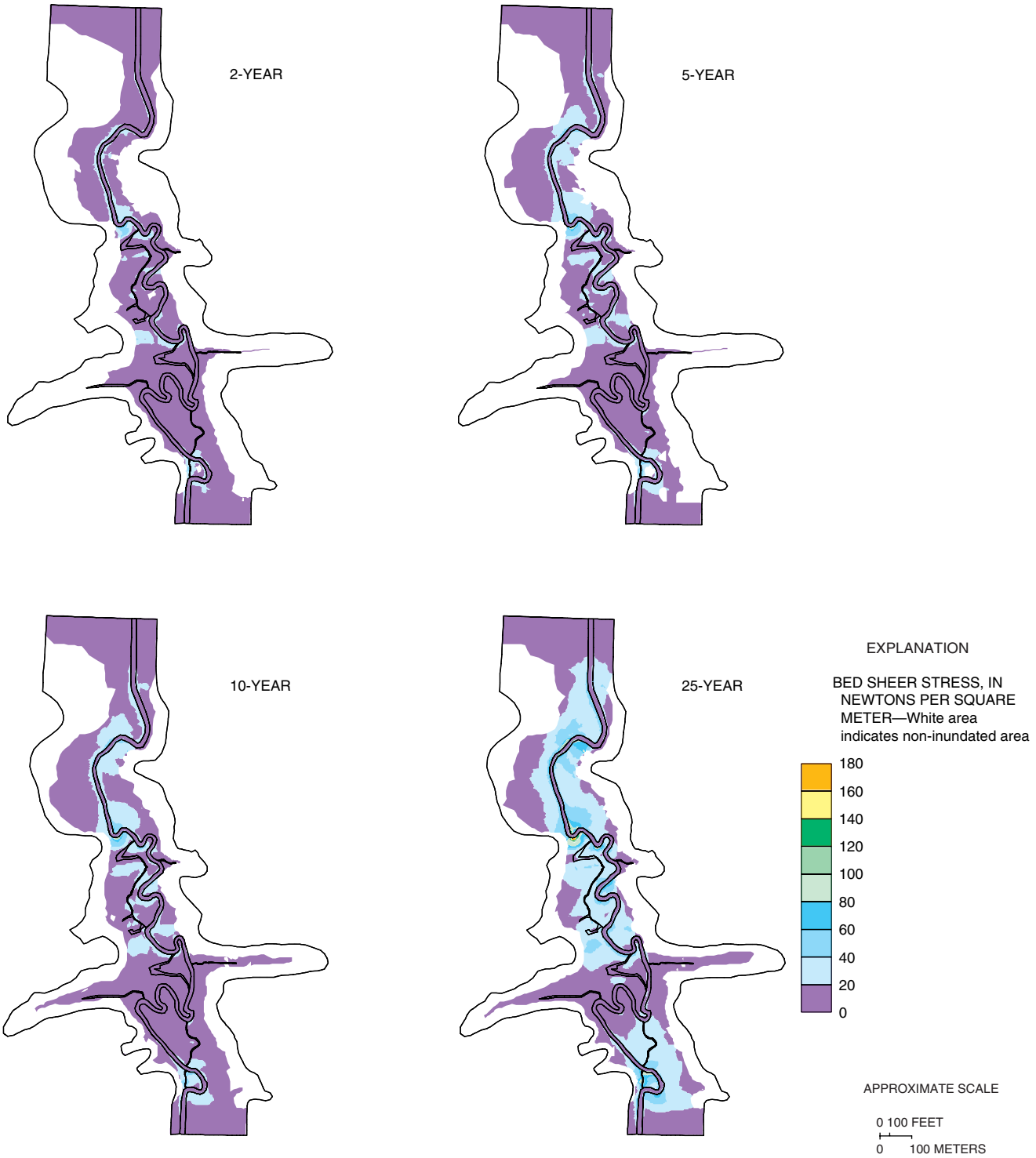

Figure 26. Spatial distribution of bed shear stress in the model reach at peak-flow conditions during 2-, 5-, 10-, and 25-year recurrence interval floods.

Table 8. Summary of sediment budget information for 2-, 5-, 10-, and 25-year floods

Sediment budget component	Total net deposition (+) or erosion (-), in kilograms	Mean deposition, in centimeters per square meter
2-year flood		
Oxbow, tributaries, and secondary channel—**A**	102,000	1.08
Floodplain (excluding oxbow and secondary channel)—**B**	1,620,000	
Floodplain (excluding oxbow and secondary channel and artificial sumps)—**C**	396,000	.09
Streambed—**D**	-3,060,000	
Inflow—**E**	697,000	
Outflow—**F**	-1,840,000	
Water column storage—**G**	52,000	
Retention ratio is **(A + C)/E = 0.71**		
Conservation of mass (ratio of sediment budget sinks/sources) is **(A + B + F + G)/(D + E) = 0.96**		
5-year flood		
Oxbow, tributaries, and secondary channel—**A**	108,000	1.14
Floodplain (excluding oxbow and secondary channel)—**B**	7,340,000	
Floodplain (excluding oxbow and secondary channel and artificial sumps)—**C**	2,510,000	.45
Streambed—**D**	-8,270,000	
Inflow—**E**	3,260,000	
Outflow—**F**	-4,550,000	
Water column storage—**G**	94,000	
Retention ratio is **(A + C)/E = 0.80**		
Conservation of mass (ratio of sediment budget sinks/sources) is **(A + B + F + G)/(D + E) = 1.05**		
10-year flood		
Oxbow, tributaries, and secondary channel—**A**	128,000	1.35
Floodplain (excluding oxbow and secondary channel)—**B**	6,350,000	
Floodplain (excluding oxbow and secondary channel and artificial sumps)—**C**	2,370,000	.43
Streambed—**D**	-6,230,000	
Inflow—**E**	3,590,000	
Outflow—**F**	-3,490,000	
Water column storage—**G**	135,000	
Retention ratio is **(A + C)/E = 0.70**		
Conservation of mass (ratio of sediment budget sinks/sources) is **(A + B + F + G)/(D + E) = 1.03**		

Table 8. Summary of sediment budget information for 2-, 5-, 10-, and 25-year floods—Continued

Sediment budget component	Total net deposition (+) or erosion (-), in kilograms	Mean deposition, in centimeters per square meter
25-year flood		
Oxbow, tributaries, and secondary channel—**A**	118,000	1.25
Floodplain (excluding oxbow and secondary channel)—**B**	8,850,000	
Floodplain (excluding oxbow and secondary channel and artificial sumps)—**C**	3,300,000	.56
Streambed—**D**	-9,450,000	
Inflow—**E**	6,370,000	
Outflow—**F**	-7,600,000	
Water column storage—**G**	-94,000	
Retention ratio is **(A + C)/E = 0.54**		
Conservation of mass (ratio of sediment budget sinks/sources) is **(A + B + F + G)/(D + E) = 1.04**		

Sediment deposition in oxbows and secondary channels was a minor component of overall deposition for all floods, but exceeded that of the remaining floodplain on a per unit area basis. Sediment deposition in the oxbows, tributaries, and secondary channels was similar between floods and was less than 20 percent of overall deposition with less than 130,000 kg of material deposited in these features. The mean deposition for these features was 1.1 to 1.4 cm/m^2 (centimeters per square meter) (table 8; fig. 27) compared with 0.1 to 0.60 cm/m^2 for the remaining floodplain. The simulated mean deposition per unit area in the oxbows, tributaries, and secondary channels was largest for the 10-yr flood and then decreased for the 25-yr flood, but the accuracy of the simulated oxbow deposition values for these larger floods was difficult to determine because verification data were lacking and the simulation data seem to conflict with measured deposition conditions for smaller floods. Measured values of oxbow deposition following the 5-yr flood indicate that erosion occurred in these features, but the 5-yr SED2D-WES simulation overestimated oxbow deposition without localized adjustment [and overestimated oxbow deposition at some sites despite localized adjustments (fig. 22)]. The velocities in these areas generated by RMA2-WES are likely insufficient to generate the measured deposition results. The lack of tributary inflows in the simulation may also account for the overestimation in deposition in these areas. The 10- and 25-yr simulated oxbow deposition amounts also are likely overestimated because these areas are without localized adjustments.

Despite the lack of adjustments, the deposition in the oxbow and secondary channels was less in the 25-yr flood simulation than in the 10-yr simulation. If the erosion conditions measured in oxbows following the 5-yr flood also occurred in the 10- and 25-yr floods, the oxbow deposition likely would be less in both the 10- and 25-yr flood simulations than that measured in the 5-yr simulation. Based on clay pad monitoring in the study reach between 1995 and 1998, oxbow deposition occurred following the smaller floods [stage less than 4.3 m (approximate bankfull stage is 3.02 m) or approximately less than 3-yr floods] and some erosion would occur at larger floods (floods corresponding to more than 4.3 m stages or greater than 3-yr recurrence interval). This is shown to some degree in figure 21 because measured oxbow deposition for the 2-yr flood was nearly twice that for the 5-yr flood.

Floodplain deposition per unit area (excluding oxbows and secondary channels) was substantially less than simulated mean oxbow/secondary channel deposition (table 8, fig. 27), but accounted for more than 80 percent of total floodplain deposition. Measured and computed values of deposition (fig. 22) indicate that deposition was underestimated, particularly in near-main channel areas, and overestimated in some near-tributary areas. Unlike deposition in oxbows and secondary channels, the floodplain deposition was lowest

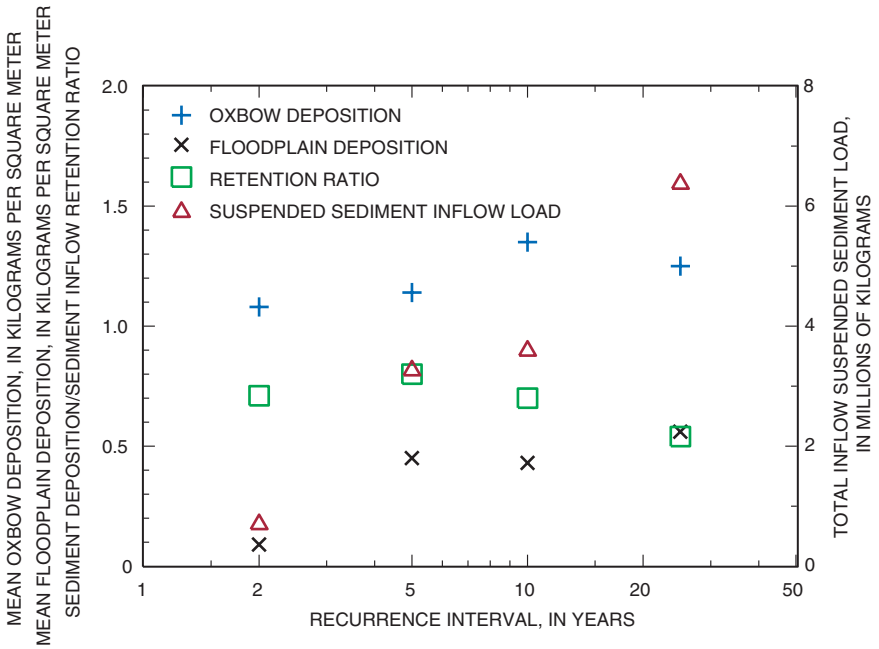

Figure 27. Summary of selected sediment budget components by flood magnitude.

for the 2-yr flood and highest for the 25-yr flood likely because of the increasing inflow sediment loads with larger floods. The double peak in the 5-yr flood may account for the relatively high sediment inflows for this flood and the resulting large floodplain and oxbow deposition. Suspended sediment concentrations are largest on the rising limbs of floods and multiple-peak floods likely have greater sediment transport than comparable single-peak floods.

Despite increases in sediment inflows from the 2- through 25-yr floods the retention of sediments was greatest for the 5-yr flood and least for the 25-yr flood. The retention ratio (ratio of mass of floodplain plus oxbow deposition to sediment inflow mass) increased between the 2- and 5-yr floods and then decreased to its lowest level for the 25-yr flood. The substantial increase in sediment deposition between the 5- and 25-yr flood did not result in proportional gains in floodplain and oxbow deposition. Therefore the retention ratio decreased. The decrease in retention ratio with increased flood flows is likely the result of higher velocities. The higher velocities result in higher bed shear stress and greater suspension time and resuspension of deposited material, which leads to greater sediment transport through the system.

Floodplain deposition (excluding oxbows and secondary channels) increased with flood sediment transport. This increase is verified by the simple linear regressions developed between mean floodplain deposition and flood characteristics (including cumulative sediment load, maximum instantaneous sediment load, cumulative streamflow, and maximum stage) for the Long Branch Creek (Heimann and Roell, 2000). The simple linear regressions were able to explain as much as 82 percent of the variability between mean floodplain deposition and flood streamflow and sediment transport characteristics.

Temporal Variability

A large variability was noted within and between graphs of simulated temporal cumulative streambed change at selected clay pad sites used as “observation” point locations (fig. 28). Those sites were the same as those selected for analyses of temporal variability in velocity and water depth shown in figure 17 (see fig. 7 for clay pad locations). At all but the oxbow sites, the peak cumulative deposition typically occurred between simulation hours 6 through 10, corresponding with the peak in suspended sediment loads (fig. 29). This peak was followed by erosional bed change, at most sites, on the hydrograph recession, presumably as a result of

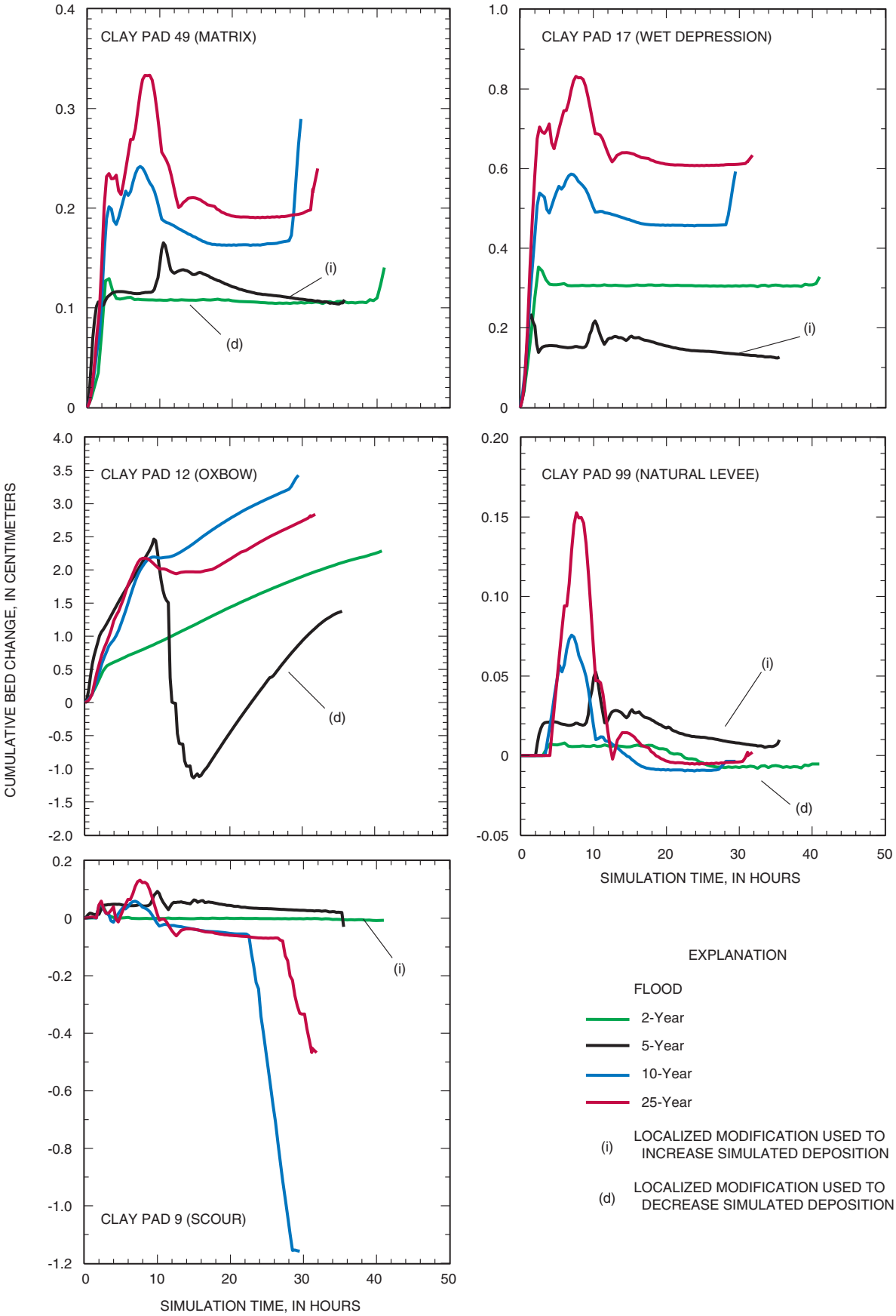

Figure 28. Temporal variation of cumulative bed changes at selected clay pad points representing different landform types for 2-, 5-, 10-, and 25-year recurrence interval floods.

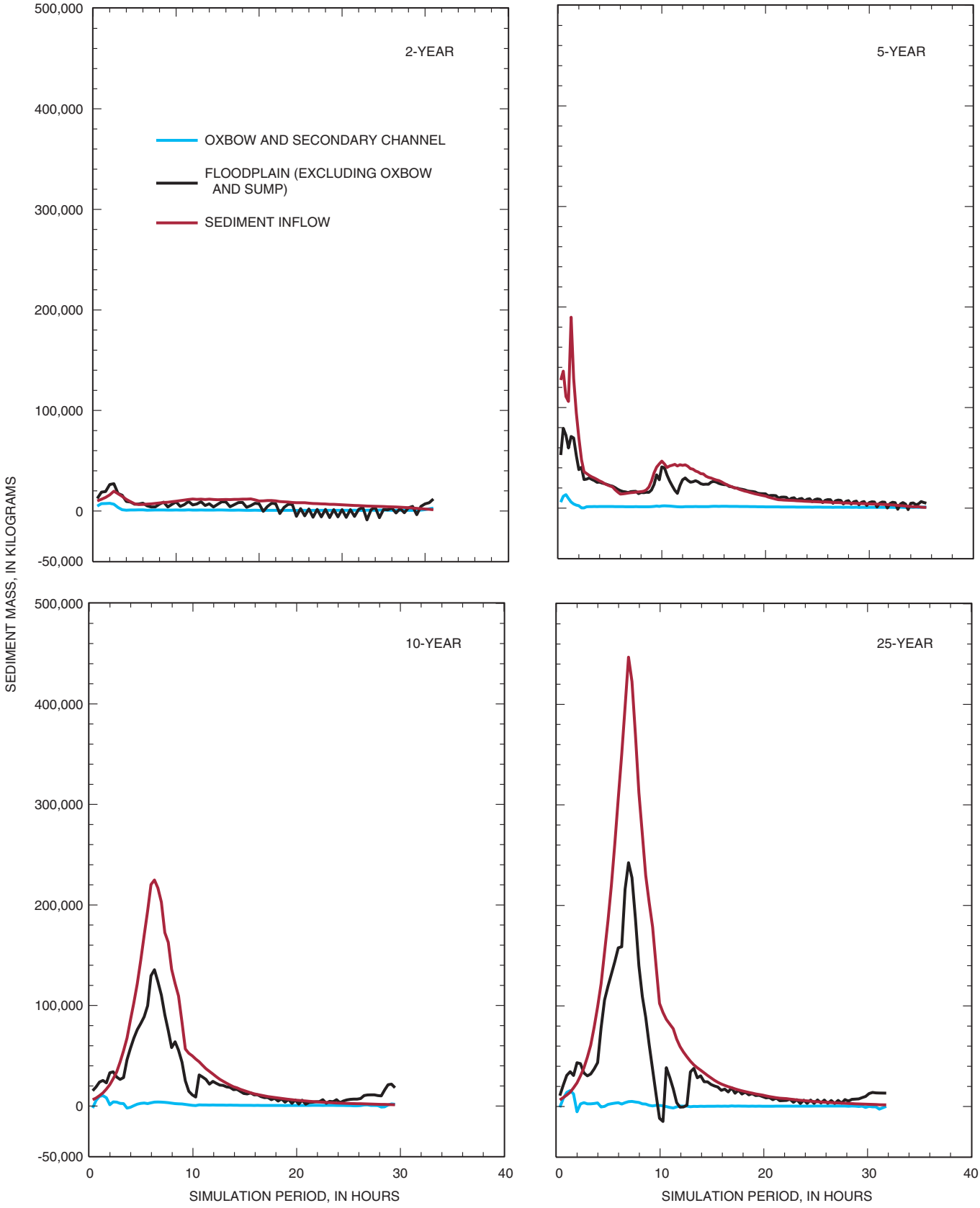

Figure 29. Temporal incremental variation in selected sediment budget components for 2-, 5-, 10-, and 25-year recurrence interval floods.

decreased sediment inflows and "sediment hungry" conditions on the event recession. The exception to this was in the graphs of bed change during 10- and 25-yr floods at the oxbow site (clay pad site 12) where deposition continued to increase following the initial peak. The temporal changes in the 10- and 25-yr flood bed change scenarios were unaffected by localized SED2D-WES bed modifications at all selected sites, but the 2- and 5-yr data may be affected by localized bed modifications.

The temporal variability of total incremental floodplain deposition was strongly related to sediment inflow concentrations. Most deposition, therefore, occurred on the rising limb of the hydrograph. The double peak in the 5-yr flood hydrograph (fig. 29) also resulted in a double peak in the sedigraph and floodplain deposition. Oscillations present on the recession of the floodplain deposition curve correspond with oscillations in streambed erosion/deposition on the flood recession. These oscillations are not present in the RMA2-WES results (temporal variation in outflow streamflow discharge, fig. 10) and velocities at selected points (fig. 17), but they could be related to how SED2D-WES responds to drying elements in the RMA2-WES solution or the aforementioned failure of SED2D-WES to update the wet/dry boundary each time step. The oscillations also may be the result of a less-than-ideal SED2D-WES input parameter value.

The increase in the mass of floodplain deposition toward the end of each simulation presumably corresponds with confinement of flows within the channel and a subsequent increase in channel velocities and erosion. The increase in sediment concentration results in increased deposition in remaining inundated floodplain areas. Measured values of suspended sediment at the upstream gaging station indicate that this phenomenon does not occur on the hydrograph recession.

Spatial Variability

Time series data describing bed shear stress provided by the SED2D-WES solution were used to explain the spatial distribution of sediment deposition on the Long Branch Creek floodplain. No discernible relation exists between sediment deposition on the Long Branch Creek floodplain and distance from a primary or secondary channel using the clay pad data collected between 1995 and 1998 (Heimann and Roell, 2000), although numerous studies have shown such relation exist for other, albeit larger, stream systems (Kleiss, 1996; Walling and others, 1996; Simm and Walling, 1998; Dunne and others, 1998). These studies have shown an exponential decrease in sediment deposition with distance from the stream channel as well as a decrease in particle size. These studies also note that the relationships vary with microtopographic variations and effects of secondary channels.

Deposition amounts from clay pads measured following the 2- and 5-yr floods were plotted with corresponding simulated maximum bed shear stress at these sites to determine if correlations existed with proximity to the channel (fig. 30). Sites were classified by landform type and subdivided into those sites within 13 m (one mean channel width) of a primary or secondary channel (near-channel sites) and those outside this distance (far-channel sites). The hypotheses tested were that the magnitude of deposition and erosion would be greater near an active channel and the deposition would vary inversely with bed shear stress. The range in sediment deposition and erosion was greater at the near-channel sites than far-channel sites. The range in deposition for the near-channel 2-yr values was 5 cm (-2 to 3 cm) whereas the range for far-channel sites was 3 cm (-1 to 2 cm). The range in deposition for the 5-yr flood for near-channel sites was 9 cm (-4 to 5 cm) and for the far-channel sites the range was 2.5 cm (-1 to 1.5 cm). As a whole, clay pad deposition had little correlation with simulated bed shear stress at either near-channel or far-channel sites for either the 2- or 5-yr floods. With the possible exception of oxbow sites, little correlation was noted between sediment deposition at sites grouped by landform type and corresponding simulated maximum bed shear stress for both near-channel and far-channel points for the 2- and 5-yr floods. The range in sediment deposition in the oxbows was within a narrow range of corresponding bed shear stress values—a possible indication of the easily erosive nature of deposits in these features.

Simulation of Floodplain Vegetation Modification

The vegetation of much of the forested riparian areas of northern Missouri has been removed or modified and the effects of vegetation modification on sediment deposition were simulated for the Long Branch Creek model reach. To simulate a modification of vegetation in the Long Branch Creek floodplain and the effects this would have on floodplain sediment deposition, the floodplain roughness was modified. A partial forest stand removal was hypothesized to increase floodplain roughness, at least temporarily, by increasing sunlight penetration and growth of understory her-

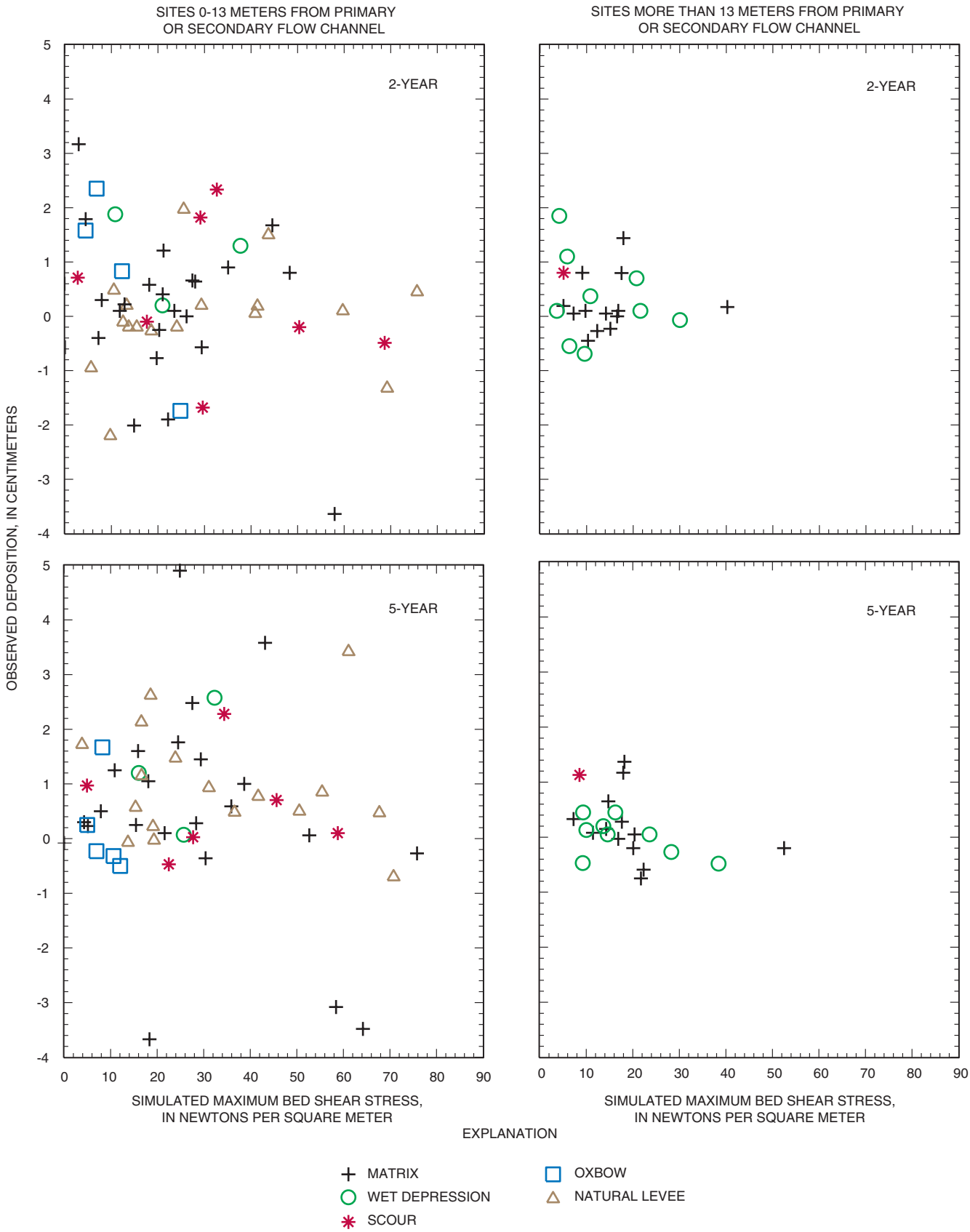

Figure 30. Comparison of event deposition and simulated maximum bed sheer stress by landform type and proximity to primary/secondary channels for the 2-, 5-, 10-, and 25-year recurrence interval floods.

baceous material. Therefore, Manning's n was increased from 0.11 to 0.12 for the entire floodplain during the first 24 hrs of a RMA2-WES 10-yr flood simulation and a solution was obtained. This solution was then used as input into SED2D-WES. The increase in floodplain sediment deposition (excluding oxbows and artificial sumps) resulting from the increase in floodplain roughness was 142,000 kg, or 6.5 percent. The increase in sediment deposits was comparable to the total oxbow and secondary channel deposition mass and translates to a mean increase in total floodplain deposition thickness of 0.025 cm. The temporal variability in sediment deposition from the two simulations is shown in fig. 31. The increased sediment deposition resulting from the modified simulation (Manning's n = 0.12) is not uniform, but rather occurs predominantly during deposition peaks. Modification of floodplain vegetation (and, therefore, roughness) would be another controllable parameter of sediment deposition on the floodplain, along with modification of sediment inflows as discussed in the "Sensitivity Analyses" section.

SUMMARY

This report summarizes the results of a study, conducted from October 1998 through December 2000, in which the two-dimensional finite element hydraulic model RMA2-WES was used in conjunction with the sediment transport and deposition model SED2D-WES to simulate flood sediment deposition on

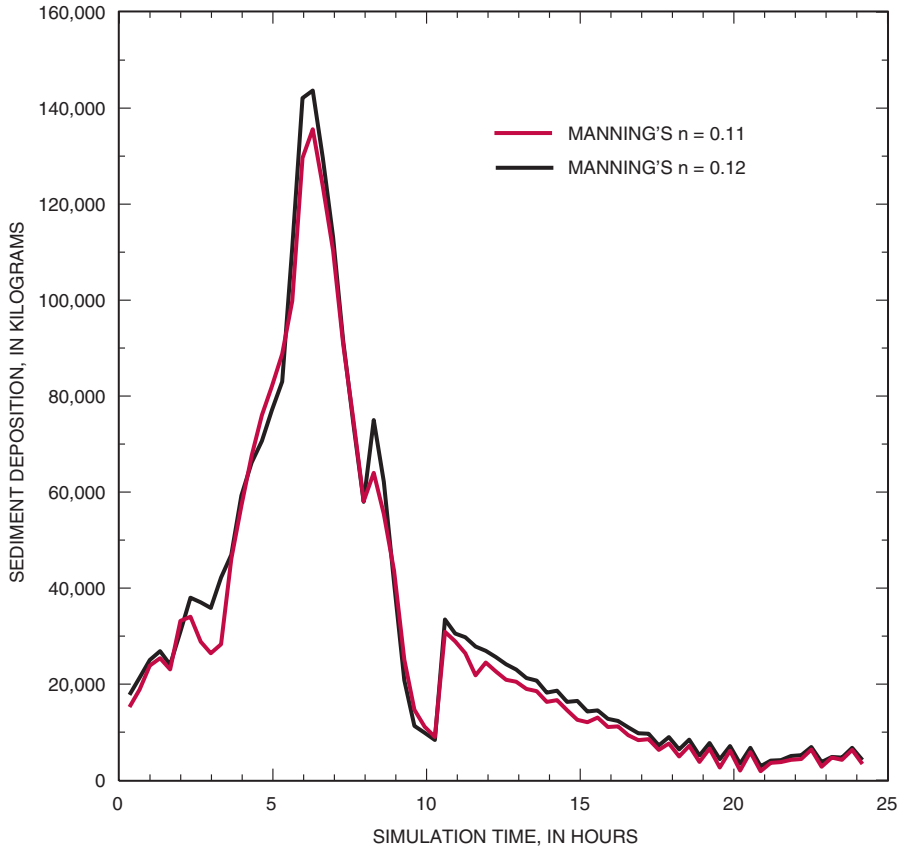

Figure 31. Temporal variability in floodplain sediment deposition (excluding oxbows and artificial sumps) for simulations using different floodplain roughness coefficients.

a 2,700 m (meter) reach of the Long Branch Creek floodplain in the Atlanta Conservation Area, Macon County, Missouri. The study was undertaken to gain a better understanding of the factors controlling sediment deposition in remnant forested riparian areas in northern Missouri including determining floodplain deposition under conditions outside the measured range of flood magnitudes. Four floods were simulated including two measured floods used for verification [2- and 5-yr (year) recurrence interval floods] and two simulated larger-recurrence interval floods (10- and 25-yr floods).

The hydrodynamic results show the importance of the secondary and meander cutoff channels in this system as these areas quickly bring floodwaters to areas not in close proximity to the main channel. The meander cutoff channels in the simulation also effectively decrease flow and velocities in some main channel sections—thereby affecting sediment deposition in these areas. The importance of select elevation control points including the secondary channel and cutoff inflow and outflow points, natural levee low points, and low points in microtopographical "ridges" on floodplain areas lacking secondary cutoff channels was also evident in constructing the model mesh and in simulation runs. The elevations at these select control points determine, to a great extent, the timing, duration, extent, and direction of overbank flows.

No discernible relationships could be found between the inside and outside bend characteristics and the simulated velocities and water depths at selected observation points. Further examination does show the controlling factor for velocities in these meander bends may be at the sub-reach channel scale. The location and carrying capacity of secondary and cutoff channels will greatly affect velocities in meander bends with similar radius/channel width characteristics. The variability in water depths were less than that for velocities for both inside and outside bend points but the bend radius/channel width ratio explained little of the variability present.

The distribution of coarse woody debris (CWD) was compared with simulated peak velocities from the 5-yr flood (the largest measured flood during the monitoring period) to determine if the simulated velocities could provide insight into the clustered distribution of CWD in the study reach. The peak in the number of CWD pieces corresponded with channel areas in the 0.3-0.39-m/s (meter per second) velocity category and over one-half of the debris pieces were in this or a lower velocity category areas. The peak CWD velocity category may provide an indication of the threshold transport velocity as number of pieces decreased with an increase in velocity class. It is likely the CWD distribution in Long Branch Creek is determined both by the nature of the source material (timber stand characteristics and size and orientation of delivered material) and also some redistribution during floods.

The 2-yr measured sediment deposition distributions by landform type were, in general, inversely related to the velocity distribution for that landform and directly related to water depth and inundation period distributions. A comparison of the relative differences in the distribution of sediment deposition with those of hydrologic characteristics for the 5-yr flood provides fewer generalized correlations and, unlike the 2-yr flood, the overall relation seemed to differ by landform type. The differences between the 2- and 5-yr flood distribution relationships not only show hydrologic differences, but is also likely an indicator of the variability in particle size of material being transported with flood magnitude.

Maximum floodplain deposition occurred in the tributary channels and artificial sumps placed in the upstream and downstream mesh boundaries while maximum erosion on the floodplain was typically found on the outside of meander bends and in cutoff channels. Deposition continues to occur in these features between the peak streamflow and final simulation time step. Floodplain erosion takes place in the simulations primarily between the peak and final time step in all flood simulations. Again, localized maximum erosion was viewed primarily on outside meanders and cutoff channels and these areas displayed the highest floodplain bed shear stress values at peak flood conditions.

Comparing deposition per unit area shows that mean deposition in oxbows and secondary channels exceeds that of the remaining floodplain areas. The simulated mass deposition per area for these features was 1.1 to 1.4 cm/m^2 (centimeters per square meters) compared with 0.1 to 0.60 cm/m^2 for the remaining floodplain. Unlike oxbows and secondary channels the floodplain deposition was lowest for the 2-yr flood and highest for the 25-yr flood in following with the increasing inflow loads with larger floods.

Despite increases in sediment inflows from the 2- through 25-yr floods the retention of sediments was greatest for the 5-yr flood and least for the 25-yr flood. The retention ratio (the ratio of floodplain plus oxbow

deposition mass to sediment inflow mass) increased between the 2- and 5-yr flood and then decreased to its lowest level for the 25-yr flood. The decrease in retention ratio at greater flows was likely the result of higher velocities resulting in higher bed shear stress, greater suspension time, and resuspension of deposited material leading to greater sediment transport through the system.

There was a large variability between graphs of temporal cumulative bed change at selected clay pad observation sites. At all but the oxbow sites the peak cumulative deposition typically occurred at the peak in suspended sediment loads. This peak was followed by erosional bed change at most sites on the hydrograph recession, presumably as a result of reduced sediment inflows and "sediment hungry" conditions on the event recession. The temporal variability of total incremental floodplain deposition was found to be strongly tied to sediment inflow concentrations. Most deposition therefore occurred on the rising limb of the hydrograph.

The range in sediment deposition and erosion was greater at near-channel (less than 13 m) sites than far-channel (greater than 13 m) sites, but clay pad deposition had little correlation with simulated bed shear stress at either near-channel or far-channel sites for either the 2- or 5-yr floods. With the possible exception of oxbow sites there was little correlation between sediment deposition at sites grouped by landform type and corresponding simulated maximum bed shear stress for both the 2- and 5-yr flood near-channel and far-channel points. The range in sediment deposition in the oxbows was located within a relatively narrow range of corresponding bed shear stress values—a possible indication of the easily erosive nature of deposits in these features.

The increase in floodplain sediment deposition (excluding oxbows and artificial sumps) resulting from a simulated vegetation modification (increase in floodplain roughness from a Manning's n of 0.11 to 0.12) was 142,000 kg (kilograms), or 6.5 percent. The increase in sediment deposits translates to a mean increase in floodplain deposition of 0.025 cm (centimeter) for a 10-yr flood. Modification of floodplain vegetation (and therefore roughness) would be another controllable parameter of sediment deposition on the floodplain comparable to modification of sediment inflows.

REFERENCES CITED

Abernethy, Y., and Turner, R.E., 1987, U.S. forested wetlands: 1940–1980: BioScience, v. 37, p. 721–727.

Alexander, T.W., and Wilson, G.L., 1995, Technique for estimating the 2- to 500-year flood discharges on unregulated streams in rural Missouri: U.S. Geological Survey Water-Resources Investigations Report 95–4231, 33 p.

Apicella, G., Norris, R., Newton, J., Ewald, W., and Forndran, A., 1994, East river modeling of water quality for multiple-project assessments: Third International Conference on Estuarine and Coastal Modeling, Oak Brook, Ill., 1994 Proceedings, p. 235–248.

Arcement, G.J., Jr., and Schneider, V.R., 1989, Guide for selecting Manning's roughness coefficients for natural channels and flood plains: U.S. Geological Survey Water-Supply Paper 2339, 38 p.

Barnes, H.B., 1967, Roughness characteristics of natural channels: U.S. Geological Survey Water-Supply Paper 1849, 213 p.

Bates, P.D., Anderson, M.G., Baird, L., Walling, D.E., and Simm, D., 1992, Modeling floodplain flows using a two-dimensional finite element model: Earth Surface Processes and Landforms, v. 17, p. 575–588.

Becker, L.D., 1990, Simulation of flood hydrographs for small basins in Missouri: U.S. Geological Survey Water-Resources Investigations Report 90–4045, 40 p.

Berger, R.C., 1990, Mass conservation in the RMA2V Code: Hydraulic Engineering National Conference, San Diego, Calif., 1990, Proceedings, American Society of Civil Engineers, Boston, MA, v. 2, p. 873–878.

Brinson, M.M., 1990, Riverine forests, *in* Lugo, A.E., Brinson, M., and Brown, S., eds., Ecosystems of the World, no.15: New York, Elsevier Publishing Co., p. 87–141.

Crowder, D.W., and Diplas, P., 2000, Using two-dimensional hydrodynamic models at scales of ecological importance: Journal of Hydrology, v. 230, p. 172–191.

Dunne, T., Mertes, L.A., Meade, R.H., Richey, J.E., and Forsberg, B.R., 1998, Exchanges of sediment between the floodplain and channel of the Amazon River in Brazil: Geological Society of America, v. 110, no. 4, p. 450–467.

Elliot, J.M., 1977, Some methods for the statistical analysis of samples of benthic invertebrates: Freshwater Biological Association, no. 25, 159 p.

Environmental Modeling Research Laboratory, 1999, Surface-water modeling system reference manual: Provo, Utah, Brigham Young University, version 6.0, 315 p.

Geier, A.R., and Best, L.B., 1980, Habitat selection by small mammals of riparian communities—Evaluating the effects of habitat alterations: Journal of Wildlife Management, v. 44, p. 16–24.

Gregory, S.V., Swanson, F.J., McKee, W.A., and Cummins, K.W., 1991, An ecological perspective of riparian zones: Focus on links between land and water: BioScience, v. 41, p. 540–551.

Guy, H.P., 1969, Laboratory theory and methods for sediment analysis: U.S. Geological Survey Techniques of Water-Resources Investigations, book 5, chap. C1, 58 p.

Guy, H.P., and Norman, V.W., 1970, Field methods for measurement of fluvial sediment: U.S. Geological Survey Techniques of Water-Resources Investigations, book 3, chap. C2, 59 p.

Hall, B.R., and Engel, J., 1995, Modeling of sedimentation processes in a bottomland hardwood wetland: International Water Resources Engineering Conference, San Antonio, Tex., 1995 Proceedings, p. 94–98.

Hardin, E.D., and Wistendahl, W.A., 1983, The effects of floodplain trees on herbaceous vegetation patterns, microtopography, and litter: Bulletin of the Torrey Botany Club, v. 110, p. 23–30.

Heimann, D.C., and Roell, M. J., 2000, Sediment loads and accumulation in a small riparian wetland system in northern Missouri: Wetlands, v. 20, p. 219–231.

Hodges, J.D., 1997, Development and ecology of bottomland hardwood sites: Forest Ecology and Management, v. 90, p. 117–125.

Hupp, C.R., and Osterkamp, W.R., 1985, Bottomland vegetation distribution along Passage Creek, Virginia, in relation to fluvial landforms: Ecology, v. 66, p. 670–681.

_____1996, Riparian vegetation and fluvial geomorphic processes: Geomorphology, v. 14, p. 277–295.

Interagency Committee, 1957, Some fundamentals of particle size analysis—A study of methods used in measurement and analysis of sediment loads in streams: Minneapolis, Minn,. St. Anthony Falls Hydraulic Laboratory, Report 12.

King, I.P., 1990, Program documentation RMA-2V. Two-dimensional finite element model for flow in estuaries and streams, version 4.3: Lafayette, Calif., Resource Management Associates.

Kleiss, B.A., 1996, Sediment retention in a bottomland hardwood wetland in eastern Arkansas: Wetlands, v. 16, p. 321–333.

Knight, D.W., and Shiono, K., 1996, River channel and floodplain hydraulics, *in* Anderson, M.G., Walling, D.E., and Bates, P.D., eds., Floodplain processes: Chichester, England, John Wiley and Sons, p. 139–181.

Koltun, G.F., Gray, J.R., and McElhone, T.J., 1994, User's manual for SEDCALC, A computer program for computation of suspended-sediment discharge: U.S. Geological Survey Open-File Report 94–459, 46 p.

Letter, J.V., Jr., Roig, L.C., Donnell, B.P., Thomas, W.A., McAnally, W.H., and Adamec, S.A., Jr., 1998, A user's manual for SED2D-WES, version 4.3 Beta—A generalized computer program for two-dimensional, vertically averaged sediment transport: Vicksburg, Miss, U.S. Army Corps of Engineers Waterways Experiment Station, 75 p.

Metzler, K.J., and Damman, A.W.H., 1985, Vegetation patterns in the Connecticut River flood plain in relation to frequency and duration of flooding: Le Naturaliste Canadien, v. 12, p. 535–547.

Murray, N.L., and Stauffer, D.F., 1995, Nongame bird use of habitat in central Appalachian riparian forests: Journal of Wildlife Management, v. 59, p. 78–88.

Nelson, P.W., 1987, The terrestrial natural communities of Missouri: Jefferson City, Missouri Natural Resources Committee, 197 p.

Patterson, G.G., Speiran, G.K., and Whetstone, B.H., 1985, Hydrology and its effects on distribution of vegetation in Congaree Swamp National Monument, South Carolina: U.S. Geological Survey Water-Resources Investigations Report 85–4256, 31 p.

Roig, L.C., Donnell B.P., Thomas, W.A., McAnally, W.H., and Adamec, Jr., S.A., 1996, A user's manual for SED2D-WES—A generalized computer program for two-dimensional, vertically average sediment transport: Vicksburg, Miss., U.S. Army Corps of Engineers Waterways Experiment Station, 75 p.

Sanchez, J.A., and Roig, L.C., 1997, Hydrodynamic and sediment transport, Mill Cove, St. John's River, Florida: Vicksburg, Miss., U.S. Army Corps of Engineers Waterways Experiment Station, Technical report CHL–97–8, 114 p.

Schroeder, W.A., 1982, Pre-settlement prairie of Missouri: Jefferson City, Missouri Department of Conservation, Natural History Series number 2, 8 p.

Sellin, R.H.J., 1964, A laboratory investigation into the interaction between the flow in the channel of a river and that over its flood plain: La Houille Blanche, no. 7, p. 793–801.

Sigafoos, R.S., 1976, Relations among surficial material, light intensity, and sycamore seed germination along the Potomac River near Washington, D.C.: Journal of Research of the U.S. Geological Survey, v. 4, p. 733–736.

Simm, D.J., and Walling, D.E., 1998, Lateral variability of overland sedimentation on a Devon flood plain: Journal of Hydrologic Science, v. 4, no. 5, p. 715–732.

U.S. Army Corps of Engineers, 1996, User's guide to RMA2, version 4.3: Vicksburg, Miss., Waterways Experiment Station, 226 p.

U.S. Department of Agriculture, 1996, Soil survey laboratory methods manual: Soil Survey Investigations Report 42, v. 3, 693 p.

Walling, D.E., He, Q., and Nicholas, A.P., 1996, Floodplains as suspended sediment sinks, *in* Anderson, M.G., Walling, D.E., and Bates, P.D., eds., Floodplain processes: Chichester, England, John Wiley and Sons, p. 399–440.

Wolfe, C.B., and Pittillo, J.D., 1977, Some ecological factors influencing the distribution of *Betula nigra* in western North Carolina: Castanea, v. 42, p. 18–30.